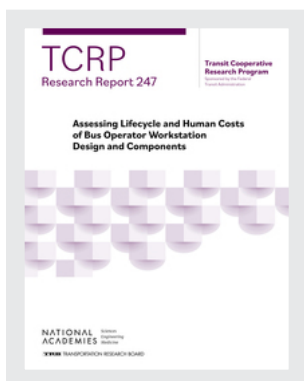


This PDF is available at <http://nap.nationalacademies.org/27858>



Assessing Lifecycle and Human Costs of Bus Operator Workstation Design and Components (2024)

DETAILS

86 pages | 8.5 x 11 | PAPERBACK

ISBN 978-0-309-70985-9 | DOI 10.17226/27858

CONTRIBUTORS

Songlin Wu, Eunsik Kim, Andris Freivalds, Yiqi Zhang, Matthew Parkinson; Transit Cooperative Research Program; Transportation Research Board; National Academies of Sciences, Engineering, and Medicine

SUGGESTED CITATION

National Academies of Sciences, Engineering, and Medicine. 2024. *Assessing Lifecycle and Human Costs of Bus Operator Workstation Design and Components*. Washington, DC: The National Academies Press. <https://doi.org/10.17226/27858>.

BUY THIS BOOK

FIND RELATED TITLES

Visit the National Academies Press at nap.edu and login or register to get:

- Access to free PDF downloads of thousands of publications
- 10% off the price of print publications
- Email or social media notifications of new titles related to your interests
- Special offers and discounts



All downloadable National Academies titles are free to be used for personal and/or non-commercial academic use. Users may also freely post links to our titles on this website; non-commercial academic users are encouraged to link to the version on this website rather than distribute a downloaded PDF to ensure that all users are accessing the latest authoritative version of the work. All other uses require written permission. ([Request Permission](#))

This PDF is protected by copyright and owned by the National Academy of Sciences; unless otherwise indicated, the National Academy of Sciences retains copyright to all materials in this PDF with all rights reserved.

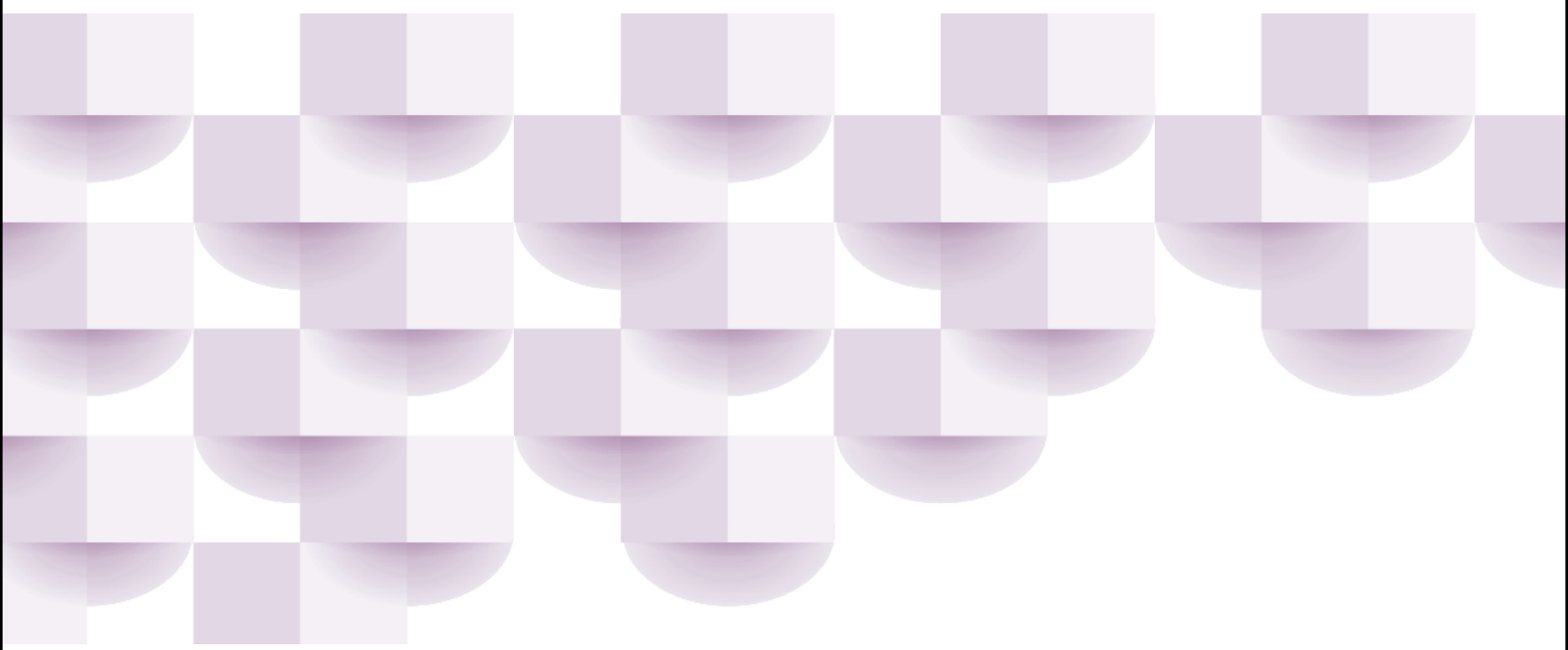
TCRP

Research Report 247

**Transit Cooperative
Research Program**

Sponsored by the Federal
Transit Administration

Assessing Lifecycle and Human Costs of Bus Operator Workstation Design and Components



**NATIONAL
ACADEMIES** *Sciences
Engineering
Medicine*

TRB TRANSPORTATION RESEARCH BOARD

TCRP OVERSIGHT AND PROJECT SELECTION COMMISSION*

CHAIR

Jeanne Krieg
Eastern Contra Costa Transit Authority (retired)

VICE CHAIR

Jameson Auten
Lane Transit District

SECRETARY/TREASURER

Ryan I. Daniel
St. Cloud Metro Bus

IMMEDIATE PAST CHAIR

Doran J. Barnes
Foothill Transit

MEMBERS

Mallory R. Avis
City of Battle Creek Transit
Alva Carrasco
Burns Engineering
Dorval Ronald Carter, Jr.
Chicago Transit Authority
Desmond Cole
Southeastern Pennsylvania Transportation Authority

Francis “Buddy” Coleman
Clever Devices Ltd.

Faye DiMassimo
Chatham Area Transit

Carolyn Flowers
InfraStrategies LLC

David Harris
New Mexico Department of Transportation

Vince Huerta
East Texas Council of Governments

Joseph Leader
HDR

Benjamin Limmer
Connecticut Department of Transportation

Bacarra Mauldin
Memphis Area Transit Authority

Jessica Mefford-Miller
Valley Metro

Brad Miller
Pinellas Suncoast Transit Authority (PSTA)

Elizabeth Presutti
Charlotte Area Transit System

Daniel J. Raudebaugh
Center for Transportation and the Environment

Jeffrey Rosenberg
Amalgamated Transit Union

Bernard Schmidt
NextEra Energy

Justin Stuehrenberg
Madison Metro Transit

Frank White, III
Kansas City Area Transportation Authority

David C. Wilcock
Vanasse Hangen Brustlin, Inc.

Kimberly J. Williams
Metropolitan Transit Authority of Harris County

Nigel H.M. Wilson
MIT

EX OFFICIO MEMBERS

Shailen Bhatt
FHWA

Victoria Sheehan
TRB

Paul P. Skoutelas
APTA

Jim Tymon
AASHTO

Veronica Vanterpool
AASHTO

TOPS COMMISSION STAFF ADVISOR

Arthur L. Guzzetti
APTA

SECRETARY

Victoria Sheehan
TRB

* Membership as of May 2024.

TRANSPORTATION RESEARCH BOARD 2024 EXECUTIVE COMMITTEE*

OFFICERS

CHAIR: **Carol A. Lewis**, *Professor, Transportation Studies, Texas Southern University, Houston*

VICE CHAIR: **Leslie S. Richards**, *General Manager, Southeastern Pennsylvania Transportation Authority (SEPTA), Philadelphia*

EXECUTIVE DIRECTOR: **Victoria Sheehan**, *Transportation Research Board, Washington, DC*

MEMBERS

Michael F. Ableson, *CEO, Arrival Automotive–North America, Detroit, MI*

James F. Albaugh, *President and CEO, The Boeing Company (retired), Scottsdale, AZ*

Carlos M. Braceras, *Executive Director, Utah Department of Transportation, Salt Lake City*

Douglas C. Ceva, *Vice President, Customer Lead Solutions, Prologis, Inc., Jupiter, FL*

Nancy Daubenberger, *Commissioner of Transportation, Minnesota Department of Transportation, St. Paul*

Marie Therese Dominguez, *Commissioner, New York State Department of Transportation, Albany*

Garrett Eucalitto, *Commissioner, Connecticut Department of Transportation, Newington*

Chris T. Hendrickson, *Hammerschlag University Professor of Engineering Emeritus, Carnegie Mellon University, Pittsburgh, PA*

Randell Iwasaki, *President and CEO, Iwasaki Consulting Services, Walnut Creek, CA*

Ashby Johnson, *Executive Director, Capital Area Metropolitan Planning Organization (CAMPO), Austin, TX*

Joel M. Jundt, *Secretary of Transportation, South Dakota Department of Transportation, Pierre*

Hani S. Mahmassani, *W.A. Patterson Distinguished Chair in Transportation; Director, Transportation Center, Northwestern University, Evanston, IL*

Scott C. Marler, *Director, Iowa Department of Transportation, Ames*

Ricardo Martinez, *Adjunct Professor of Emergency Medicine, Emory University School of Medicine, Decatur, GA*

Michael R. McClellan, *Vice President, Strategic Planning, Norfolk Southern Corporation, Norfolk, VA*

Russell McMurry, *Commissioner, Georgia Department of Transportation, Atlanta*

Craig E. Philip, *Research Professor and Director, VECTOR, Department of Civil and Environmental Engineering, Vanderbilt University, Nashville, TN*

Steward T.A. Pickett, *Distinguished Senior Scientist, Cary Institute of Ecosystem Studies, Millbrook, NY*

Susan A. Shaheen, *Professor and Co-director, Transportation Sustainability Research Center, University of California, Berkeley*

Marc Williams, *Executive Director, Texas Department of Transportation, Austin*

EX OFFICIO MEMBERS

Michael R. Berube, *Deputy Assistant Secretary for Sustainable Transportation, U.S. Department of Energy, Washington, DC*

Shailen Bhatt, *Administrator, Federal Highway Administration, U.S. Department of Transportation, Washington, DC*

Amit Bose, *Administrator, Federal Railroad Administration, Washington, DC*

Tristan Brown, *Deputy Administrator, Pipeline and Hazardous Materials Safety Administration, U.S. Department of Transportation, Washington, DC*

Steven Cliff, *Executive Officer, California Air Resources Board, Sacramento*

Rand Ghayad, *Senior Vice President, Association of American Railroads, Washington, DC*

LeRoy Gishi, *Chief, Division of Transportation, Bureau of Indian Affairs, U.S. Department of the Interior, Germantown, MD*

William H. Graham, Jr. (Major General, U.S. Army), *Deputy Commanding General for Civil and Emergency Operations, U.S. Army Corps of Engineers, Washington, DC*

Robert C. Hampshire, *Deputy Assistant Secretary for Research and Technology, U.S. Department of Transportation, Washington, DC*

Sue Lawless, *Acting Deputy Administrator, Federal Motor Carrier Safety Administration, Washington, DC*

Niloo Parvashtiani, *Engineer, Mobility Consultant Solutions, Iteris Inc., Fairfax, VA, and Chair, TRB Young Members Coordinating Council*

Sophie Shulman, *Acting Administrator, National Highway Traffic Safety Administration, Washington, DC*

Karl Simon, *Director, Transportation and Climate Division, U.S. Environmental Protection Agency, Washington, DC*

Paul P. Skoutelas, *President and CEO, American Public Transportation Association, Washington, DC*

Polly Trottenberg, *Deputy Secretary of Transportation and Acting Administrator, Federal Aviation Administration, U.S. Department of Transportation, Washington, DC*

Jim Tymon, *Executive Director, American Association of State Highway and Transportation Officials, Washington, DC*

Veronica Vanterpool, *Acting Administrator, Federal Transit Administration, Washington, DC*

* Membership as of May 2024.

TRANSIT COOPERATIVE RESEARCH PROGRAM

TCRP RESEARCH REPORT 247

**Assessing Lifecycle and Human Costs
of Bus Operator Workstation
Design and Components**

Songlin Wu
Eunsik Kim
Andris Freivalds
Yiqi Zhang
Matthew Parkinson
PENN STATE UNIVERSITY
University Park, PA

Subject Areas

Public Transportation • Safety and Human Factors • Vehicles and Equipment

Research sponsored by the Federal Transit Administration in cooperation with the American Public Transportation Association

NATIONAL
ACADEMIES

Sciences
Engineering
Medicine

 TRANSPORTATION RESEARCH BOARD

2024

TRANSIT COOPERATIVE RESEARCH PROGRAM

The nation's growth and the need to meet mobility, environmental, and energy objectives place demands on public transit systems. Current systems, some of which are old and in need of upgrading, must expand service area, increase service frequency, and improve efficiency to serve these demands. Research is necessary to solve operating problems, adapt appropriate new technologies from other industries, and introduce innovations into the transit industry. The Transit Cooperative Research Program (TCRP) serves as one of the principal means by which the transit industry can develop innovative near-term solutions to meet demands placed on it.

The need for TCRP was originally identified in *TRB Special Report 213—Research for Public Transit: New Directions*, published in 1987 and based on a study sponsored by the Urban Mass Transportation Administration—now the Federal Transit Administration (FTA). A report by the American Public Transportation Association (APTA), *Transportation 2000*, also recognized the need for local, problem-solving research. TCRP, modeled after the successful National Cooperative Highway Research Program (NCHRP), undertakes research and other technical activities in response to the needs of transit service providers. The scope of TCRP includes various transit research fields including planning, service configuration, equipment, facilities, operations, human resources, maintenance, policy, and administrative practices.

TCRP was established under FTA sponsorship in July 1992. Proposed by the U.S. Department of Transportation, TCRP was authorized as part of the Intermodal Surface Transportation Efficiency Act of 1991 (ISTEA). On May 13, 1992, a memorandum agreement outlining TCRP operating procedures was executed by the three cooperating organizations: FTA; the National Academies of Sciences, Engineering, and Medicine, acting through the Transportation Research Board (TRB); and APTA. APTA is responsible for forming the independent governing board, designated as the TCRP Oversight and Project Selection (TOPS) Commission.

Research problem statements for TCRP are solicited periodically but may be submitted to TRB by anyone at any time. It is the responsibility of the TOPS Commission to formulate the research program by identifying the highest priority projects. As part of the evaluation, the TOPS Commission defines funding levels and expected products.

Once selected, each project is assigned to an expert panel appointed by TRB. The panels prepare project statements (requests for proposals), select contractors, and provide technical guidance and counsel throughout the life of the project. The process for developing research problem statements and selecting research agencies has been used by TRB in managing cooperative research programs since 1962. As in other TRB activities, TCRP project panels serve voluntarily without compensation.

Because research cannot have the desired effect if products fail to reach the intended audience, special emphasis is placed on disseminating TCRP results to the intended users of the research: transit agencies, service providers, and suppliers. TRB provides a series of research reports, syntheses of transit practice, and other supporting material developed by TCRP research. APTA will arrange for workshops, training aids, field visits, and other activities to ensure that results are implemented by urban and rural transit industry practitioners.

TCRP provides a forum where transit agencies can cooperatively address common operational problems. TCRP results support and complement other ongoing transit research and training programs.

TCRP RESEARCH REPORT 247

Project G-17
ISSN 2572-3782
ISBN 978-0-309-70985-9

© 2024 by the National Academy of Sciences. National Academies of Sciences, Engineering, and Medicine and the graphical logo are trademarks of the National Academy of Sciences. All rights reserved.

COPYRIGHT INFORMATION

Authors herein are responsible for the authenticity of their materials and for obtaining written permissions from publishers or persons who own the copyright to any previously published or copyrighted material used herein.

Cooperative Research Programs (CRP) grants permission to reproduce material in this publication for classroom and not-for-profit purposes. Permission is given with the understanding that none of the material will be used to imply TRB, AASHTO, APTA, FAA, FHWA, FTA, GHSA, or NHTSA endorsement of a particular product, method, or practice. It is expected that those reproducing the material in this document for educational and not-for-profit uses will give appropriate acknowledgment of the source of any reprinted or reproduced material. For other uses of the material, request permission from CRP.

NOTICE

The research report was reviewed by the technical panel and accepted for publication according to procedures established and overseen by the Transportation Research Board and approved by the National Academies of Sciences, Engineering, and Medicine.

The opinions and conclusions expressed or implied in this report are those of the researchers who performed the research and are not necessarily those of the Transportation Research Board; the National Academies of Sciences, Engineering, and Medicine; or the program sponsors.

The Transportation Research Board does not develop, issue, or publish standards or specifications. The Transportation Research Board manages applied research projects which provide the scientific foundation that may be used by Transportation Research Board sponsors, industry associations, or other organizations as the basis for revised practices, procedures, or specifications.

The Transportation Research Board; the National Academies of Sciences, Engineering, and Medicine; and the sponsors of the Transit Cooperative Research Program do not endorse products or manufacturers. Trade or manufacturers' names or logos appear herein solely because they are considered essential to the object of the report.

Published research reports of the

TRANSIT COOPERATIVE RESEARCH PROGRAM

are available from

National Academies Press
500 Fifth Street, NW, Keck 360
Washington, DC 20001

(800) 624-6242

and can be ordered through the Internet by going to
<https://nap.nationalacademies.org>

Printed in the United States of America

NATIONAL ACADEMIES

Sciences
Engineering
Medicine

The **National Academy of Sciences** was established in 1863 by an Act of Congress, signed by President Lincoln, as a private, non-governmental institution to advise the nation on issues related to science and technology. Members are elected by their peers for outstanding contributions to research. Dr. Marcia McNutt is president.

The **National Academy of Engineering** was established in 1964 under the charter of the National Academy of Sciences to bring the practices of engineering to advising the nation. Members are elected by their peers for extraordinary contributions to engineering. Dr. John L. Anderson is president.

The **National Academy of Medicine** (formerly the Institute of Medicine) was established in 1970 under the charter of the National Academy of Sciences to advise the nation on medical and health issues. Members are elected by their peers for distinguished contributions to medicine and health. Dr. Victor J. Dzau is president.

The three Academies work together as the **National Academies of Sciences, Engineering, and Medicine** to provide independent, objective analysis and advice to the nation and conduct other activities to solve complex problems and inform public policy decisions. The National Academies also encourage education and research, recognize outstanding contributions to knowledge, and increase public understanding in matters of science, engineering, and medicine.

Learn more about the National Academies of Sciences, Engineering, and Medicine at www.nationalacademies.org.

The **Transportation Research Board** is one of seven major program divisions of the National Academies of Sciences, Engineering, and Medicine. The mission of the Transportation Research Board is to mobilize expertise, experience, and knowledge to anticipate and solve complex transportation-related challenges. The Board's varied activities annually engage about 8,500 engineers, scientists, and other transportation researchers and practitioners from the public and private sectors and academia, all of whom contribute their expertise in the public interest. The program is supported by state transportation departments, federal agencies including the component administrations of the U.S. Department of Transportation, and other organizations and individuals interested in the development of transportation.

Learn more about the Transportation Research Board at www.TRB.org.

COOPERATIVE RESEARCH PROGRAMS

CRP STAFF FOR TCRP RESEARCH REPORT 247

Waseem Dekelbab, *Deputy Director, Cooperative Research Programs*
Gwen Chisholm Smith, *Manager, Transit Cooperative Research Program*
Stephan A. Parker, *Senior Program Officer (retired)*
Stephanie Campbell-Chamberlain, *Senior Program Assistant*
Natalie Barnes, *Director of Publications*
Heather DiAngelis, *Associate Director of Publications*
Claire Aelion-Moss, *Editor*

TCRP PROJECT G-17 PANEL

Field of Administration

Roland Cordero, *Foothill Transit, West Covina, CA (Chair)*
Jack Dennerlein, *Boston University, Boston, MA*
Shawn M. Donaghy, *C-TRAN, Vancouver, WA*
Danielle Julien, *Amalgamated Transit Union, Local 1576, Everett, WA*
Rodney P. Massman, *Missouri Public Service Commission, Columbia, MO*
David L. Mayer, *Washington Metrorail Safety Commission (WMSC), Washington, DC*
Raymond J. Melleady, *United Safety & Survivability, Exton, PA*
Brian L. Sherlock, *Amalgamated Transit Union, Silver Spring, MD*


FOREWORD

By **Gwen Chisholm Smith**
Staff Officer
Transportation Research Board

This is a toolkit for predicting the long-term safety and health performance of bus operator workstations. The toolkit allows a user to (1) assess bus operator workstation options available and (2) estimate the percentages of driver populations who will be accommodated by a candidate vehicle design. These assessments provide insight into what changes might improve short- and long-term performance, comfort, safety, and health of bus drivers. This report will be of immediate use to safety regulators, transit vehicle operators, risk and safety managers, chief engineers, directors of maintenance at transit agencies who oversee specifications for procurements, human resources departments, writers of specifications for contracted services, manufacturers, and suppliers.

Time loss at public transportation agencies is significantly higher than the average U.S. working population, and human costs are considerable. Musculoskeletal problems, such as low back, wrist, elbow, and shoulder pain, are endemic in public transportation. Significant changes have been made in the designs of critical systems for bus operator workstations, such as seats, pedals, and steering. This report considers the effect of bus drivers' body dimensions and postural preferences and their interaction with bus cab spatial layouts. The information may help the public transportation industry understand, evaluate, and implement options to improve operator health while reducing time loss, injury, disability, and external liability.

The objective of TCRP Project G-17 was to assess bus operator workstation technologies that improve bus operator health and well-being and reduce external risk. This research supplements the work of *TCRP Report 25: Bus Operator Workstation Evaluation and Design Guidelines* and *TCRP Report 185: Bus Operator Workstation Design for Improving Occupational Health and Safety*, covering progress in the design of seats, steering, pedals, and controls where significant advances have been shown to reduce injuries, reduce costs, and improve safety performance.

Led by Mathew Parkinson and coinvestigators Songlin Wu, Eunsik Kim, Andris Freivalds, and Yiqi Zhang of Penn State University and based on direction from the project panel, the research team focused on the features of the workstation that most improve health, well-being, and performance, considering the attributes of the bus operator population. The research team considered:

- relative health and turnover rate of current bus operator populations (compared to other occupations)
- features of the workstation that would most improve health, well-being, and performance, considering the attributes of the bus operator population
- components in isolation and in the context of the workstation envelope
- performance implications to the safe and efficient operation of the vehicle (e.g., dwell time and customer service implications)

This report describes the methods used; an accompanying “Bus Accommodation” Excel tool to estimate what percentage of a bus driver population is accommodated by a candidate bus workstation design is available on the National Academies Press website (nap.nationalacademies.org) by searching for *TCRP Research Report 247: Assessing Lifecycle and Human Costs of Bus Operator Workstation Design and Components*.



CONTENTS

1	Chapter 1 Introduction
1	1.1 Design for Human Variability
1	1.2 Anthropometry
2	1.3 Accommodation
2	1.4 Body Dimensions
3	1.5 Postural Preference
4	1.6 Vehicle Packaging
4	1.7 Research Overview
5	Chapter 2 Literature Review
5	2.1 Vehicle Packaging
10	2.2 Manikin Approach
12	2.3 Population Model Approach
13	2.4 Hybrid Approach
18	Chapter 3 Bus Operator Posture and Associated Risk of CTDs
18	3.1 Background
18	3.2 Research Activities
22	3.3 Results
25	Chapter 4 Bus Packaging Methods
25	4.1 Model Selection
27	4.2 Cascade Model for Buses
36	4.3 Bus Driver Population
42	Chapter 5 Bus Packaging Results
42	5.1 Steering Wheel
46	5.2 H-Point
48	5.3 Eye Point
51	5.4 Overall Accommodation
52	5.5 Other Body Landmarks
52	5.6 “Average” Driver
57	5.7 RULA
59	Chapter 6 Discussion and Bus Packaging Software Tools
59	6.1 Observation and Reflection
60	6.2 Cascade Model Overview
60	6.3 Applications
60	6.4 Limitations and Future Work
63	References
68	Appendix A Data Processing in Excel
71	Appendix B U.S. Bus Driver Demographics



CHAPTER 1

Introduction

The objective of this project was to create an easy-to-use toolkit for predicting the long-term safety and health performance of bus operator workstations. The toolkit helps assess the effects of operator size and shape, workstation geometry, and vehicle technologies. These assessments are performed through a process called virtual fit testing (VFT), where thousands of virtual users' interactions with the bus operator workstation is simulated.

The success of designs intended for human use is determined by a wide range of factors, such as safety, aesthetics, effectiveness, portability, and cost. Although one factor may be the driving force for a specific design, the impact of each factor requires a significant amount of research and is its own field of study (11). Through theoretical analysis and practical experiment, researchers explore how each factor contributes to the overall outcome. As many industries become more transparent, companies are evolving to meet shifting needs; among these are user-centric elements such as human variability.

1.1 Design for Human Variability

Design for human variability (DfHV) considers the inherent variability in the target user population during the creation of designed artifacts. Several factors influence this variability, including when and where someone is born, cultural background, family atmosphere, and religion (12). Other factors such as sex, race, ethnicity, and age can dramatically impact how humans act, react, and interact (13). DfHV is the practice of designing artifacts, tasks, and environments that are robust to the variability in their users. This requires clearly defining the user population and understanding attributes that affect their interaction with the design.

1.2 Anthropometry

Anthropometry, one of the major fields of research in human variability, is a systematic and statistical study of the measurements and proportions of the human body. A combination of these measurements and proportions describes the size and shape of a human body, which makes individuals unique (14). There are many ways to categorize anthropometric variables. One common way is to distinguish them as length-related variables, such as stature, trochanter height (leg length), and hand length, and width-related variables, such as hip breadth, calf circumference, and chest breadth. Intuitively, taller people are expected to be wider than their shorter counterparts. This inference is usually true; however, there are exceptions due to human variability. For instance, the width of a human body is not only an indicator of its size, it can also be a measure of obesity. In this case, body width is independent of body length. Therefore, careful consideration is required to choose the most appropriate anthropometric indicators while making design decisions.

2 Assessing Lifecycle and Human Costs of Bus Operator Workstation Design and Components

Anthropometry is commonly considered in industrial practice; anthropometry-focused concepts can be found in vehicle packaging, furniture designs, sport equipment innovation, and clothing design. The expectation of this practice is to achieve a greater outcome while minimizing cost so the final product is effective yet efficient. A poorly designed product can cause discomfort and dissatisfaction in users and result in a decrease in productivity (15). In certain circumstances, it can even put users in life-threatening danger. Thus, designers must diligently study the anthropometry of a target population and use the associated artifacts to guide their designs.

1.3 Accommodation

A good design should accommodate its users so they can perform the required tasks without encountering limitations (3). When a user is accommodated, they will feel safe and comfortable doing physical tasks, which can increase their productivity. In contrast, when a user is disaccommodated—they are unable to interact with the artifact, task, or environment in their preferred manner—their job satisfaction level is generally low, and the likelihood of safety hazards increases significantly (16). In many cases, companies and designers invest resources to achieve a better accommodation level. Practically speaking, perfect accommodation usually does not exist. When designing for a large audience, it usually costs a tremendous quantity of resources to accommodate the users with extreme body dimensions; as a result, companies tend to target the majority rather than all users.

Although most designs are not expected to accommodate every user in the target population, there are times when it is necessary. In competitive indoor and outdoor activities, sports equipment is frequently custom-made for best performance (17). For instance, NBA players are known for their elite performance on a basketball court. Competing with other extraordinary athletes, it is a significant advantage to jump a little higher or change direction a little faster. This pursuit of excellence inspires top shoe companies to take 3D scans of professional athletes' feet and analyze the loading condition on their shoes to design shoes specific to the athlete that enhance their performance (18, 19, 20).

Customized designs can sometimes maximize the performance of a product, but they usually raise the cost significantly. They not only require more design considerations, but also bring challenges to the manufacturing process (17). For instance, many plastic products are formed through injection molding, which is a process of melting and injecting material into a mold. Due to the dimensional precision of the molds, they are expensive to produce. With machine testing and labor cost, it is difficult to justify the cost when only a small quantity of parts is needed (21). Alternatively, additive manufacturing saves on tooling, but requires additional research and time. Because of its layered nature, it may lead to structural failures (22).

1.4 Body Dimensions

Human bodies vary significantly in size and shape, which creates a difficulty in providing universally functional solutions for a population. One of the common approaches to resolve this issue is to create various sizes of a product and let users or retailers determine which size is most suitable for each consumer. Shoes are a great example of this strategy (23). In the United States, shoe sizes are typically designed in increments of 0.5 or 1. With help from the elasticity of the materials, these increments are small enough to accommodate most users (24). One of the greatest advantages of this approach is its simplicity; however, it is not suitable when users desire different sizes. Another approach to accommodating variability is to implement adjustability in product dimensions. For instance, a belt allows the user to adjust the tightness of it around the waist. Instead of having to purchase belts of various sizes, the user only needs one

adjustable one (25). However, the major disadvantage of adjustable components is the increase in complexity of a system, which can cause a higher failure rate (26). An adjustable product also frequently involves a higher part count, which often means higher cost (16).

Analysis of anthropometric data has shown that many anthropometric measurements can be approximated as normal distributions, especially length-related ones, with the majority of the data clustering in the middle and the extremity of the data spreading at the tails (27). In product design, it is neither economical nor realistic to accommodate 100% of the user population due to the large spread of body dimensions. Thus, a design usually aims to accommodate a proportion of the user population (15). In practice, a target percentage of accommodation is pre-selected, 90% for instance, and serves as an assessment goal for the final product. Users who are disaccommodated can sometimes still achieve compromised comfort by adjusting their posture.

In other cases, however, disaccommodation may lead to safety hazards. Such phenomena exist throughout the world but are more common in developing countries because resources are more limited. Agriculture plays an important role in northern China's economy, and large machines are used to reduce the amount of manual work. If a worker has a difficulty operating these machines due to physical limitations, the probability of injury is much higher. In fact, a study observed a 13.1% prevalence of machinery-related injuries from the surveyed agricultural workers due to machine sizes and other limitations (28). A similar point can be made in vehicle interior design. Failure to reach the instruments to operate a vehicle or inability to maintain an adequate field of view are associated with car accidents (29). Therefore, designers and engineers must ethically investigate the consequences of disaccommodation before making design decisions.

1.5 Postural Preference

Human interaction is not only impacted by the physical dimensions of the human body but also by a user's postural preference. Postural preference is unique and can be dramatically different from person to person (30). For instance, the purpose of a chair is to provide a sturdy seating surface that supports the user. However, the action of sitting is very complex. Given a standard chair, some like to lean backward, some like to cross their legs, some prefer to sit high, some do not use the armrests (31). Assessment of success is no longer limited to the fundamental purpose of a chair, but rather the capability to accommodate the postures of as many users as possible to provide the most comfort.

Collecting data on postural preference can be a costly process because it requires user participation, which involves experiment design, user testing, data collection, and user feedback. In many cases, the size of a testing group is critical to an unbiased solution. With a small testing group, extreme behaviors are sometimes magnified and can be overanalyzed, which can lead to biases (32). The testing group must also represent the actual user population in terms of demographic descriptors, such as male-female ratio, age, race, and ethnicity. Thus, doing market research in preparation for any postural experiment is essential (33, 34).

Occasionally, postural preference can be transferable across products when the two products are used in a similar way, but careful consideration needs to be given to the risk of oversimplifying the problem (35). For example, ice skates and running shoes are comparable in shape and are worn similarly, but they serve different purposes. Ice skates must be stiff enough to protect users from twisting their ankles, but running shoes need to provide shock absorption and comfort, which is why new products usually need to run their own user interaction experiment. Unlike interaction preference, physical dimensions of a human body usually only need to be measured once. These dimensions can be simulated in space using software to display results in dimensional fitting (36).

4 Assessing Lifecycle and Human Costs of Bus Operator Workstation Design and Components

1.6 Vehicle Packaging

The knowledge of spatial dimension and postural preference is useful in many fields of design, especially vehicle packaging. As defined by Roe, vehicle packaging is a subject that studies a vehicle's interior spacing and components layout for the purpose of providing safety, spatial accommodation, and comfort to drivers and passengers (27). Of all the components inside a vehicle, the two most critical in this work are the steering wheel and driver's seat, because they determine the driver's capability to operate the vehicle (37). By the definition of accommodation, drivers must be able to adjust these two components without encountering any limitations to comfortably turn the steering wheel and step on the accelerator pedal or the brake pedal. One other consideration is driving safety (3). While operating a vehicle, drivers must maintain awareness of the surrounding traffic to make proper decisions (8). The goal of vehicle packaging is to scientifically design vehicle layouts to accommodate driver anthropometry so that both spatial fit and driver field of view can be achieved.

1.7 Research Overview

Driving trucks and buses is a physically demanding occupation that carries one of the highest injury rates of major occupational categories in the United States. Drivers often work in postures that increase risk of low back pain and other musculoskeletal disorders, slow their response time, and put them at increased risk for acute injuries due to crashes. Poor exterior visibility for drivers also increases the risk to other drivers, pedestrians, and workers. This report investigates bus cab spatial layouts and considers the effect of bus drivers' body dimensions and postural preferences.

Literature Review

Human variability exists in various forms. Such variability is responsible for a broad spectrum of user responses to one solution, and it multiplies the ambiguity in the design process (38). In some cases, users give dissimilar or even conflicting feedback, which pulls the design in opposite directions (34). In vehicle packaging, for instance, drivers vary in body dimensions and have different driving postures. The ideal situation is to design a vehicle package that allows all drivers to safely and comfortably perform all driving tasks without encountering any limitation; however, such high expectation of accommodation requires large adjustment ranges that are not always achievable due to cost, safety, and the desire to reduce vehicle size (3). While packaging a vehicle, all these factors must be considered, and compromises need to be made to find the best possible solution based on these considerations and accommodation possibilities.

This chapter introduces the concept of vehicle packaging and reviews design objectives that are used to measure success. It also presents several approaches that have been developed to design for human variability and discusses the advantages and disadvantages of each.

2.1 Vehicle Packaging

Vehicle packaging is designing the interior layout of a vehicle with the goal of achieving a certain level of accommodation (27). It involves a broad range of design considerations that determine whether the fundamental driving components, such as the pedals and the steering wheel, are within reach (3). Further design considerations include button controls, digital displays, and other elements the driver interacts with. In the automotive industry, designing for vehicle interior layout is one of the first steps, after the body exterior contour design and window openings design (3). Besides spatial fitting, safety-related vision requirements are crucial factors to provide accommodation and comfort for drivers (27).

The transportation industry has been evolving, and this trend is not slowing down. The demand for vehicles for uses other than daily commuting has increased greatly and the variety of vehicle class divisions has also multiplied as vehicles of different shapes are developed to suit societal needs (39). Categorizing by interior volume and gross weight, the three major classes are car class (various sizes of compacts, sedans, and wagons), sport utility vehicles (SUVs; various sizes of crossovers and SUVs, and minivans), and trucks (mid- and full-size regular/extended/crew) (40). Vehicles in each class share a similar shape and similar design objectives. While designing the frame, a number of concerns need to be considered; one of the most important is the field of view. The upper daylight opening (UDLO) is the point where the top of the windshield meets the car frame (Figure 2.1), which limits the angle that drivers can see upward. The upvision requirements are different for different categories of vehicles. Drivers must also maintain sufficient downvision; depending on the driver's eye location, downvision can be limited by either the hood point (a point that represents the tip of the hood) or the cowl point

6 Assessing Lifecycle and Human Costs of Bus Operator Workstation Design and Components

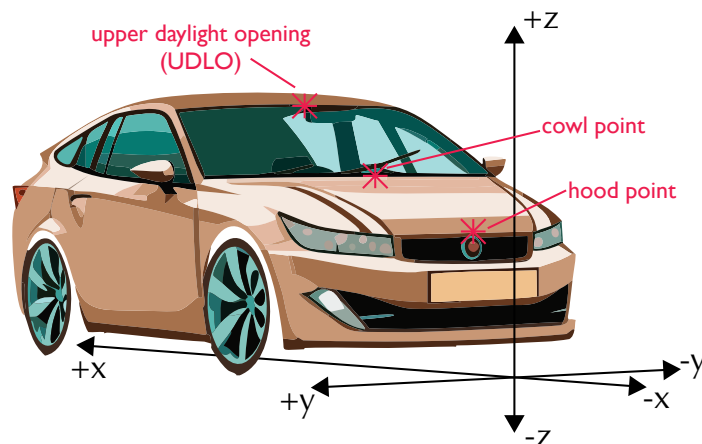


Figure 2.1. The standard reference coordinate planes for vehicle design and packaging (1).

(where the bottom of the windshield meets the hood) (41). These points are commonly measured from the ground in the Z direction and from the accelerator heel point (AHP) in the X direction (Figure 2.3). Although vehicle packaging is a 3D design, only the X-Z plane is studied in this work because the adjustable components of interest, such as the steering wheel and the seat, are designed on the center line on the driver's side. Future work could consider the design objectives in the Y direction.

To properly and efficiently design a vehicle package, understanding human anthropometric variability is key. In general, there are two categories of data involved: conventional static measurements and functional task-oriented measurements. Conventional static measurements are done when subjects are in standardized rigid positions, which typically involve lengths, widths, and circumferences (Figure 2.2). They are the fundamental descriptors of a driver's size and shape, and they do not change due to the driver's posture, unlike the functional task-oriented measurements. These descriptors are the basis of driver-vehicle spatial fitting (27).

Functional task-oriented measurements indicate the driver's ability to perform certain tasks, and they can vary among drivers—even among those with similar body dimensions. These are

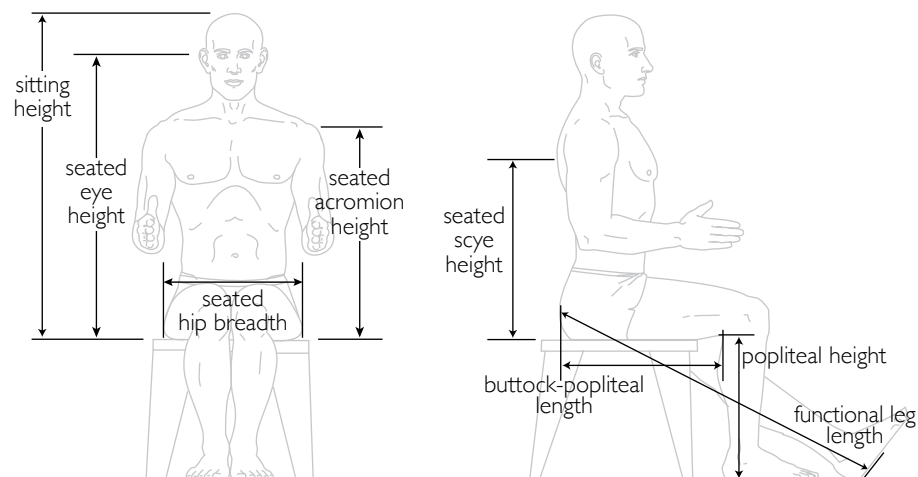


Figure 2.2. Typical seated anthropometric measures.

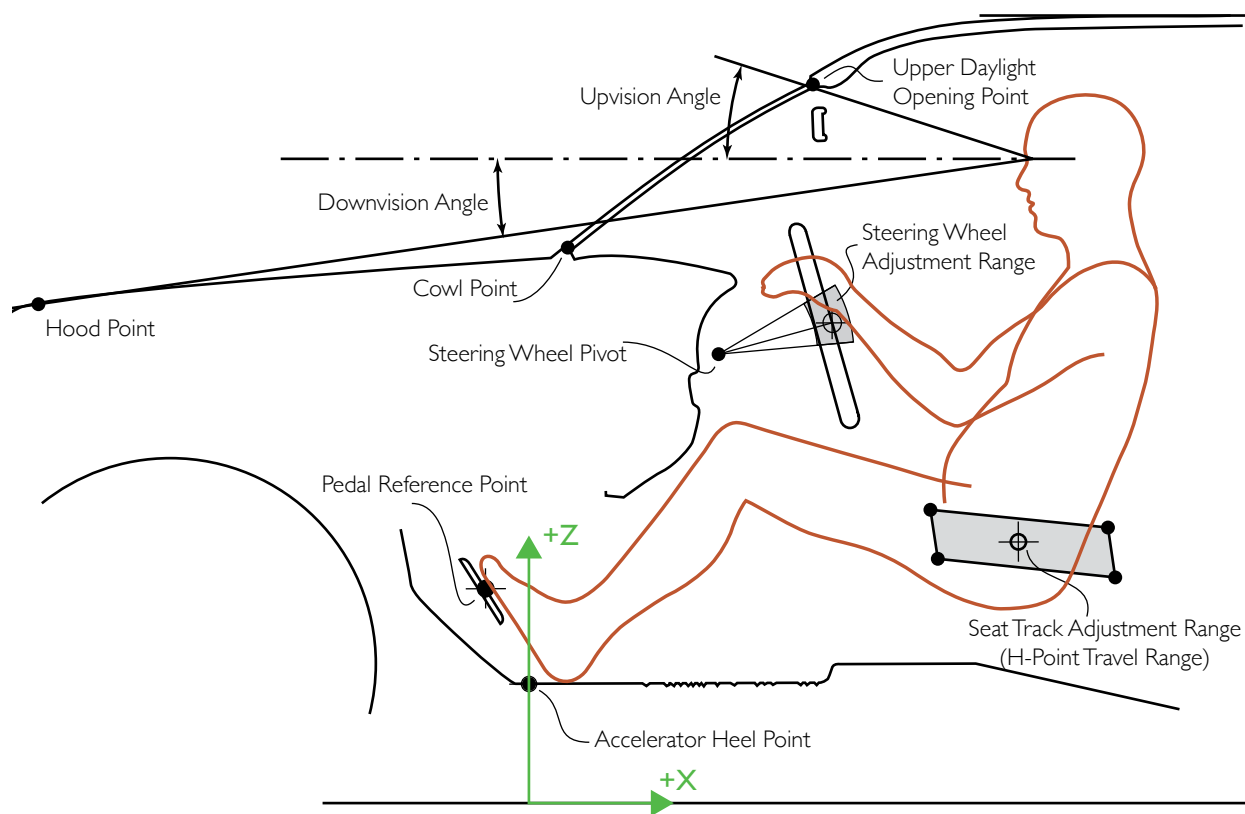


Figure 2.3. *The dimensions and reference locations used in 2D vehicle packaging.*

a function of body segment parameters, strength, and range of motion and include things like reach envelopes and manipulation zones. Vehicle packaging is a complex task: a cab needs to be designed such that drivers not only fit in it, but are able to perform functional tasks, such as turning the steering wheel.

One of the most important reference points is the AHP, the intersection between the accelerator and the floor. Components of vehicle frame geometry (roof, UDLO, cowl point, hood point, etc.) are measured from the ground in the Z direction and from the AHP in the X direction. This reference system works for these components, but is unsuitable for the interior components, such as the seat and the steering wheel, because there is not a direct way of measuring them from the ground. The difficulty of measuring interior components from the ground causes inaccuracy in these measurements. Instead, these interior components are measured from the AHP, since the AHP is a fixed distance from the ground (1). In vehicle packaging research, the AHP is commonly referred to as the origin of the system; this report follows that convention to refer to interior measurements.

When designing the interior layout of a vehicle, it is important to understand each component and its contribution to the overall accommodation. In most vehicles, the steering wheel can tilt around a pivot point, and some can telescope in and out (Figure 2.3). Ideally, a driver's preferred steering wheel location should fall within the adjustment envelope. In that case, that aspect of driver preference is considered accommodated. If the preferred location lies outside the envelope, the location preference is not accommodated, and the driver would compromise by adjusting the steering wheel center to the nearest point on the envelope. Although the driver cannot obtain the most desirable steering wheel location, they can often achieve moderate comfort by adjusting the rest of their body to adapt (37).

8 Assessing Lifecycle and Human Costs of Bus Operator Workstation Design and Components

Another adjustable component is the seat. Most seats can move in the fore-aft direction (i.e., horizontally toward the front and rear of the vehicle). For large vehicles, such as trucks and buses, the seat can also move vertically. The adjustment envelope is a rectangle (Figure 2.3), and the goal is to design a seat adjustment envelope to accommodate the majority of drivers. If a driver's preferred seat position lies outside the envelope, they will adjust the seat to the nearest point on the envelope, as with the steering wheel adjustment (42). Once the locations of the most critical components, steering wheel and seat, are determined, an assessment on eye location can be conducted. Although eye location is rarely a concern of spatial fitting, it is an important consideration in vehicle packaging because it determines the driver's field of view, which is directly related to driving safety (3). Previous research has found success in estimating drivers' eye locations as an elliptical model (41), which can be a useful tool to assess vehicle layout reference points, such as cowl point, hood point, and UDLO. This report explicitly studies eye locations, together with steering wheel and seat locations.

In vehicle packaging, the results of accommodation are usually expressed as a percentage. An accommodation rate can be defined as the proportion of the driver population able to meet the spatial fitting requirements and safety requirements (27). For instance, a seat adjustment envelope can be designed to accommodate 95% of the population and implies that 95% of drivers can move the seat to their desired location without encountering any limits, while 5% cannot. The assessment of one objective is intuitive, but the design task becomes challenging when more than one component is adjustable. Therefore, it is important to first distinguish a multivariate problem from a univariate problem (43).

2.1.1 Univariate and Multivariate Analyses

Univariate analysis has guided vehicle packaging practice for over 50 years (44, 45). However, some of the limitations of the method have been understood for nearly as long (46, 47). For example, recommendations for seat height adjustment range may be based on the popliteal height of seated operators. Similarly, seat width recommendations are typically based on seated hip breadth (Figure 2.4). The 95th percentile value is the location separating the lower 95% of the distribution from the upper 5%.

In univariate analysis, each workstation dimension is considered independently of the others. In other words, the data under consideration are analyzed and conclusions drawn without considering other factors (48). Using univariate analysis to solve multivariate problems is known to produce inaccurate estimates of accommodation (49). Historically, the univariate data could be

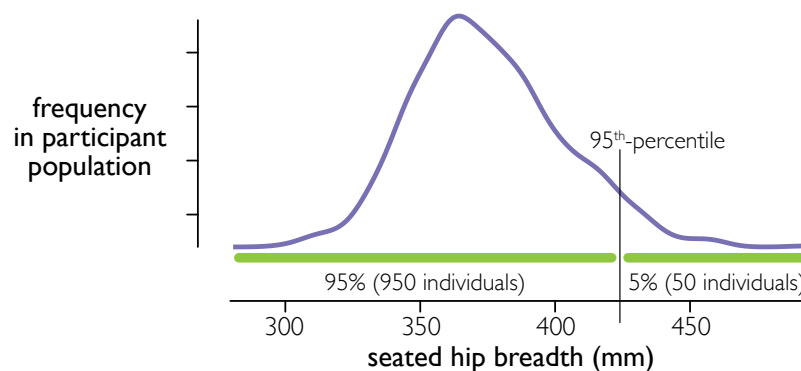


Figure 2.4. The distribution of seated hip breadth for a population of 500 men and 500 women selected randomly from the ANSUR population.

represented in tables and templates. This simplicity of representation coupled with a long tradition of practice may explain the popularity of the method today despite its known problems.

For most design problems, univariate analysis is not sufficient to achieve the overall goal of a specific level of accommodation; Figure 2.5 illustrates this for two dimensions. Since anthropometric measures are not perfectly correlated, accommodating 95% of the population on two dimensions individually will usually not result in accommodating 95% on both. Individuals disaccommodated on one measure are not the same as those disaccommodated on another. For example, when 95th-percentile values of both popliteal height and seated hip breadth are selected, the overall accommodation for this population is 902/1000 people = 90.2%. Note that it is not possible to determine in advance how much the accommodation level will be affected when multiple variables are considered.

When two or more variables are considered simultaneously, many possible designs will achieve the same level of accommodation. In general, decreased accommodation on one dimension can be traded off for increased accommodation on another while maintaining the same overall level of accommodation. Of course, the accommodation level on each dimension must be at least at the target level (for example, 95%). If the selected anthropometric dimensions are fully independent, the disaccommodated fractions are additive. For example, the two variables in Figure 2.5 are nearly independent. Univariate disaccommodation of 5% of the population on hip breadth and 5% on popliteal height results in a total accommodation of just over 90%—only two individuals in this population are disaccommodated on both dimensions. Accommodating 95% of the population on these two uncorrelated dimensions would require disaccommodating no more than approximately 2.5% on each individual dimension.

This principle is true when looking exclusively at anthropometry, but it extends to all aspects of the operator experience. For example, if 10% of operators are disaccommodated based on fore-aft seat location, there is no reason to expect those individuals are the same as those disaccommodated by vision requirements, strength requirements, or limitations due to fatigue.

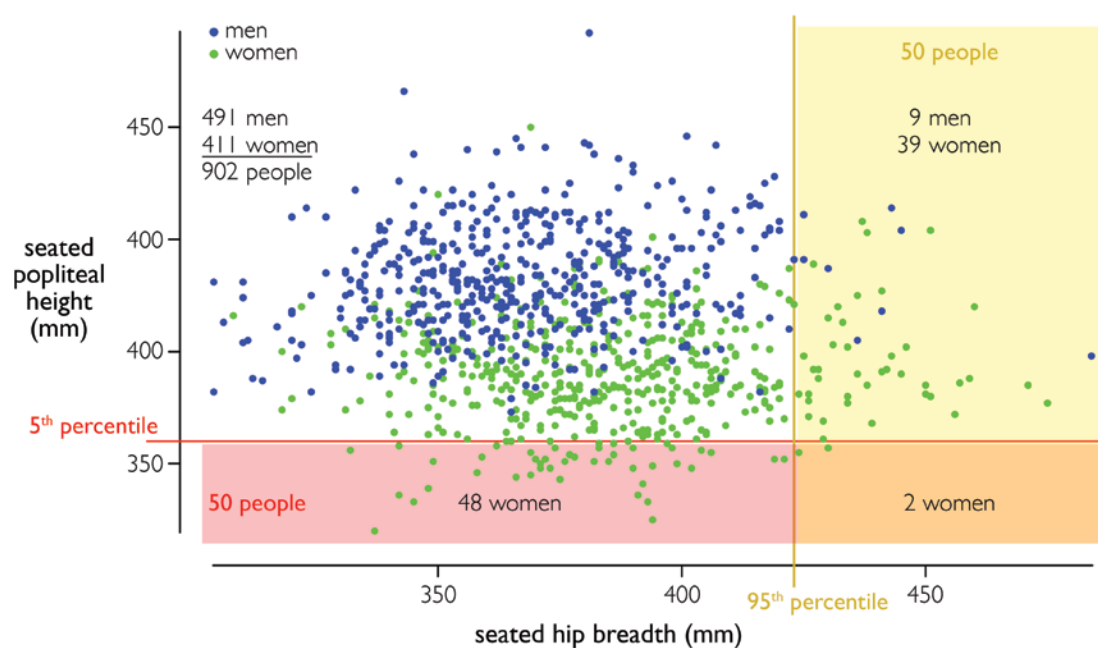


Figure 2.5. The bivariate distribution of seated popliteal height and seated hip breadth for 500 men and 500 women selected randomly from the ANSUR population. The lines show 5th-percentile popliteal height and 95th-percentile hip breadth.

Due to these limitations of univariate analysis, a multivariate approach is the best practice for multivariate design problems such as vehicle packaging. Multivariate analyses allow designers to investigate the accommodation level of a combination of design objectives, which reveals the underlying relationships between the different objectives (50) and provides important information on design decision-making.

2.2 Manikin Approach

The variability in human anthropometry is a difficult subject because human bodies vary in size and shape. However, the randomness in most length- or width-related measures follow a distribution, so statistical tools, such as percentiles, are frequently used. Given a group of people ordered from least to greatest by stature, the 5th percentile is that surpassed by 95% of the group and the 95th percentile is that surpassed by 5% of the group. Using percentiles allows for estimating the proportion of a group that meets a certain requirement and determining design limits (51).

A direct way to apply percentiles is through manikins. Each manikin is built to a unique combination of body dimensions suitable for the design project and used to predict human interaction. To detect design limits, boundary manikins are frequently used to represent the extremes of the population. A design that can accommodate the extremes is expected to accommodate those with less extreme body dimensions. In many cases, a small female and a large male are used to approximate the extremities. For instance, a 2.5th-percentile female manikin and a 97.5th-percentile male manikin are frequently used to assess a 95% accommodation level, assuming female and male body dimensions are approximately normally distributed and male bodies are bigger than female bodies.

A Gaussian or “normal” distribution contains higher-frequency data in the middle and low-frequency data at the tails. Because of the increased density in the central region of a distribution, relatively small amounts of adjustability, properly located, can accommodate large percentages of a population’s preferred design configuration. A similar amount of adjustability focused on the tails of the distribution will yield much lower accommodation rates. Consider Figure 2.6, a probability density plot for stature, a measure that is approximately normally distributed. The total range across these data is 545 mm, but a design that accommodates the central 219 mm (40%) of the data will accommodate 90% of the individuals. For this reason, it is usually most cost-effective to design for the central portion of the distribution. For some design conditions there is no practical limitation on either the lower (seat width; narrower individuals are not disaccommodated) or upper (seat height; taller lengths are not disaccommodated) bound, so the design is limited by one tail or the other, rather than both.

The manikin approach is relatively easy to understand and is easier to implement, but it has certain limitations; one of these is the reliability of manikins. During the approach, each manikin is a percentile model and represents one user with extreme body dimension. Intuitively, a 90th-percentile manikin is expected to be composed of 90th-percentile body segments, but in reality, these segments would add up to be much taller. By accommodating this 90th-percentile manikin, designers assume those with less extreme body dimensions are also accommodated. However, this assumption has major flaws, especially in complex design problems. A design that accommodates the users with extreme body dimensions will not necessarily accommodate all the users in between the extremes, and an n th-percentile individual does not exist (47).

The manikin approach has been applied in various design fields. For instance, a systematic ergonomics study using manikins was conducted on industrial workstation design in 1996 (52). In 1998, a study was conducted on the optimization of viewing angle for touchscreen displays using a similar approach (53). Manikins have been used in the automotive industry as early as 1962. In the late 1950s, the Society of Automotive Engineers (SAE) first proposed the concept

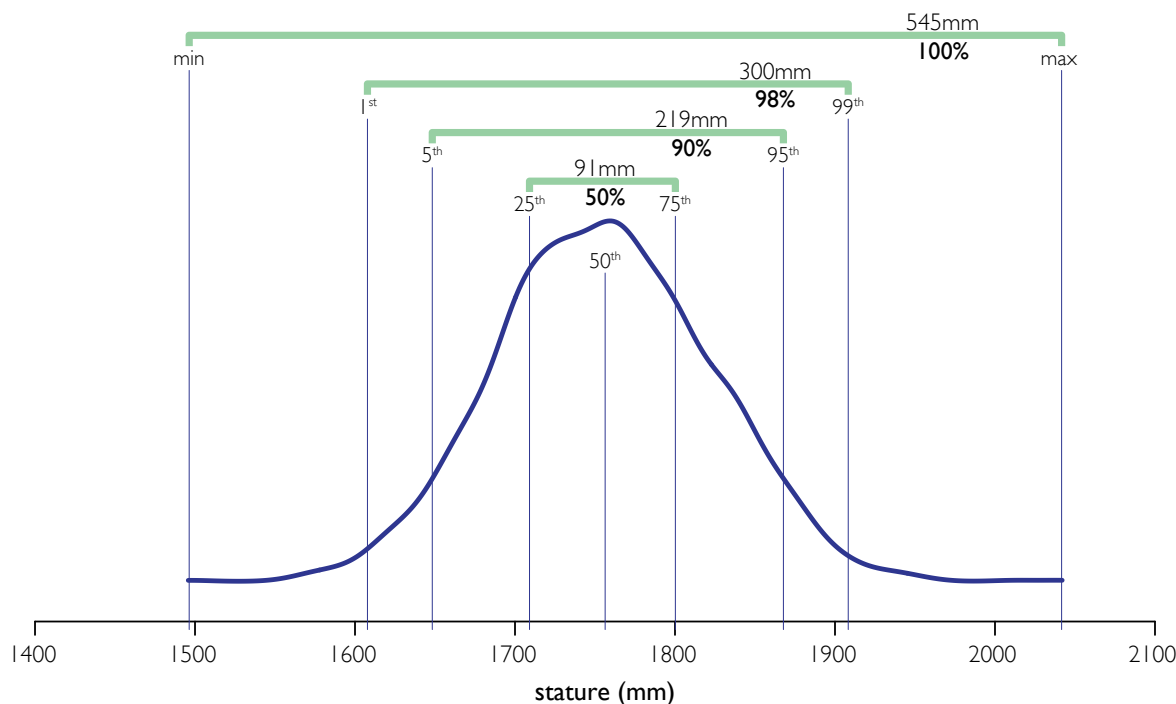


Figure 2.6. A probability density plot showing the distribution of stature. A large percentage of the individuals are captured by a relatively small amount of the total range.

of applying standardized procedures and tools in vehicle packaging and composed J826, which introduced a 2D H-point template to estimate packaging profile and a 3D H-point machine for defining and measuring occupant seating accommodations. This machine, one of the first uses of manikins in the automotive industry, defines the location of the H-point (generally, where a driver's hips would be), which is specific to a seat (42). An update to J826 uses the improved Automotive Seat and Package Evaluation and Comparison Tools (ASPECT) manikin, shown in Figure 2.7 (54).

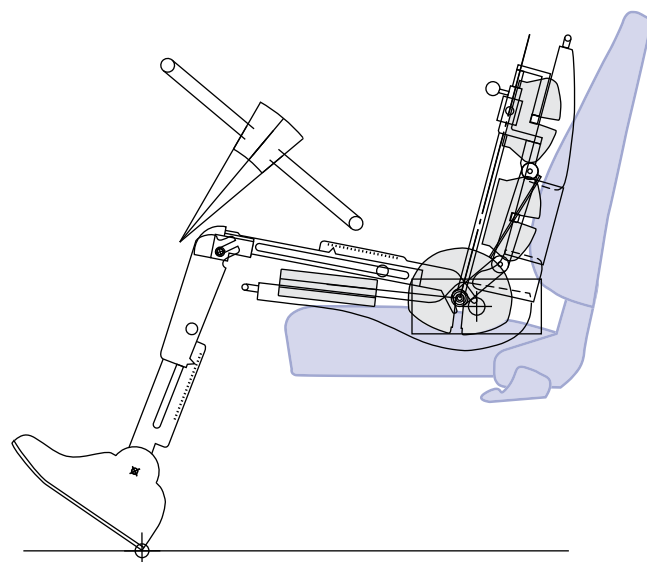


Figure 2.7. The ASPECT manikin.

The manikin approach, or the percentile model, is one of the most commonly used approaches in ergonomic design, and it studies the distribution aspect of anthropometric measurements. The investigation of how an individual relates to a population is its core concept. For example, when designing for a single measure, the 5th and 95th percentile values might be specified as limits. The expectation would be that individuals smaller than the 5th and larger than the 95th percentile would not be able to use the design in the intended manner (55). This simple and intuitive approach remains reliable for most univariate problems. In many design practices, by designing for both the lower extreme user and the upper extreme user, designers assume all the users in the middle are accommodated. This assumption is valid in simple design cases but loses its validity when assessing a full body that consists of multiple measurements. Although statistics and research (including this report) often refer to an “*n*th-percentile user,” such a person does not really exist, because of human variability. There are countless measurements to define a human body, and it is impossible to find one person who is *n*th percentile on every single measurement (56).

Manikins are frequently used in vehicle packaging to simulate how a user would interact with the main components in a vehicle based on body anthropometry. It is a simple and visual way to assess multivariate accommodation, but it has major flaws. Specifically, driving posture plays a critical role in vehicle packaging, but it is not considered in the manikin approach (57). In practice, designers often posture the manikins manually based on either personal intuition or a standardized procedure, which poorly quantifies human postural variability. In order to solve this bias, several methods with a focus on posturing were developed.

2.3 Population Model Approach

The manikin approach provides a visual and intuitive way to estimate user interaction under the assumptions given in section 2.2, but it cannot provide knowledge on human posturing. The population model approach, on the other hand, directly investigates the interaction between users and a design. This approach first identifies a sample group, then conducts a human interaction experiment for this group and establishes a model based on the results. This model is then applied to the user population so a certain percentage of the population can be accommodated (57).

Unlike the manikin approach, which simulates a percentile-based user who frequently represents an extremity, the population model approach targets the actual users. To lower the cost of the design, a sample group, rather than the entire population, is commonly selected for an experiment or a focus study. Although there are advantages to reducing the size of the sample group, it must be relatively large to ensure it can adequately represent the target user. Certain traits could be magnified when the group is small, which could lead to biases. In addition, a random sampling method must be used; this is essential to the validity of the results (27).

During the experimental study with the sample group, participants are frequently invited to interact with a robust prototype that provides an excessive range of adjustment, and their responses are recorded and analyzed. Due to the interactive nature of the population model and its use of prototypes, it is frequently used in product design. For instance, a research group used a 3D laser scanner to measure standoff distance between the head and the back of the helmet of a representative sample group of 30 participants. This information was used to guide future ballistic helmet design (58). Similarly, a study was conducted using a population model approach to determine the optimal grip span with respect to hand anthropometry. During the process, a total of 12 participants were invited to interact with the hand-grip device (59).

In order to study postural preferences through a population model approach, participation from a large number of randomly sampled drivers is required. While each participant is in a testing environment, a tracking system can be used to continuously monitor the location of the body landmarks of interest. The relative spatial locations of these landmarks show the subject's

body configuration, which indicates their postural preference, and the absolute spatial locations determine whether the subject is accommodated by the vehicle layout or not.

There are many examples of the population model being applied in the automotive industry. In a study published by the University of Michigan Transportation Research Institute (UMTRI) in 2017, a statistical body shape model was used for seated vehicle occupants to study their driving preference. This reliable model was established from 147 participants. The data of various seating postures was captured with a laser scanner together with manually measured body landmarks (60). There are many more applications of the population model approach in the SAE as it is one of the fundamental concepts in the SAE International recommended practices (61).

2.4 Hybrid Approach

Although the population model approach shows improvement from the manikin approach by considering postural preferences, it still has several limitations that cannot be ignored. The most important one is that the population model can only be applied to one single design case. Since the sample group is selected from the user population, this model is limited to that user population and can only be applied in an identical design case, which rarely happens in real life. Even when designing the same product for a slightly different user population, the entire process must be repeated. An adequately large group needs to be sampled randomly, and participants have to participate in the accommodation experiment individually, after which data can be analyzed. The process of creating a valid model this way is time-consuming and costly. It would be more efficient to be able to reuse the previous data.

To conquer the issues with the population model, a hybrid approach was developed. The hybrid approach merges the strengths of the postural preference model and the anthropometry-configurable manikins (57). The goal is to confidently apply the same model to a different user population, so a quantitative relationship must be found that relates the desired outcome to anthropometric measurements. These anthropometric measurements serve as predictors of the model. When applying the model to a different user population, anthropometric measurements can be modified to best match the new user population, and the results from the hybrid model are adjusted accordingly.

By diligently collecting data and interpreting the underlying relationships, researchers have found success in the hybrid model. For example, a group of researchers used an adjustable bicycle simulator to assess comfort level on bicycles and validate commercial bicycle accommodation. To do so, they performed correlation analysis on preferred bicycle dimensions and body anthropometric measurements and found that saddle-pedal distance is strongly related to crotch height (62). A similar approach, relating outcome variables with anthropometric measurements, can be found in the Yakou et al. study on evaluation of cylindrical objects, which examines handle diameter and hand length (63).

2.4.1 Virtual Fit Testing

The most accurate assessment of the level of accommodation provided by a design would be obtained by having a large population of individuals representative of the target user population interacting with a high-fidelity physical prototype. Because such testing is generally not feasible due to cost and time requirements, virtual fit testing (VFT) can be conducted using abstract representations of individuals suitable for computational evaluation. In a traditional application of anthropometric data, only summary statistics for each variable across the population would be used. The interactions among the various variables are not considered in this approach. In contrast, VFT examines each individual and their simulated interaction with the design, then computes the fraction of the total population that is accommodated.

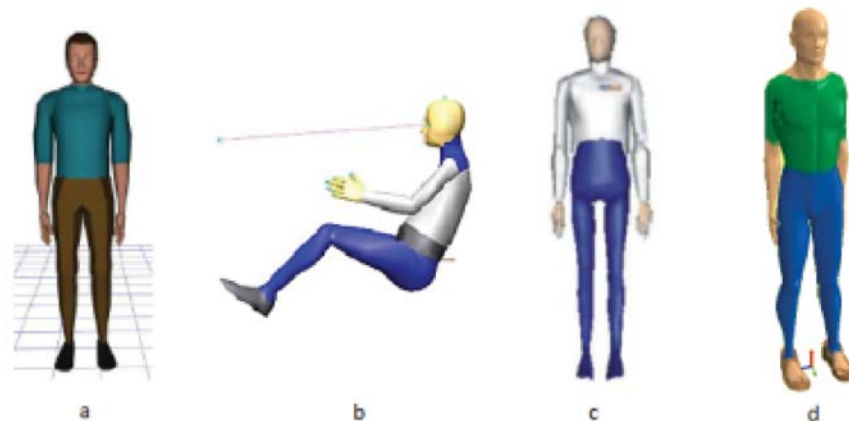


Figure 2.8. A sampling of four digital human models: Jack (a), RAMSIS (b), HumanCAD (c), and 3DSSPP (d) (2).

Digital human models (DHMs) are one strategy for conducting virtual fits. They were developed in the 1990s to virtually represent humans as an improvement to the manikin approach. Since then, DHMs have increasingly been used for vehicle packaging and other ergonomics design (64). Since the creation of DHMs, they have been widely used for task performance simulation. One of their advantages is the facilitation of a quicker design process (36). With the development of computers, DHMs can be an important part of product design and provide insights on product usability (65). Instead of competing on money investment, companies shift their focus to engineering research and computing power. Figure 2.8 shows the DHMs generated in four different software tools.

Using DHMs, designers can visually assess the fit of all interior components and make appropriate adjustments to improve overall accommodation (Figure 2.9). While DHMs produce useful visualizations and the opportunity to simultaneously consider a number of measures, there are also limitations. In particular, each model only represents one user and one of their associated preferences (e.g., posture). Since each model requires meaningful amounts of time to place and posture, the use of more than a few manikins is rare.

Improvements to the VFT approach can be made by using large numbers of manikins. For example, Figure 2.10 is the result of analyses from a study assessing posturing and fit involving 23 SAE Class B truck drivers in several different truck and bus cabs (66). The four panels show a cross section of the workstation. The green stick figure shows the anthropometry and as-measured posture for that individual. The other dots show estimated preferred location for 100 individuals

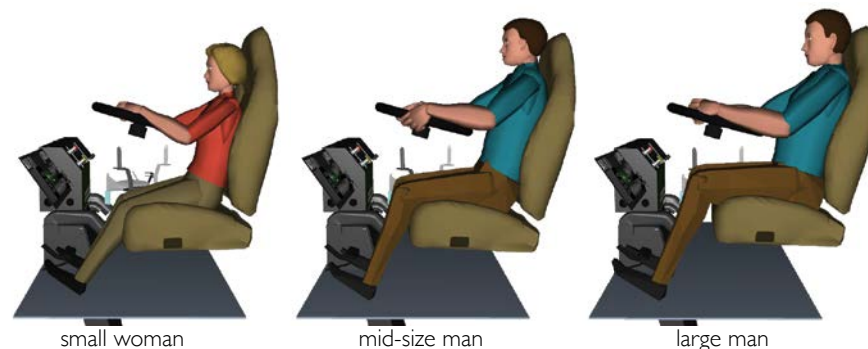


Figure 2.9. Package assessment via three virtual fit tests conducted using digital human models of various sizes.

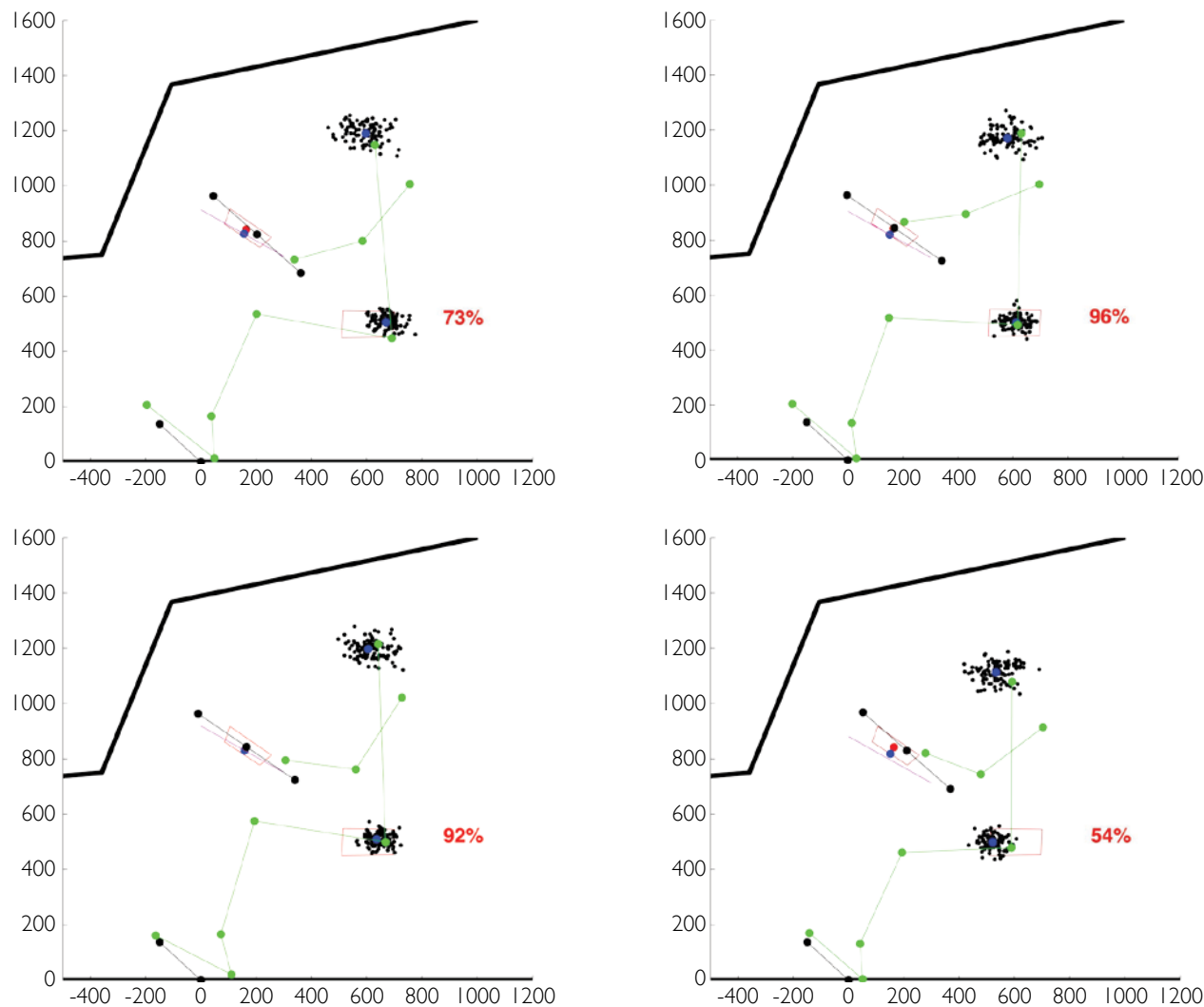


Figure 2.10. Each pane shows a postured individual and their preferred component locations in the vehicle package. The simulated distribution of locations for 99 additional participants of that same size and shape as well as the overall accommodation rate are also shown.

of that same size and shape. The blue dot shows the centroid or average behavior for each location (seat, steering wheel, and eye). Based on those analyses, the likelihood of accommodation for an individual of that size and shape is shown. This ranges from 54% to 97% for the four individuals shown.

When the interaction of large numbers of virtual drivers can be assessed quickly, the virtual fitting method can provide high-resolution estimates of true multivariate accommodation. Models like the cascade prediction model (described in section 2.4.2) allow the manikins to be postured almost instantaneously and the effects of anthropometry, preference related to anthropometry, and preference unrelated to anthropometry to be considered simultaneously. The method is especially useful for Class B vehicles, such as trucks and buses, because they usually involve more design considerations besides spatial fitting due to the driving tasks. For instance, Class B vehicles commonly use height-adjustable seats so drivers can maintain adequate vision of the surroundings (67).

Another significant advantage of applying VFT in vehicle packaging is its seamless adaptability to the hybrid model. As discussed, the manikin approach does not usually have a scientific way

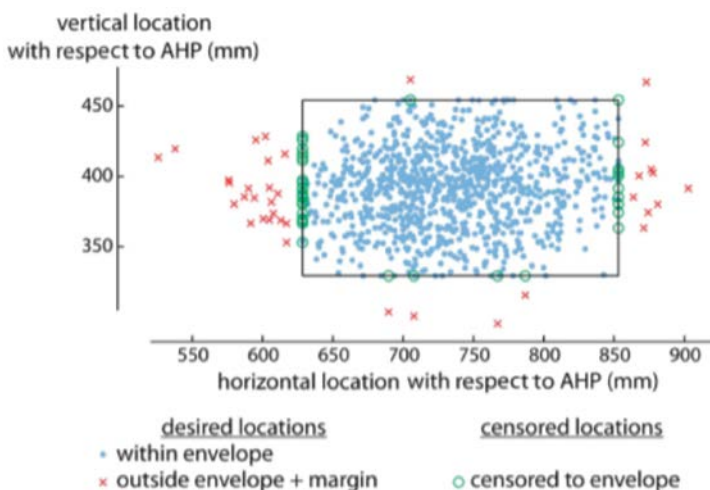


Figure 2.11. An example showing the preferred and censored seat locations of a virtual population of truck drivers (3).

of posturing the manikins. The designers usually posture the manikins manually, which introduces bias. Using a hybrid approach can resolve this issue. The hybrid approach establishes a model relating driver anthropometry to their body landmark locations in space. By creating a large number of virtual driver profiles and feeding their body anthropometric data into the hybrid model, designers can accurately and quantitatively simulate how each driver would posture themselves in a cab. It allows the designers to visually assess the accommodation level of any vehicle layout (Figure 2.11) (3).

2.4.2 Cascade Prediction Model

The SAE is an organization of professional engineers that aims to come up with standards and conduct research to bring safe and innovative design to the world. In the past several decades, many SAE J tools have been developed and heavily used for vehicle packaging in the automotive industry. For instance, SAE J1517 examines driver seat position, SAE J941 investigates driver eye position, and SAE J1052 specifically studies driver head location (Figure 2.12). These SAE J tools provide thorough guidelines on each individual component. Since these tools are not reconfigurable and generally consider a single design variable, they can produce vehicle package designs that accommodate a smaller percentage of the driver population than expected.

In the early 2000s, a cascade prediction model (CPM) was developed (68). From analyzing drivers' postures captured with a sonic digitizer, researchers found that drivers frequently react to their surroundings by moving their limbs while keeping their torso position still. Since locating the torso is a crucial step that lays the foundation for limb posturing, the CPM puts great emphasis on predicting hip and eye locations, which are recognized to be the most important measurements in vehicle packaging. Hip location is critical for seat position design and lower limb posturing, while eye location is a direct assessment of a driver's field of vision (69). With these two critical body landmarks created from the models of experimental data, researchers can establish submodels and apply inverse kinematics to predict the secondary body landmarks, such as shoulder location, elbow location, and knee location (37).

Even though the CPM is relatively recent compared to other vehicle packaging methods, such as the manikin approach, it is proven to be reliable. In a study conducted by UMTRI, a group

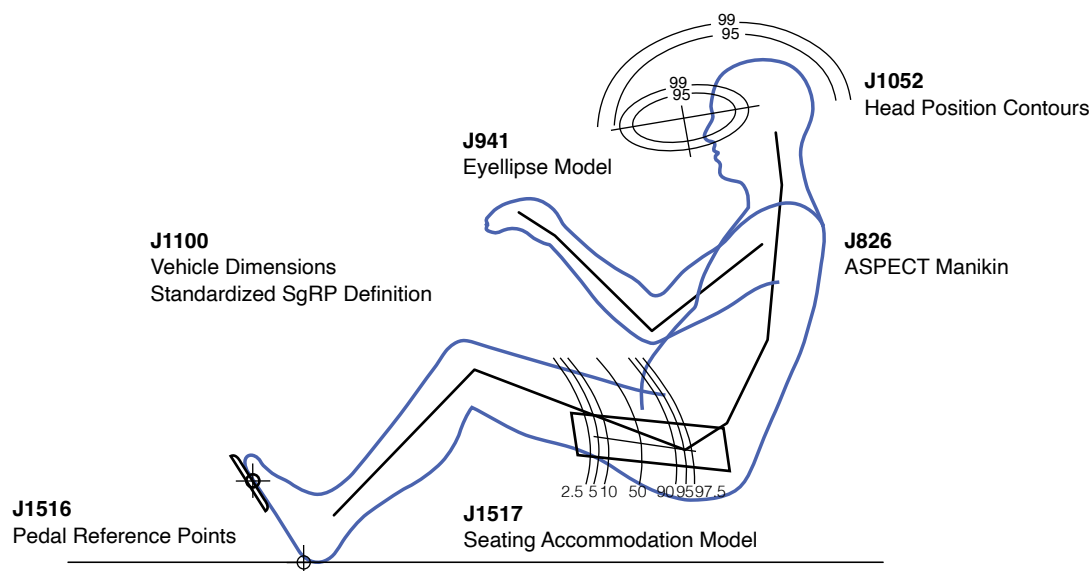


Figure 2.12. SAE International provides a number of J tools that can assist with vehicle packaging.

of researchers aimed to estimate driver postures with a CPM and compare them to laboratory observations (60). A total of 63 participants were studied in a laboratory setting to create the CPM while being given 27 vehicle package and seat conditions. The results matched the observed postures of 24 participants from an earlier in-vehicle study. The differences in mean eye and hip locations were within a few millimeters, and the differences in standard deviation were comparable as well. The CPM is used for subsequent analyses in this report.



CHAPTER 3

Bus Operator Posture and Associated Risk of CTDs

Professional drivers are a high-risk group for work-related musculoskeletal disorders (WRMSDs). There are a number of different kinds of WRMSDs; this project examined the risk associated with one specific class: cumulative trauma disorders (CTDs). Analysis using three different assessment tools found that in typical situations the majority of bus drivers are not at particular risk for CTDs.

3.1 Background

Any repetitive job having potentially excessive frequencies, high forces, and extreme limb postures can result in WRMSDs of the upper extremities. Six major surveys (70) have estimated the prevalence of these to be on the order of 15% for the U.S. population. Professional drivers are a high-risk group for WRMSDs involving the spine (71) and the shoulder and knee joints (72); in particular, there is a high incidence of early degenerative spine changes among truck drivers (73). Also, Tse et al. reported the negative impact of bus operators' stress on physical (cardiovascular diseases, gastrointestinal disorders, musculoskeletal problems, fatigue, etc.), psychological (depression, anxiety, post-traumatic stress disorder), and behavioral outcomes, with a very detailed review of 50 years of research on their injuries (74). Thus, the workplace of the driver, which includes the cabin climate, exposure to vibration and noise, and changing climatic conditions and driving postures, must be considered in relation to WRMSDs. These disorders contribute to low retirement age and high morbidity in drivers (75). Drivers are often exposed to repetitive and awkward postural stress in their working environment, contributing to back, neck, and upper extremity discomfort (76). Activities that include vibration and driving 30 km or more in a single trip increase the risk of back pain, disc rupture, tension, and fatigue. Although that research reported a limited examination of musculoskeletal disorders, later research focused specifically on the upper extremities with considerable detail from Washington State (77), Hong Kong (78), and Israel (79).

3.2 Research Activities

An experiment was designed to determine if bus drivers were at specific risk for CTDs. Video was captured for a number of professional bus drivers at the beginning and end of their shifts. This video was analyzed using three different assessment tools: the CTD risk index, rapid upper limb assessment (RULA), and the strain index.

3.2.1 Participants

Motion analysis was performed on existing videos of 14 bus operators. Participants were professional drivers who worked testing buses at the Larson Transportation Institute test track. All

bus operators were male and were included in the study's analysis. The oldest study participants were over 40 years of age and drove 50–60 hours each week. The majority of drivers were driving more than 250 km per day. Anthropometric data such as stature, mass, sitting height, seated hip breadth, and seated bideltoid breadth were measured (Table 3.1). All study procedures were approved by the Pennsylvania State University's Office for Research Protections.

3.2.2 Observation

Each bus operator was required to drive an electric transit bus for two rounds (long and short tracks) at the Larson Transportation Institute test track facility. Participants drove three loops on each track at the beginning and three loops on each track at the end of their 1-hour driving shift, so the research team recorded six loops on the long track and six loops on the short track for each driver. The total recorded time per bus driver across the four conditions was approximately 20 minutes. Interior cameras recorded their posture. They were positioned to record the right and front profiles of the drivers. The cameras were placed to ensure they were not in the driver's usual field of view. Specific tasks such as turning, lane changes, and avoidance of road hazards were incorporated into the driving schedule and were signaled in the video. This allowed decomposition of the video by task.

3.2.3 Assessment Tools

Three different risk analyses were performed on these motion data to ascertain potential risk for WRMSDs. A quantitative CTD risk index was developed by Weston and Freivalds (4) that evaluates all three major risk factors: force, frequency, and joint posture (Figure 3.1). This has been used quite successfully by Freivalds in his research at the Center for Cumulative Trauma Disorders in approximately 89 different industries over the last 30 years. That risk index was somewhat based on the second assessment tool used in this project: the more basic posture analysis index, the RULA developed by McAtamney and Corlett (5). A RULA worksheet is shown in Figure 3.2; this tool has been used to evaluate bus drivers (80) but was focused on trunk and neck regions rather than the upper extremities. A third assessment tool, the strain index, was developed by Moore and Garg to predict the risk of injury due to task attributes like intensity, duration, frequency, speed, and posture (6).

Due to the differing natures of the analyses, the data were processed slightly differently. For the CTD risk index and the strain index, a 2-minute segment of data was analyzed. For the RULA analysis, images were extracted at 1-second intervals from the videos. Among them, 10% were randomly selected for analysis. Thus, the total was 1,666 driving postures (20 min * 60 s * 14 drivers * 0.1 sampling) evaluated.

Table 3.1. Summary of the anthropometric data of study participants.

Measure	Mean	SD
Stature	1,788 mm	59.1 mm
Mass	104.6 kg	19.5 kg
Hip breadth, seated	427 mm	35.0 mm
Bideltoid breadth, seated	519 mm	102 mm
Sitting height	903 mm	38.3 mm

CTD Risk Index

Job Title:	VCR Counter No.:	Date:
Job Description:	Department:	Analyst:

Cycle Time (in minutes; obtain from videotape)		ⓐ	ⓑ
# Cycle/Day = $\frac{(480 - \text{Lunch-Breaks})}{\text{Cycle Time}}$	=	ⓐ	ⓓ Larger of ⓐ or ⓑ:
# Parts / Day (if known)	=	ⓑ	
# Handmotions / Cycle			ⓔ
# Handmotions / Day (ⓓ x ⓔ)			ⓕ
Frequency Factor (Divide ⓕ by 10,000) =			

<i>(Circle appropriate condition)</i>	Points			
	0	1	2	3
Working Posture	Sit	Stand		
Hand Posture 1: Pulp Pinch	No	Yes		
Hand Posture 2: Lateral Pinch	No	Yes		
Hand Posture 3: Palm Pinch	No	Yes		
Hand Posture 4: Finger Press	No	Yes		
Hand Posture 5: Power Grip	Yes	No		
Type of Reach	Horizontal	Up/Down		
Hand Deviation 1: Flexion	No	Yes		
Hand Deviation 2: Extension	No	Yes		
Hand Deviation 3: Radial Dev.	No	Yes		
Hand Deviation 4: Ulnar Dev.	No	Yes		
Forearm Rotation	Neutral	In/Out		
Elbow Angle	=90°	≠90°		
Shoulder Abduction	0	<45°	<90°	>90°
Shoulder Flexion	0	<90°	<180°	>180°
Back/Neck Angle	0	<45°	<90°	>90°
Balance	Yes	No		
Total the Points for the Circled Conditions ⓖ				
Posture Factor (Divide ⓖ by 10) =				

Grip or Pinch Force Used on Task	ⓗ	lbs.	ⓓ Divide ⓗ by ⓓ:
Max Grip or Pinch Force	ⓙ	lbs.	
Force Factor (Divide ⓙ by .15) =			

<i>(Circle appropriate condition)</i>	Points			
	0	1	2	3
Sharp Edge	No	Yes		
Glove	No	Yes		
Vibration	No	Yes		
Type of Action	Dynamic	Intermittent	Static	
Temperature	Warm	Cold		
Total the Points for the Circled Conditions ⓚ				
Miscellaneous Factor (Divide ⓚ by 3) =				

$CTD\ Risk\ Index = .3 \times (Frequency + Posture + Force\ Factors) + .1 \times (Miscellaneous\ Factor)$				
CTD Risk Index = .3 x (+) + .1 x () =				

Figure 3.1. The CTD risk index assessment tool (4).

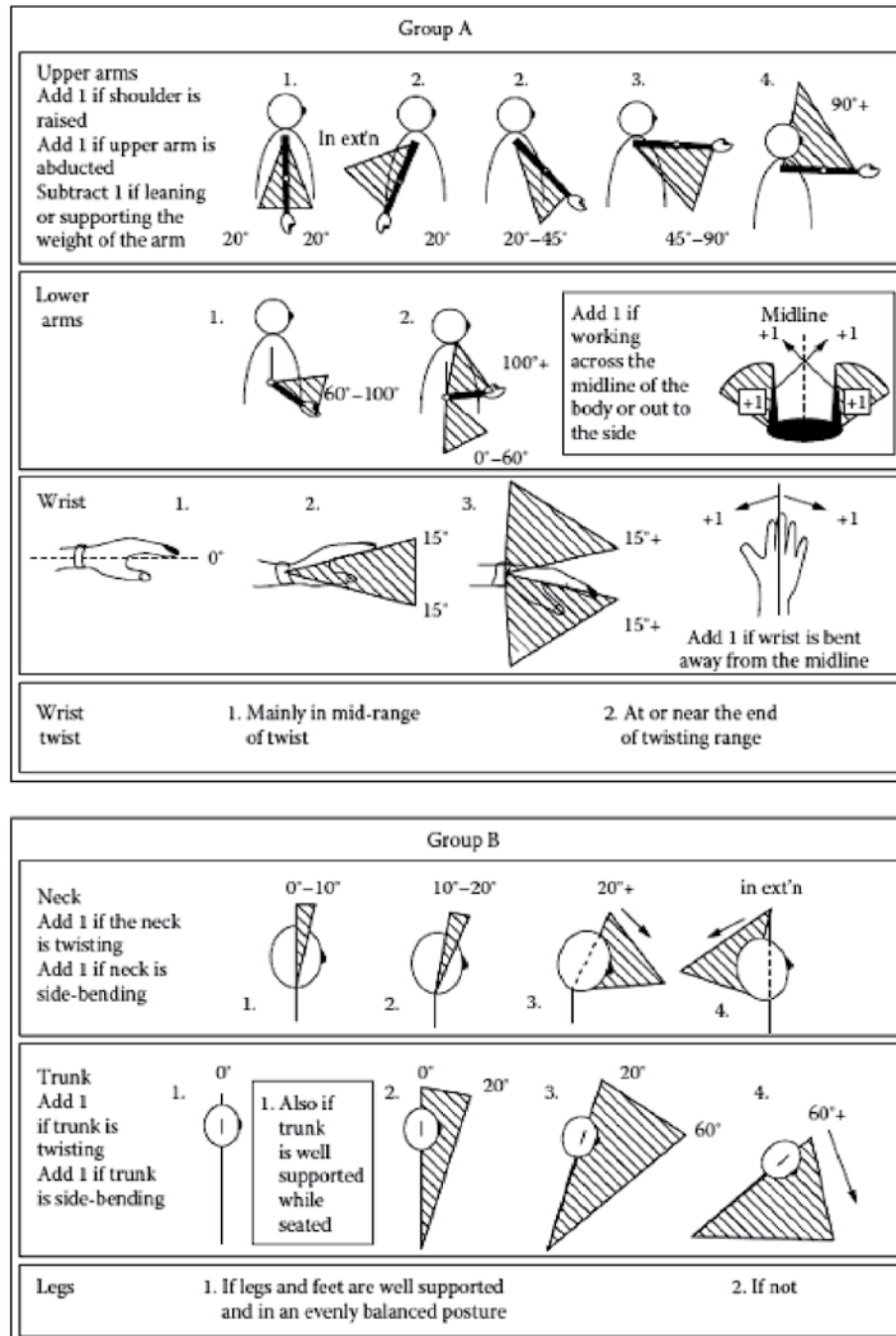


Figure 3.2. The RULA tool (5).

3.3 Results

3.3.1 CTD Risk Index

The results of the CTD risk index assessment for the participants are summarized in Table 3.2. The force factor and miscellaneous factor parameters were assumed to be 1.0 and 0.66, respectively. There is no CTD risk score greater than 1.0 across all the conditions. The highest score, which occurred at the beginning of the short durability track, was 0.56. There was no significant difference between tracks (p -value = 0.909) under the conditions examined here (Figure 3.3). Also, there was no significant difference in results from the beginning of the shift vs. the end of the shift (p -value = 0.308), an indication of fatigue.

Table 3.2. Results of the CTD risk index assessment.

Track	Timing	Frequency Factors	Posture Factors	Force Factors	Misc Factors	CTD Risk Score
S	B	0.392	0.907	1.00	0.660	0.756
S	E	0.389	0.886	1.00	0.660	0.748
L	B	0.376	0.893	1.00	0.660	0.724
L	E	0.363	0.864	1.00	0.660	0.736

3.3.2 RULA

Table 3.3 reports the results of the RULA. The driving postures are categorized into groups of low, average, and high posture and the corresponding component ratio of each posture group is reported. Score A represents wrist and arm scores and Score B refers to neck, trunk, and leg scores.

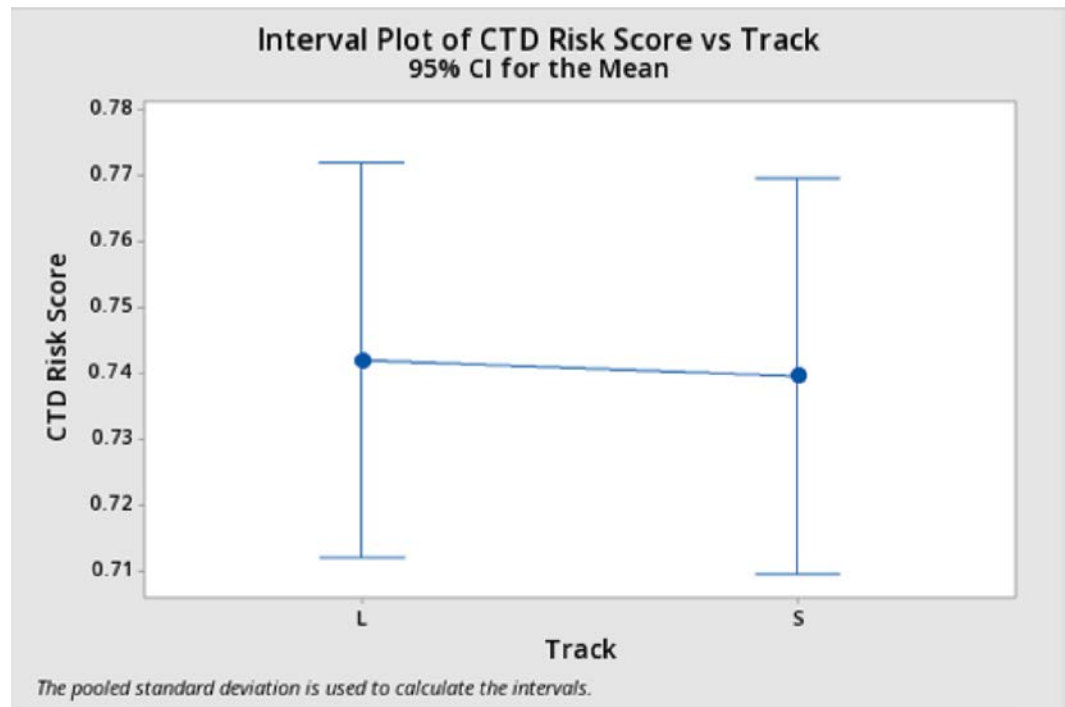


Figure 3.3. CTD risk score based on the track (L = long durability track; S = short durability track).

24 Assessing Lifecycle and Human Costs of Bus Operator Workstation Design and Components

disorders; only one scored above 7, which implies bus operation is probably hazardous. Like the other results, strain index shows there was no significant difference between tracks (p-value = 0.637) and no significant fatigue for 1 hour of driving (p-value = 0.920).

3.3.4 Summary

Overall, the scores from the three evaluation tools showed that there may be some risk for CTDs for some drivers in terms of posture and movement during bus operation. Most of the drivers are in a low-risk state. One of the objectives of this research effort is to mitigate the risk for all drivers through improved bus workstation packaging.



CHAPTER 4

Bus Packaging Methods

The objective of this work is to study driving postures of U.S. bus operators and make design recommendations regarding bus cab layout. The various approaches to vehicle packaging each have advantages and disadvantages. One might be suitable for one scenario and inappropriate for another. When deciding which method to use, many factors need to be considered, including available data, cost, and fidelity of results. An appropriate approach should be able to provide results of sufficient accuracy within a reasonable budget and meet the project expectations.

Besides selecting an appropriate model, another challenge is understanding the bus operator population as a whole. The work requirements and other considerations make the demographics of U.S. bus operators unique from the general population. The differences can be reflected in descriptors such as gender ratio, race/ethnicity composition, and age distribution. This information is vital to good design for human variability practice since it defines some of the variability that must be considered in the creation of the artifact, task, or environment. A poorly defined user population can result in designs that don't meet accommodation expectations. This is especially problematic with designs like bus operator workstations, where adjustability is used to improve overall accommodation rates. Improperly allocated adjustability increases costs without improving performance.

The first half of this chapter discusses the approach used in this work and presents the models to predict driver posture. The second half of this chapter presents the demographics of U.S. bus drivers.

4.1 Model Selection

Vehicle packaging considers the spatial placement of components including displays, controls, and the seat. Recommendations should consider the driver population and the postures they are likely to prefer or exhibit while driving. These behaviors are a compound result of body dimensions and postural preferences. A successful package provides sufficient adjustability to accommodate a large fraction of these individuals and postures while minimizing the associated costs.

This research results in a toolkit to accurately predict the postures and associated joint center locations of populations of U.S. bus operators in response to a candidate cab geometry. The tool reports what fraction of operators in the specified population are capable of reaching the steering wheel and the pedals without any difficulty while simultaneously maintaining the ability to see target locations. Cascading posture prediction was selected for a number of reasons, including the experimental validation and its ability to conduct simultaneous multivariate prediction.

The toolkit provides numeric/tabular results as well as visual ones. Research has shown that including visuals can increase an individual's patience in learning and understanding (81). Additionally, on average, 83% of what a person learns is through sight (82). Therefore, it would significantly reduce the learning curve associated with this new toolkit to include a visual representation

of the accommodation results. To be specific, the toolkit should clearly and accurately identify the critical landmarks (preferred steering wheel location, H-point location, and eye location), and accurately display the rest of the landmarks (shoulder location, elbow location, knee location, and ankle location).

As mentioned previously, industry users currently rely heavily on the SAE J tools and conduct mostly univariate analyses by designing interior components independently. The J tools provide sufficient information on how people react to each design objective and estimate how a driver's interaction varies within a certain population, but they cannot provide a coherent understanding of how individuals adapt to several spatial requirements simultaneously. The correlation between the requirements is disjointed, especially from an individual level. More importantly, the SAE J tools are incapable of predicting postural adjustments due to disaccommodation. In other words, they provide information on the preferred location for a control, but not on what a driver might do when that preferred location is unattainable.

Current industry standards describe driver posture by estimating the distribution of the preferred locations of each landmark, such as steering wheel, H-point, and eye location. Assuming these are normally distributed, they can be represented with a mean and standard deviation. The advantage of such an approach is that distributions are continuous. Without needing an infinite number of drivers, it produces results of infinite resolution. The disadvantages are apparent as well. The main issue is the model cannot adjust based on bus geometric constraints, because the underlying relationship between meeting multiple design objectives remains uncertain. While designing an adjustment envelope for the steering wheel, for instance, a high accommodation rate is desired, but disaccommodated drivers are expected as well. When a driver's preferred steering wheel location is not in the adjustment envelope, they will move the steering wheel to the nearest point on the envelope and adjust the rest of their body to accommodate this change (Figure 4.1) (37).

The purpose of a new design is to minimize these required changes to a driver's preferred posture. In order to visually reflect how adjusting one landmark can impact the location of other landmarks for every virtual bus operator, it is important to approach vehicle packaging from an individual perspective. That is the strength of the VFT approach—each virtual driver is allowed to interact with the candidate design individually and their responses are predicted. Then the individual results are aggregated to predict behavior for an entire population. This mirrors what would happen in a real usage scenario.

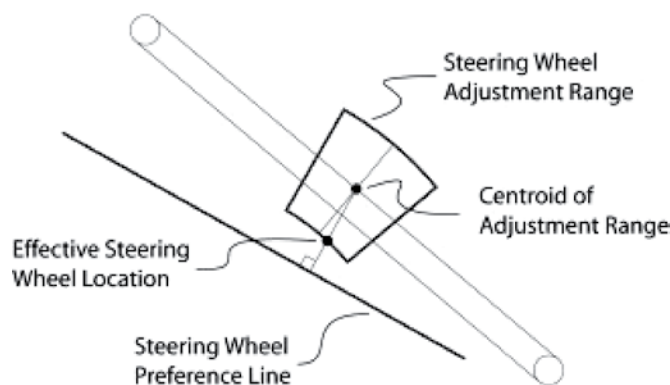


Figure 4.1. When the preferred steering wheel location is not attainable (e.g., due to limitations in the hardware), it is adjusted to the nearest location in the adjustability envelope.

Overall, the model needs to be able to (1) predict locations of critical landmarks with high accuracy, (2) assess design objectives using a multivariate approach, and (3) use visuals to present packaging results. Considering all the available approaches discussed in Chapter 2, the first two needs can be met using cascade modeling, and data visualization can be achieved through virtual fitting.

4.2 Cascade Model for Buses

Previous research has laid a foundation in Class B vehicle packaging, and a cascade model for buses and trucks was developed in 2005. Its core concepts can be summarized in a flowchart (Figure 4.2). This section details the cascading procedure of driving posture prediction.

4.2.1 Steering Wheel Location

In posture prediction, identifying the preferred steering wheel location is one of the first steps. Most vehicles now include adjustable steering wheels. Due to the spatial demand of the operator cabs among large vehicles, especially buses and trucks, steering wheels need to provide suitable adjustment ranges for drivers to maintain sufficient vision while driving. There are two common modes of adjustment: tilting and telescoping. Tilting is when a steering wheel rotates about its pivot point, located at the base of the steering wheel. Telescoping is when a steering wheel moves parallel to the shaft (Figure 4.1). With the two modes of adjustment, the steering wheel can move in both X and Z directions.

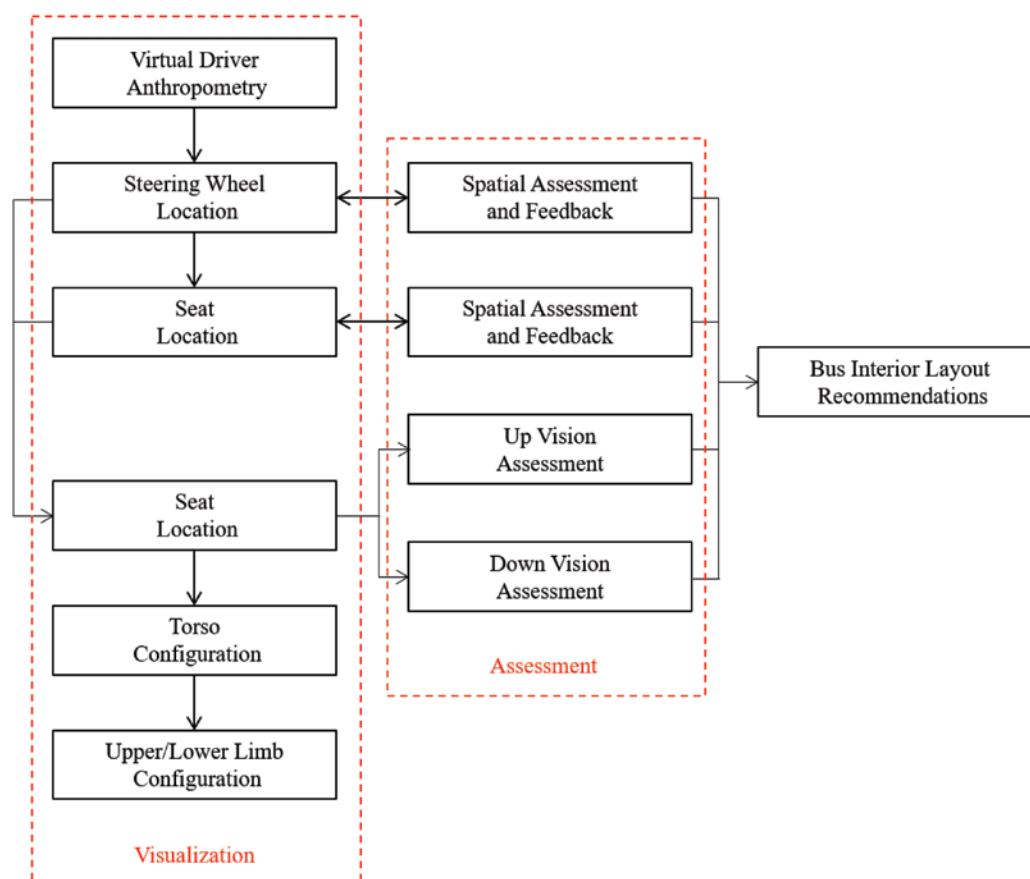


Figure 4.2. A schematic diagram of the cascade posture prediction model.

Drivers tend to place the steering wheel at the most comfortable location for them to perform normal driving tasks. Preferred steering wheel locations vary from person to person, which makes it challenging to predict driver preference. In an attempt to understand such variability, a laboratory study was conducted to investigate preferred steering wheel location for vehicle operators. Participants were asked to sit in a simulated cab and adjust the floor height and the pedals in the X (fore-aft) and Z (vertical) directions. Instead of the steering wheel, the origin of the cab (AHP) was adjusted because steering wheels were fixed in space in the experiment setup. This allowed the relative location between the steering wheel and the pedals to vary based on driver preference. After each driver adjusted to their preferred posture, data were collected (37).

The preferred steering wheel location data (measured from the AHP) indicated that the vertical location of the steering wheel is negatively impacted by its horizontal location, and a near-linear relationship was discovered. The average ratio (mean) was calculated to be -0.559 with a standard deviation (SD) of 0.305 . In other words, the vertical location is expected to decrease by an average of 0.559 mm for every 1 mm the steering wheel travels back horizontally. And 67% of the drivers will likely choose a ratio between $-0.864 * (\text{Mean} - \text{SD})$ and $-0.254 * (\text{Mean} + \text{SD})$.

$$\text{SWpref}_z - 0.559 * \text{SWpref}_x \quad (4.1)$$

where SWpref_z is the steering wheel preference Z coordinate and SWpref_x is the steering wheel preference X coordinate.

The variance of the ratio was also derived from the driver's preference, and it was independent of driver anthropometry (37). However, the preferred total height of the steering wheel is strongly dependent on the driver's stature (height). Stature is a widely available anthropometric measure and a common predictor in postural models, including in vehicle packaging. The preferred vertical location is found to be

$$\text{SWpref}_z@175(\text{mm}) = 524 + 0.1613 * \text{stature}, R^2 = 0.32, \text{RMSE} = 23.4 \quad (4.2)$$

when the horizontal location is at 175 mm with respect to the AHP. The horizontal location of 175 mm does not hold actual meaning and is chosen merely for mathematical convenience. In fact, any horizontal location can be chosen because the preferred vertical locations move along a slope of 0.559 , as mentioned. These preferred vertical locations can be found by using the equation:

$$\text{SWpref}_z(\text{mm}) = 524 + 0.1613 * \text{stature} - 0.559 * (x - 175) \quad (4.3)$$

This line represents the steering wheel preferred vertical locations. Based on their stature, each driver has a unique preferred steering wheel vertical height line (Figure 4.1).

One preference line is not enough to locate a preferred steering wheel location in a 2D space because there are two degrees of freedom (DoF); a minimum of two lines are needed. Besides steering wheel vertical height, human variability can also be reflected in the steering wheel tilt angle. Rotating the steering wheel about the pivot point not only allows drivers to control the face angle of the steering wheel so it is easier to grab, but also enables the steering wheel to move in the horizontal direction to adapt fore-aft preference. By drawing a line connecting the steering wheel pivot of rotation to the center of the steering wheel, a driver's preferred tilt angle can be found. These two lines can be used to find the intersection that represents the driver's preferred steering wheel location (37).

For a properly designed vehicle, the majority of preferred steering wheel locations should be accommodated. In fact, the adjustment envelope should be selected after the preferred locations are found. Once the envelope is determined, it can be used to locate the fore-aft and vertical locations of the center of the steering wheel with respect to the AHP, which are to be used as

inputs for the rest of the posture prediction. If the preferred location lies outside the adjustment envelope, the nearest point to the envelope is used (37). Specifically, two measures need to be assessed: tilt angle and telescope distance. Both need to be within the vehicle adjustment range. If one exceeds that range, the most extreme location in the range will be selected (Figure 4.3).

This model provides a mathematical understanding of how drivers would adjust the steering wheel to a preferred location based on their body dimensions and their driving preference. It was developed using laboratory data and has been verified in the field.

4.2.2 H-Point Location

The seat is another adjustable component inside a vehicle. Its location is usually defined by the H-point, which generally represents where a driver's hips would be. One of the design concerns of seat location is that drivers must be able to comfortably reach the pedals with their feet. This is a fundamental requirement of vehicle packaging and an indicator of spatial accommodation. Another concern of locating the driver's H-point is to provide reasonable relative location between the hand grip and the torso. Similar to reaching the pedals with the feet, reaching the steering wheel with the hands is important. Once the steering wheel location and the seat location are chosen, driver eye location will be assessed for safety considerations. A more detailed discussion on driver field of view is presented in section 4.2.3.

The cascade model used for some of the posture prediction was developed based on linear regression, in the form of constant coefficients multiplying predictors (c).

$$y = c_0 + c_1 * x_1 + c_2 * x_2 \dots \quad (4.4)$$

Here, y represents the dependent variable, which is the variable of interest. The independent variables (x_1 , x_2 , etc.) are predictors. In vehicle packaging, two kinds of predictors are common: driver anthropometry and vehicle geometry. Driver anthropometry describes body size and

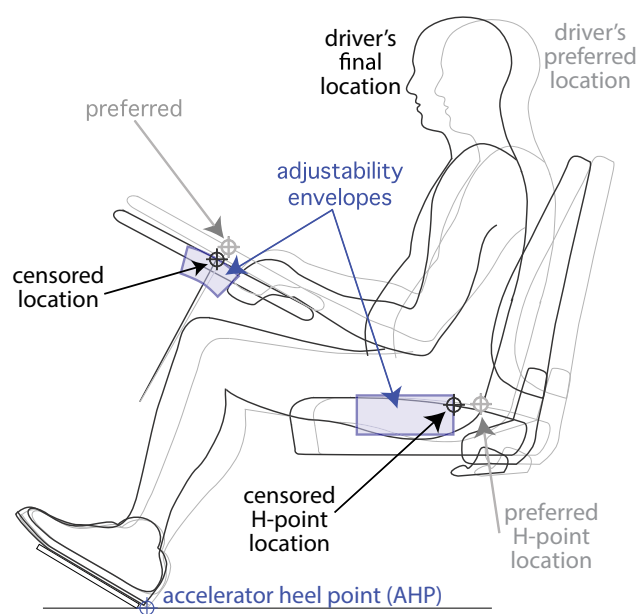


Figure 4.3. The preferred and actual driver locations, selected as a result of the cascading posture prediction algorithm and considering the adjustability limits of the vehicle components.

shape and plays a major role in spatial fitting, which mostly determines body landmark locations. Vehicle geometry also contributes to the effect because drivers commonly adjust their posture to adapt to the vehicle's interior component layout. Taking these two predictors into account allows for accurate prediction of the average location of a desired landmark.

This linear regression is useful for predicting drivers' average behavior but is insufficient to express the ranges of individual preference uncorrelated with anthropometry that most drivers exhibit. To include this factor, the residual variance from the regression model is reintroduced into the equation (43). The error term $N(0, s)$ is a randomly generated number from a Gaussian distribution. This distribution has a mean of zero and a standard deviation of s , the square root of the residual variance. By studying the size of the error and augmenting this error to the linear regression, a complete spectrum of driver preference can be captured through this model.

$$y = c_0 + c_1 * x_1 + c_2 * x_2 \dots + N(0, s) \quad (4.5)$$

As discussed in Chapter 2, an H-point is a fixed point on a car seat near the driver's hip. Unlike a hip point that moves with the driver's posture, an H-point is a characteristic of the seat. Given an H-point location with respect to the AHP, it's possible to accurately locate the seat. One of the objectives of vehicle packaging is to design a proper seat adjustment envelope (the region the H-point can move through). Thus the H-point, instead of the hip point, is commonly used.

The H-point can be measured on a physical seat using an H-point machine and the procedures outlined in SAE J826 (42). Researchers have also created a linear regression model that can predict the preferred H-point location of a population with high accuracy (37). One of the factors that led to its success is that it uses a stepwise approach in an iterative manner (83). For instance, there are a number of anthropometric measurements that are related to the length of a human body, including stature, leg length, arm length, erect sitting height, and acromial height. This introduces more predictors than needed and can lead to more errors because certain body characteristics are overanalyzed. A stepwise approach carries out an automatic process of choosing predictors to fit regression models. During each step, one predictor is analyzed to determine whether to add it to or subtract it from the current list of predictors.

Through an iterative stepwise approach, two predictors regarding vehicle geometry (fore-aft and vertical locations of the center of the steering wheel with respect to AHP) and five predictors regarding anthropometric measurements (stature, erect sitting height, ratio of erect sitting height to stature, difference between stature and erect sitting height, and natural log of body mass index [BMI]) were identified (37). Since anthropometric measurements are approximately normally distributed, each measurement of a population can be represented with a mean and a standard deviation. The stepwise regression results indicate that the horizontal location of the H-point is largely dependent on the horizontal and vertical location of the steering wheel, which is a sign of drivers adjusting their seating to adapt to vehicle interior components. For this reason, steering wheel location is predicted first and is used as inputs for seat location prediction, although drivers usually adjust both of them simultaneously in an iterative manner. The driver's functional leg length is estimated by taking the difference between stature and erect sitting height. A positive coefficient shows that drivers with longer legs tend to adjust the seats backward.

BMI is the other predictor that indicates body width. Usually, a wider driver would need more space to operate a vehicle. The purpose of using the natural log is to normalize the BMI measurements of the population, which otherwise exhibit a long right tail. The standard deviation of the error term is 37.7 mm, which represents a driver's postural preference unrelated to anthropometry (37).

$$H_x(\text{mm}) = -53.6 + 0.6081 * \text{SWpivot}_x - 0.3343 * \text{SWpivot}_z + 0.6394 * l_{\text{leg}} + 89.07 * \text{Ln}(\text{BMI}) + N(0, 37.7) \quad (4.6)$$

where

H_x = H-point location X coordinate

SWpivot_x = steering wheel pivot point X coordinate

SWpivot_z = steering wheel pivot point Z coordinate

l_{leg} = functional leg length

Ln(BMI) = natural log of BMI

Unlike the horizontal location, which uses four predictors, the vertical location of the H-point is dependent solely on the vertical location of the steering wheel. Anthropometric measurements regarding body length or width had a minimal effect. The standard deviation of a driver's preferred seat vertical location is 22.9 mm, which is smaller than horizontal (37).

$$H_z = -200.3 + 0.8545 * SWpivot_z + N(0, 22.9) \quad (4.7)$$

where H_z is the H-point location Z coordinate.

While designing a seat adjustment envelope for the preferred seat location of a driver population, the huge amount of potential variability makes it impossible to accommodate 100% of them. Consequently, the accommodation goal is commonly set at 95% or lower for economic and/or practical reasons. For virtual drivers who are accommodated by the candidate design (i.e., they can put the seat in their preferred location), the cascade posture prediction model will proceed to the next step. For the disaccommodated virtual driver, the predicted location becomes the nearest point on the adjustability envelope to the preferred location. Then their posture is adjusted accordingly (37).

4.2.3 Eye Location

The cascade model received its name from its cascading nature; a sequence of actions must take place in order to achieve the desired goal. The first step is to predict the virtual driver's preferred steering wheel location. After this, seat location can be predicted. The cascade model can then proceed to estimate the driver's eye location. In vehicle packaging, the location of the eye center is represented by the eye point (Figure 4.4). The range of eye locations in the 2D X-Z plane for a population of drivers is referred to as the eyellipse. Generally, the movement limits are 45° upward, 65° downward, and 30° left and right, but for comfort, a 15° turn in all four directions is considered "easy eye rotation" (29). In SAE J1050, the eye point is defined in 3D space with the left and right eyes fixed 65 mm apart. Since this work studies vehicle packaging in the 2D X-Z plane, only the eye point on the X-Z plane is calculated and used for performance assessment.

In the referenced cascade model, the eye point was studied in a similar manner as the H-point, through laboratory data, and the same set of predictors are used. Both steering wheel location

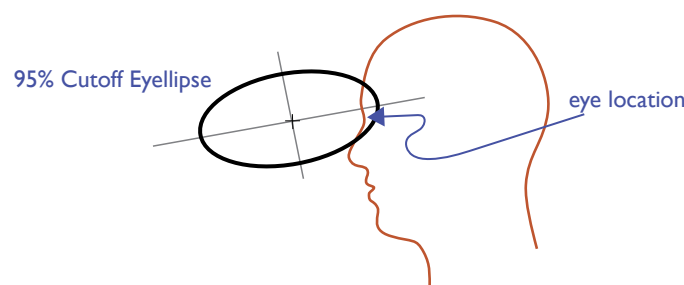


Figure 4.4. Eye location and a sample 95% cutoff eyellipse for a population of drivers (7).

and seat location are predicted from the AHP, the origin of vehicle interior component packaging. However, the eye point location developed in this model is expressed relative to a different datum. Due to the limited movement of the driver's neck during driving, the driver's head and torso are relatively static. In other words, the driver's eye point is largely dependent on the seat location, so eye points are expressed in terms of H-point (37). In the horizontal direction, the eye point is found to be a function of three predictors: the horizontal location of the steering wheel, the ratio of sitting height to stature, and BMI. This regression model (Equation 4.8) also incorporates a residual variance term that represents preference unrelated to anthropometry. The square root of the residual variance was found experimentally to be 41.0 mm. In the vertical direction, the eye point (Equation 4.9) is a function of only one predictor, erect sitting height, and has $s = 22.3$ mm (37).

$$\text{Eye}_x = -334.0 + 0.0809 * \text{SWpivot}_x + 1142 * \text{ratio} - 87.98 * \text{Ln}(\text{BMI}) + N(0, 41.0) \quad (4.8)$$

where Eye_x is the eye point X coordinate.

$$\text{Eye}_z = -47.3 + 0.7812 * \text{SittingHeight} + N(0, 22.3) \quad (4.9)$$

where Eye_z is the eye point Z coordinate and SittingHeight is the driver's sitting height.

Driving requires a number of actions that involve the steering wheel, foot pedals, buttons, and other interior components. These actions are essential to operating a vehicle as desired, but the ability to see outside of the vehicle is even more important because the driver's sight is the main source of information they use to make decisions. The central vision field, straight through the front windshield, allows drivers to see cars, pedestrians, traffic lights, and signs in the front. Besides central vision, peripheral vision is also important because it captures cars and other potential hazards. The quality of driver vision can directly impact driver safety and performance (84). Since this work is conducted only in the X-Z plane, only central vision is considered.

A driver's central vision in two dimensions is bounded by the driver's ability to look both upward and downward. Upvision angle is measured from the horizontal plane to the highest angle the driver can see, and downvision angle is measured to the lowest angle. The sum of the two angles makes up the driver's central vision. In most vehicles, the upvision angle is limited by the UDLO, where the top of the windshield meets the frame of the vehicle. An adequate upvision angle permits the driver to read road signs, respond to traffic lights, and see traffic on uneven roads. According to the American Public Transportation Association (APTA) bus design guideline, the windshield must ensure a minimum of a 14° upvision angle (8).

Downvision is also important, particularly because buses are typically higher than the vehicles around them. This makes it challenging for drivers to see immediately in front of the bus. This issue is especially profound in urban areas where traffic and pedestrians are primary concerns. Additionally, school transportation is one of the main ways buses are used, where picking up and dropping off children is the most essential part of the job. Bus drivers must be able to maintain adequate downward vision to ensure clearance in front of the bus. Thus, APTA requires all bus drivers to detect an object 42" high and 24" in front of the bus (Figure 4.5). These upvision and downvision requirements agree with SAE practice (29), and they are used as design guidelines in this work.

Upvision is usually defined by the location of the UDLO, but downvision requires more consideration. Depending on the geometric layout, a few interior components could be the limiting factor. The most common consideration is the location of the cowl point—where the bottom of the windshield meets the body of the bus. If it was designed to be above the line connecting the driver's eye point and the tip of the 42" object, the requirement would be unmet. Besides the

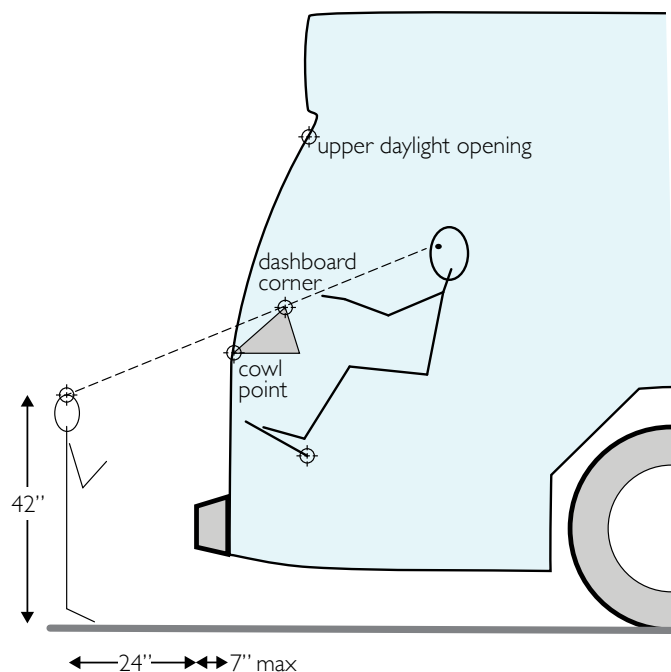


Figure 4.5. The downvision requirement for bus drivers states that a 42" object located 24" in front of the bus must be visible (8).

cowl point, some buses are equipped with a hood. The hood point, which represents the highest point on the front end of the hood, can also be a limiting factor. Another candidate is the dashboard. As more functionalities are added to buses, the dashboard is growing bigger to fit an increased number of buttons and screens. As designers assess a bus package, all the potential obstacles need to be considered to ensure a safe downvision angle.

4.2.4 Secondary Body Landmarks

The purpose of vehicle packaging is to apply an understanding of drivers' behavior inside a vehicle and make design decisions on the layout of the interior components to best accommodate them. In this work, most of the essential components in the X-Z plane are included: steering wheel, seat, and vision-related components. They are assessed with drivers' preferred steering wheel location, H-point, and eye point. This knowledge allows for successfully packaging many elements of a bus layout. As discussed at the beginning of this chapter, besides accurately predicting drivers' postures, visually representing these postures is significantly useful for industry users. This section briefly discusses how secondary body landmarks (hip point, shoulder point, grip point, elbow point, ankle point, and knee point) are predicted.

In the study of biomechanics, a human body can be presented using body landmarks. In vehicle packaging this is often accomplished through representations of the body as body segments and joints (85, 86, 87). This approach not only gives a visual representation of the drivers but also works seamlessly with the cascade model. As a continuation of the cascade model, the next step is to use inverse kinematics to estimate the locations of other body landmarks, which is useful to assess accommodation and visualize the driver.

In previous sections, linear models of finding the preferred H-point were presented. The H-point is a fixed location on a seat and does not move relative to the seat based on driver

preference. A hip point, however, is the joint center of a driver's hip. It is a commonly used body landmark when configuring driver posture since it is part of the kinematic chain connecting the upper and lower body segments.

The location of the hip for each virtual driver can be estimated using linear regression. The offset vector from the H-point to the hip point is a function of the driver's body dimensions (37). Specifically, the horizontal offset distance is negatively proportional to the driver's BMI, and the vertical offset distance is positively proportional to both the driver's BMI and erect sitting height. By adding these offset distances to the H-point location, the hip point location can be found. Since the following body landmarks are mainly used for visualization and have minimal impact on vehicle interior layout, simple linear regression models are used without variance. Hip point location is calculated as follows:

$$\text{Hip}_x = 90.2 - 5.27 * \text{BMI} + H_x \quad (4.10)$$

$$\text{Hip}_z = -109.9 + 1.51 * \text{BMI} + 0.0813 * \text{SittingHeight} + H_z \quad (4.11)$$

where Hip_x is the hip point X coordinate and Hip_z is the hip point Z coordinate.

For consistency of terminology, the shoulder joint center, elbow joint center, and knee joint center are referred to in this report as the shoulder point, elbow point, and knee point. Once the hip point is located, the next joint center in the kinematic chain—the shoulder—can be predicted. While driving, the shoulder point and hip point together represent the driver's torso. Commonly, drivers lean their torso against the back of the seat to reduce stress. Taking this slouching factor into consideration, researchers have found the distance between the hip point and the shoulder point to be a function of the driver's erect sitting height. As Equation 4.12 indicates, the distance is solely impacted by the driver's length. However, the angle between the two is largely dependent on the driver's width (Equation 4.13). This angle (measured from the vertical direction) can be predicted:

$$\text{HipShoulderDist} = 0.49 * \text{SittingHeight} \quad (4.12)$$

$$\text{HipShoulderAngle} = -25.1 + 0.297 * \text{BMI} + 67.6 * \text{ratio} \quad (4.13)$$

where the distance (HipShoulderDist) and angle (HipShoulderAngle) between the two points, the X- and Z-offsets, can be calculated using trigonometry. The location of the shoulder point can be obtained by augmenting the offsets to the hip location:

$$\text{Shoulder}_x = \text{Hip}_x + \text{HipShoulderDist} * \sin(\text{HipShoulderAngle}) \quad (4.14)$$

$$\text{Shoulder}_z = \text{Hip}_z + \text{HipShoulderDist} * \cos(\text{HipShoulderAngle}) \quad (4.15)$$

where Shoulder_x is the shoulder joint center X coordinate and Shoulder_z is the shoulder joint center Z coordinate.

The next step is locating the center of the steering wheel. The preferred steering wheel angle was also calculated, measured from the vertical direction by convention. This angle is the same as the angle formed between the wheel face and the horizontal direction. Knowing the steering wheel diameter (SWD), once again, the X- and Z-offsets can be found using trigonometry and can then be added to the steering wheel location, which indicates the driver's grip point.

$$\text{Grip}_x = \text{SW}_x + \text{SWD}/4 * \cos(\text{SW angle}) \quad (4.16)$$

$$\text{Grip}_z = \text{SW}_z - \text{SWD}/4 * \sin(\text{SW angle}) \quad (4.17)$$

where

Grip_x = grip point X coordinate

Grip_z = grip point Z coordinate

SWD = steering wheel diameter

SW angle = preferred steering wheel angle

The grip point, the shoulder point, and the elbow point form a triangle. With two of the vertices and one side being known, the third vertex can be positioned by knowing the lengths of the other two sides. One of the sides is the upper arm length, which is measured from the shoulder center joint to the elbow center joint, and this length can be estimated using the acromial radial length from an anthropometry database, such as the second U.S. Army Anthropometric Survey (ANSUR II) (9) which is discussed in section 4.3.1. In the survey, distances are measured from landmarks to landmarks, such as the acromion and the radial. Although these landmarks are different from the joint centers, researchers have quantified the offsets between them (88). Likewise, the length between the elbow joint center and the grip center can be estimated to represent forearm length. After knowing both upper arm length and forearm length, the elbow joint center can be estimated.

Due to the similarities between the upper limbs and the lower limbs, the same trigonometric procedure can be applied to lower-body configuration. Instead of the grip point, an ankle joint center is used. Relative to the AHP, researchers estimated the ankle to be 32 mm in the X direction and 128 mm in the Z direction (89). This is approximated as a constant since there is relatively little variation from the base of the heel to the malleolus landmark across individuals. Besides the ankle point, leg lengths are needed. One of them is the thigh length, which represents the distance between the hip joint center and the knee joint center. The other is the shank length, which represents the distance between the knee joint center and the ankle joint center. After knowing the lengths and locations of two vertices, the third vertex can be configured using the fundamentals of trigonometry, which represents the knee joint center.

4.2.5 Estimation of Accommodation

The cascade model used in this project advocates the principle of letting information flow down from experts through layers of customized treatment to obtain desired outcomes (90). In vehicle packaging, the cascade model applies a similar concept. The driver's anthropometric dimensions and vehicle geometry are the high-level data. With these data, preferred steering wheel location is predicted. Using preferred steering wheel location as an input, preferred seat location is then predicted. Although these two steps usually take place iteratively in a laboratory setting or in real life, they are carried out sequentially in the VFTs because the model was developed based on final locations of these reference points. From here, eye point is predicted and field of vision is assessed. Once these primary locations are predicted, secondary body landmarks can be estimated, starting with hip point and shoulder point. After this, grip point, ankle point, elbow point, and knee point can be calculated.

Throughout the process of cascade posture prediction, a total of four design objectives were assessed. They are (in order of prediction):

1. Steering wheel adjustment envelope accommodation
2. Seat adjustment envelope accommodation
3. Upward vision (minimum of 14°)
4. Downward vision (must see a 1,067-mm object 610 mm in front of the vehicle)

The multivariate approach of assessing the accommodation condition of each virtual driver is a significant component of this work. With a large population of drivers as inputs, it provides

high resolution and allows designers to study the aggregated effects of design decisions. For each driver, designers can directly assess how they are accommodated on each of the four objectives. This approach facilitates an understanding of the underlying relationship between the objectives. When calculating overall accommodation, which is the proportion of drivers who have met all four design objectives, an accurate result can be given. Otherwise, assumptions would need to be made on who is disaccommodated on more than one design objective.

Anthropometric accommodation is described as the proportion of intended users who are within the range of desired objectives (91). Frequently, a percentile method is only suitable for univariate accommodation models. With multiple objectives, adding and subtracting cannot accurately combine accommodation results (92). One common approach to assess multivariate accommodation is through the intersections of sets, because of the comparable nature of the two mechanisms (93). While performing set intersection, set correlation is considered. For a pair of positively related variables, the intersection can be calculated as:

$$P(A \cap B) = r_{AB} * (SD_A * SD_B) + P(A) * P(B) \quad (4.18)$$

where r_{AB} is the correlation between the two variables, and SD_A and SD_B are the standard deviations. For negatively related (disjoint) variables, the correlation is zero, which simplifies the calculation to:

$$P(A \cap B) = P(A) * P(B) \quad (4.19)$$

Intersection of sets is a well-known method and has been validated with simulation data (93). However, the effort of studying variable correlations is costly. Since this work conducts design assessments for each individual in the population, a sequence of true/false indicators can be assigned to them instead. The outcome of assessing each design objective is either true or false. For such binary assessment, an indicator function assigns a value of 0 or 1 to each event based on the accommodation condition (93). In this work, a total of four design objectives were assessed, so each virtual driver was assigned four binary digits to indicate their accommodation. For instance, if the indicator functions generate 1-1-1-1 for a driver, the driver is expected to be accommodated on all four objectives. Similarly, a 1-1-1-0 indicates that the driver failed the downward vision requirement (the fourth test) but is accommodated on all others.

4.3 Bus Driver Population

The cascade model used in this work passes information through a sequence of models. The outputs from the previous model become the inputs to the next model. To improve the reliability of the final results, users can (1) choose the most appropriate model and (2) increase the fidelity of the inputs, namely vehicle geometry and driver population anthropometry. This section discusses the U.S. bus driver population and the available information that can be used in this work.

4.3.1 Anthropometric Database

Conventionally, military studies are the main source of anthropometric data for many design references and standards. Due to the large quantity of reported measures and rigorous methods of data collection, the 1988 U.S. Army Anthropometry Survey (ANSUR I) has been arguably the most frequently used anthropometric database globally. ANSUR I reported 132 directly measured dimensions and derived an additional 60 dimensions from each of the 3,982 U.S. military personnel (1,774 men and 2,208 women). It also included the demographic information, such as age, race, and ethnicity, to make it possible to sample from the most appropriate population (94). However, this does not represent the general U.S. civilian population well, especially

for dimensional extremities. For instance, obesity is underrepresented in the military. Because of the military's strict selection requirements, ANSUR I and II data reflect a young, healthy, and athletic population. If a design for the civilian population uses ANSUR I or II data to simulate user interaction, the result will not be reliable (95).

Over time, secular trends in increased body size made the ANSUR I data inappropriate for even military use and a follow-up study was conducted in 2012. This used a broader sampling strategy and added whole-body scans. ANSUR II collected measurements from a total of 6,068 participants (4,082 men and 1,986 women), including reservists, and found that weight, circumferences, and breadths had all increased. It also found that the variation in these measurements had increased (Figure 4.6). ANSUR II replaced ANSUR I and was made publicly available in 2017 (9). Even though it is not an explicitly accurate approximation of the U.S. civilian population, it still contains useful information and can be used in the early phases of research.

The results from ANSUR II reflected that secular trends over the previous 30 years are noticeable and significant. Unlike ANSUR I and II, the National Health and Nutrition Examination Survey (NHANES) has been conducted continuously in the United States since 1999 (96). This sampling method makes it a suitable tool to analyze demographic trends in civilian populations. The most important observation is that mean mass (body weight) and BMI have both been increasing, especially weight, which agrees with ANSUR II (97). One of the biggest advantages of NHANES is the oversampling strategy. By oversampling the tails of the anthropometric distribution, the underrepresented groups are included at a higher frequency, which ensures that there are plenty of data in these groups. Thus, each measured individual has an associated weight that indicates the size of the population they represent. In the 1980s, UMTRI designed manikins of various sizes by combining NHANES anthropometric data and stereophotogrammetry. This knowledge was then applied in automobile design (98, 99, 100). One distinct disadvantage of the NHANES data is that they only collect a limited number of measurements, such as stature, mass, and BMI. However, data synthesis methods (101, 102, 103) can be used to estimate the desired body dimensions through known relationships in more detailed datasets like ANSUR II. Once the appropriate detailed U.S. bus driver anthropometry data are available, they can be used as inputs to the cascade model.

4.3.2 Bus Driver Demographics

The four main types of bus drivers in the United States are school bus drivers, local transit bus drivers, intercity bus drivers, and charter bus drivers. Data from the Bureau of Labor Statistics show that in 2018, among all 681,400 bus driver jobs, 497,500 (73%) were provided by schools and special clients. Transit and intercity bus drivers held about 183,800 (27%) of jobs (Table 4.1).



Figure 4.6. Examples of ANSUR II data collection methods (9).

Table 4.1. Industry composition of U.S. bus drivers in 2018.

Type	Count	Percentage
School and client	497,500	73.01%
Intercity and transit	183,800	26.97%
Others	100	0.015%
Total	681,400	100%

Many bus drivers operate through heavy traffic or bad weather, and sometimes deal with unruly passengers. Because of the road hazards and mental stress, bus drivers have one of the highest rates of injuries and illnesses of all occupations (104). Unlike many other jobs, bus drivers have a spatially limited workstation. While driving, they frequently maintain a driving posture for hours before taking a break. Thus, a well-designed bus cab can significantly improve the working conditions for a driver.

While designing a bus cab, proper driver demographics must be specified. Otherwise, the final design would be inappropriate and ineffective. In 1987, a study on urban transit buses used in Hong Kong discovered that many buses were designed based on European anthropometric data and were built in the United Kingdom. This resulted in bus workstations that were not suitable for the Cantonese workforce (105). This study showed that the designs for one racial or ethnic group do not necessarily accommodate another racial or ethnic group. This fact raises the challenge in the United States because the U.S. workforce has become more diverse not only in racial or ethnic composition, but also in gender composition, age, and other aspects. The next few sections report and discuss U.S. bus driver demographics, with the aim of understanding the driver population and providing important design guidelines.

4.3.3 Gender Composition

In the past several decades, many occupations have been dominated by either men or women. This was true especially before World War II. For instance, the secretarial workforce was almost exclusively women, and the commercial driver workforce was limited to men (106). However, the demographics have shifted in the United States in recent years. In 2020, the U.S. Department of Labor reported that women comprised 47% of the total U.S. labor force (107). This trend of improved participation of women is also present in the commercial driver workforce.

Despite earlier increases in participation from women in the commercial driver workforce, according to the American Community Survey (ACS) provided by the Census Bureau, the ratio of men to women has been consistent over the past few years (2014–2017). In 2018, men were 54.7% of the workforce to 45.3% women (108). As the years go by, a small fluctuation is observed in the total number of drivers and the gender composition, but overall they remain about the same (Table 4.2). Thus, this ratio should be used as the default for driver demographics, posture

Table 4.2. U.S. bus driver gender composition 2014–2017.

Year	Men	Women	Total by Year	Percentage Men	Percentage Women
2014	401,946	331,576	733,522	54.8%	45.2%
2015	424,168	347,898	772,066	54.9%	45.1%
2016	406,475	333,660	740,135	54.9%	45.1%
2017	393,972	334,603	728,575	54.1%	45.9%
Total by Gender	1,626,561	1,347,737	2,974,298	—	—
Average	—	—	—	54.7%	45.3%

prediction, and accommodation assessment. However, this ratio only represents the national average and could vary in different regions or due to specific driving responsibilities. To maintain reliability of the bus design, industry designers need to conduct driver demographics studies and modify the men-to-women ratio to best represent the driver population. More detailed information on gender composition can be found in Appendix B.

4.3.4 Race and Ethnicity

The United States is currently the third-largest country in the world by population and is known for its diversity. As of 2018, the White population constituted the majority at 76.4%, and the Black or African American population stood second at 13.4% (108). Such racial and ethnic composition is reflected in the employment market. In 2018, the White and Black or African American population made up 73.6% and 12.0% of total employment in the United States, respectively, which matches closely with the racial and ethnic composition of the population.

Similar to most other occupations, racial and ethnic diversity can be found in the bus driver workforce. ACS showed that the bus driver workforce consists of 62.9% White drivers, 27.7% Black or African American drivers, 2.2% Asian drivers, and 7.2% drivers of other races in 2017. Comparing the racial and ethnic composition of the bus driver workforce to that of the general U.S. workforce, the White population (62.9%) and the Black or African American population (27.7%) dominated with a total of 90.6% of the workforce, which is expected. This was found in previous years as well (Table 4.3). Detailed data of racial and ethnic composition in the bus driver workforce and the entire U.S. job market from 2014 to 2017 are in Appendix B. The percentage of White bus drivers fluctuated between 62.0% and 64.4%, and the percentage of Black or African American bus drivers fluctuated between 27.0% and 28.0% within these 4 years. This indicates that the relatively high prevalence of White and Black or African American drivers is likely to continue for the next several years.

The bus driving occupation is more common in some racial and ethnic groups than others. In 2017, 12.0% of the U.S. workforce was Black or African American employees, but 27.7% of bus drivers were Black or African American. Using racial and ethnic composition in general society as a reference, there were proportionally more Black or African American drivers than White drivers or Asian drivers by a large margin. This phenomenon exists in the previous 4 years as well (as shown in Appendix B). This is strong evidence that the proportion of Black or African American bus drivers in the workforce is about twice the proportion of Black or African American people in the U.S. workforce. Even though the previous observation shows that racial and ethnic diversity in bus drivers mostly match racial and ethnic diversity in the general population, proper adjustments still need to be made for more accurate simulation results.

4.3.5 Age

Besides the men-to-women ratio and racial and ethnic composition, age is another important descriptor of the U.S. bus driver demographics. Most states require their bus drivers to be at least

Table 4.3. U.S. bus driver ethnicity 2014–2017.

Year	White	Black	Asian	Other
2014	64.4%	27.0%	1.9%	6.7%
2015	63.1%	27.5%	2.3%	7.1%
2016	62.0%	28.0%	2.5%	7.5%
2017	62.9%	27.7%	2.2%	7.2%
Average	63.1%	27.6%	2.2%	7.1%

18 years old. Some require commercial drivers who drive across state lines to be 21 or older. A maximum age limit does not exist. Instead, interstate bus drivers must successfully complete a physical exam every 2 years, per federal regulations (108).

As discussed, men constitute 54% of the bus driver workforce and women constitute 46%. The data show a noticeable age difference in the two genders as well. According to the ACS, with a 95% confidence level, the average age for bus drivers in 2017 was 54.5 years for men and 49.7 years for women (Table 4.4), an age difference of 4.8 years. In the previous 3 years, 2014 to 2016, a similar age difference was observed at 4.6, 4.1 and 4.8 years, respectively. This trend is plotted in the average age chart in Appendix B. This trend is expected to continue.

The age distribution charts from 2014 to 2017 (see Appendix B) not only indicate an age difference between these two genders, but also showed how age impacts the bus driver workforce. One of the observations is that the age distribution is skewed left. In other words, the number of drivers gradually increases with age until it reaches the average age. Once past the average age, the number of drivers decreases with age at a faster rate. This observation is likely to be the result of a combination of experience requirements and physical capabilities. Another observation is that the majority of the bus driver workforce is between 45 and 70 years of age for men and between 40 and 65 years for women. Thus, designers need to strategically tailor the anthropometry database by matching population characteristics to best represent bus driver demographics.

4.3.6 Weighted Population Approach

In the previous sections, descriptors (gender ratio, racial/ethnic composition, and age distribution) regarding bus driver demographics were drawn from the ACS. Many similarities exist between the U.S. bus driver population and the U.S. civilian population, but there are noticeable differences. One of the solutions to address this issue is to start over and conduct a new survey specifically designed for the U.S. bus driver population. This solution is intuitive and direct, but the disadvantages outweigh the advantages. To capture most characteristics of the desired demographics without biases, the sample size must be large enough for the data to be reliable. In addition, the participants must be recruited from all over the nation to avoid regional bias. After collecting data from this large sample group, it would be equally challenging to sync and analyze the data. For these and other reasons, conducting a new survey is impractical.

As discussed, many surveys, such as ANSUR I, ANSUR II, and NHANES, have already been conducted to gather detailed anthropometric data from military and civilian populations. Identifying methods that would facilitate the use of these existing data would be advantageous. Consequently, methods that will allow the use of existing data for new populations are needed.

Table 4.4. U.S. bus driver age distribution 2014–2017.

Year/Gender	30 or lower	30 to 40	40 to 50	50 to 60	60 to 70	70 or older
2014/Men	6.8%	10.0%	17.8%	30.7%	25.9%	8.9%
2014/Women	5.7%	15.4%	29.5%	34.2%	13.4%	1.7%
2015/Men	7.1%	10.2%	19.3%	28.7%	25.4%	9.3%
2015/Women	6.8%	13.9%	29.3%	32.2%	16.0%	1.9%
2016/Men	7.2%	10.8%	17.5%	28.3%	26.8%	9.5%
2016/Women	7.3%	16.3%	26.8%	32.8%	14.8%	2.1%
2017/Men	6.5%	10.5%	17.8%	27.9%	27.6%	9.8%
2017/Women	6.5%	16.8%	26.5%	31.6%	15.9%	2.8%
Men Average	6.9%	10.4%	18.1%	28.9%	26.4%	9.4%
Women Average	6.6%	15.6%	28.5%	32.7%	15.0%	2.1%

Fortunately, researchers have studied this subject and have come up with a number of methods. Among these, downsampling and weighting are the most effective for the situation at hand.

Downsampling removes individuals from an existing database until those that remain represent the desired population, i.e., the target user population. This method is simple and intuitive, but it has its limitations. One of the associated weaknesses is that the downsampling wastes a lot of information. Depending on how well the unmodified database matches the target population, a significant amount of data can be lost (103). Without adequate data, there is a high risk of introducing bias. Another challenge is the difficulty of maintaining flexibility in the data. As mentioned, industry users may need to adjust the driver demographics to suit a specific need. Once the database is downsampled, the change is irreversible. There may not be enough data to produce accurate results for a specific driver group. For these reasons, downsampling is not suitable for this work.

Unlike downsampling, weighting the data uses all the available data. A sampling weight is assigned to each person, indicating the proportion of the target population who have similar characteristics (103). In other words, the weighting method manipulates the demographic composition of the database by modifying how much each person matters. Designers are usually responsible for adjusting the weights. For example, if a database contains 500 men and 100 women, designers can make this 5:1 men-to-women ratio behave as 1:1 by assigning a weight of 1 to all the men and assigning a weight of 5 to all the women. Weighting is a common method of modifying a database to meet requirements. An example can be found in the National Automotive Sampling System (NASS), which modified a civilian database into a desired vehicle crash population using weighting (109).



CHAPTER 5

Bus Packaging Results

When packaging a bus, several design parameters need to be considered. This work exclusively discusses drivers' accommodation in the X-Z plane and addresses concerns regarding spatial fitting of components, driver safety, and a driver's ability to see objects around the cab. To provide meaningful feedback to the industry users, the following design parameters are used:

- Steering wheel pivot location
- Steering wheel tilt angle adjustment
- Steering wheel telescope distance adjustment
- Steering wheel diameter
- Seat fore-aft adjustment
- Seat vertical adjustment
- UDLO location
- Cowl point location
- Tip of dashboard location
- Tip of front bumper location
- AHP location

When packaging a bus, industry users must carefully select these parameters to ensure the majority of the driver population are accommodated on all four design objectives, as discussed in Chapter 3.

Apart from bus geometry, driver population profile is also a critical contributor to the success of a design because a bus package made for one population may not be suitable for another. In fact, the wrong match could cause driver fatigue and other safety hazards (110). The United States is known for its diverse population, and this diversity is reflected in the bus driver workforce. To reflect U.S. bus drivers, this chapter uses a 55:45 men-to-women ratio.

This chapter presents the outcomes of the cascade model by showing the predicted reference points and body landmarks in a virtual bus cab. It is important to be aware that the location of these points depends on bus cab geometry. The virtual bus cab shown in this chapter only serves as visual representation and can be altered to meet the specific needs of the industry user. Similarly, the population is reduced to 1,000 individuals (550 men and 450 women) to make the accommodation rate math easier to follow in the example.

5.1 Steering Wheel

Steering wheel location prediction is the first step of cascade modeling and becomes the input for the following steps. Each preferred location is described with an angle and a distance from the pivot. With a total of 1,000 virtual drivers, 1,000 steering wheel locations are generated, and they

form a fan-shaped cluster of points where purple represents men and yellow represents women (Figure 5.1).

Through calculation, men's preferred steering wheel locations were found to be farther away from the pivot than women's by 20 mm on average, which is expected given that stature is an input to the model and, as a population, men are generally taller than women. The steering wheel tilt angles are almost identical across the two genders. This outcome indicates that driver's postural preference is independent of gender when controlled for stature.

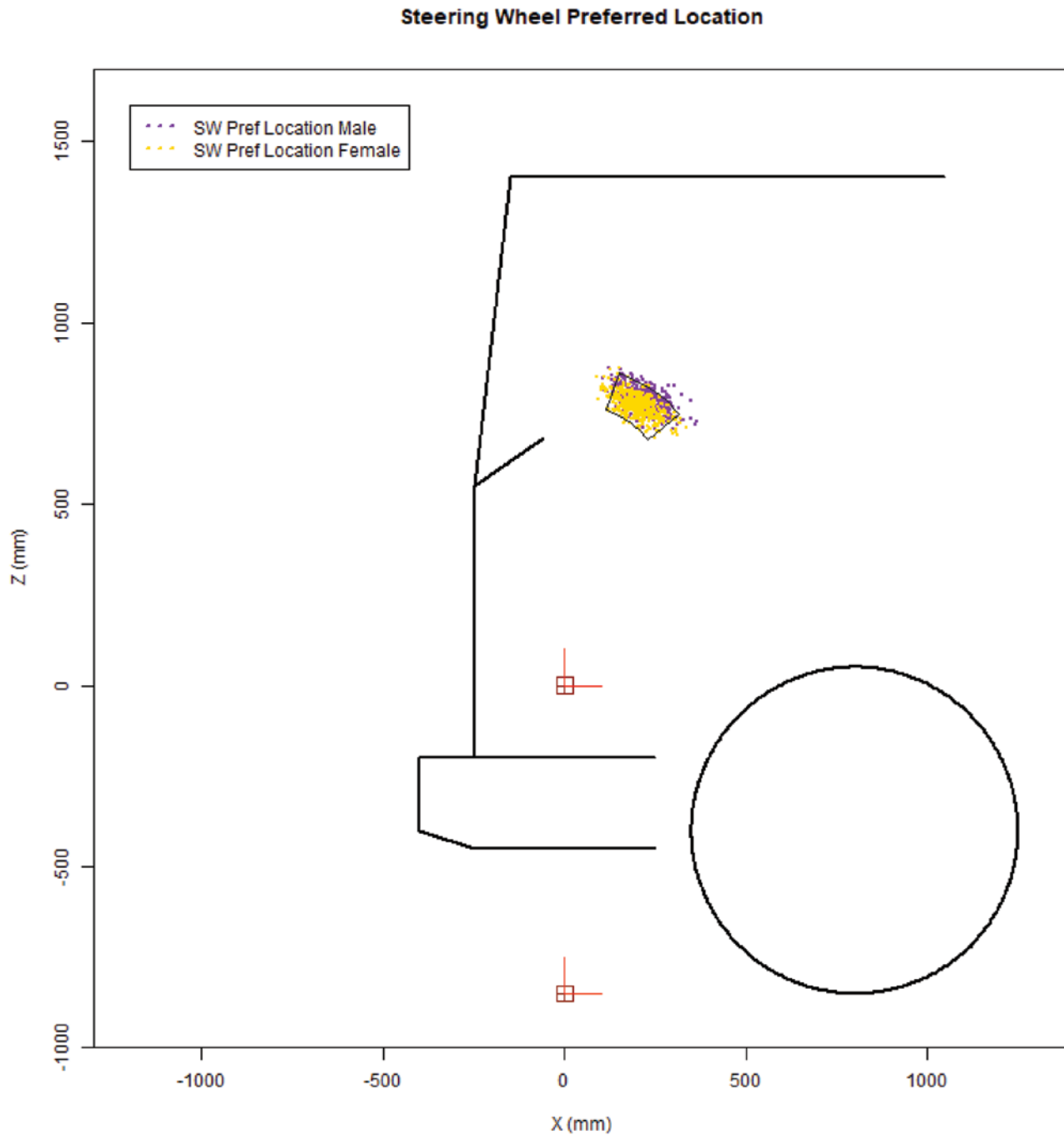


Figure 5.1. The preferred steering wheel locations for the virtual population of men and women truck drivers.

44 Assessing Lifecycle and Human Costs of Bus Operator Workstation Design and Components

In some cases, a large enough adjustment envelope may be constructed to accommodate all the virtual drivers, but for the purpose of demonstration, a smaller adjustment envelope is chosen, and the disaccommodated drivers are marked in red (Figure 5.2). The adjustment is provided through a combination of telescoping and tilting about the pivot point.

For this specific bus layout, the pivot of the steering wheel is at (20 mm, 500 mm) with respect to the AHP. The steering wheel has a telescoping range of 275 mm to 385 mm and a tilt angle

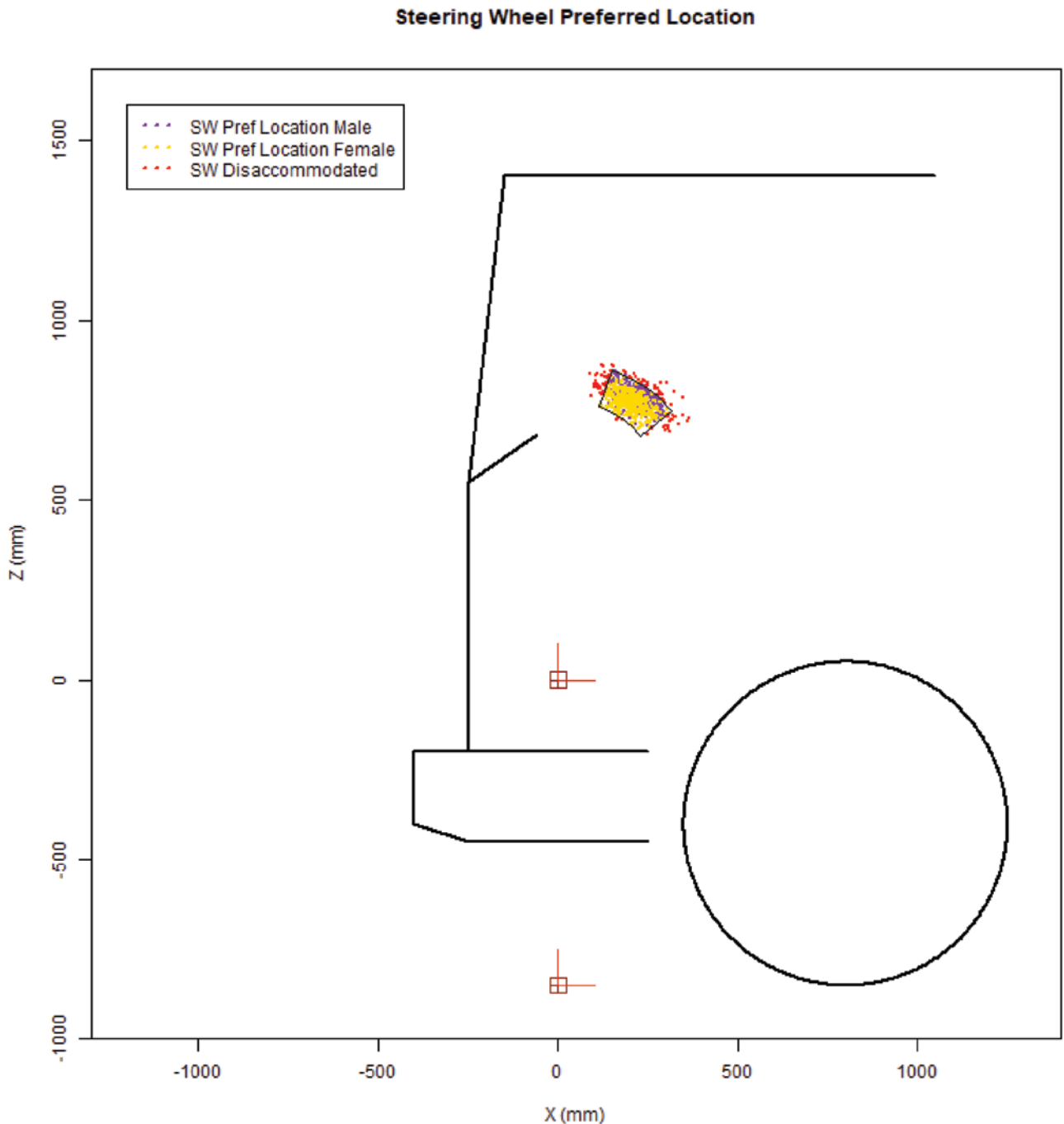


Figure 5.2. The preferred steering wheel locations that are not accommodated by the steering wheel adjustability range.

of 20° to 50° from the vertical direction. Among the 1,000 virtual drivers, a total of 100 were disaccommodated (52 men and 48 women), which means an 89.6% and 90.4% accommodation rate for men and women, respectively. Considering gender ratio, the total accommodation is 90.0%. When a driver is disaccommodated, they would adjust the steering wheel to the nearest point on the envelope and adjust the rest of their body to adapt to the change. After applying such adjustment to all 100 disaccommodated drivers, the steering wheel locations shown in Figure 5.3 are achieved.

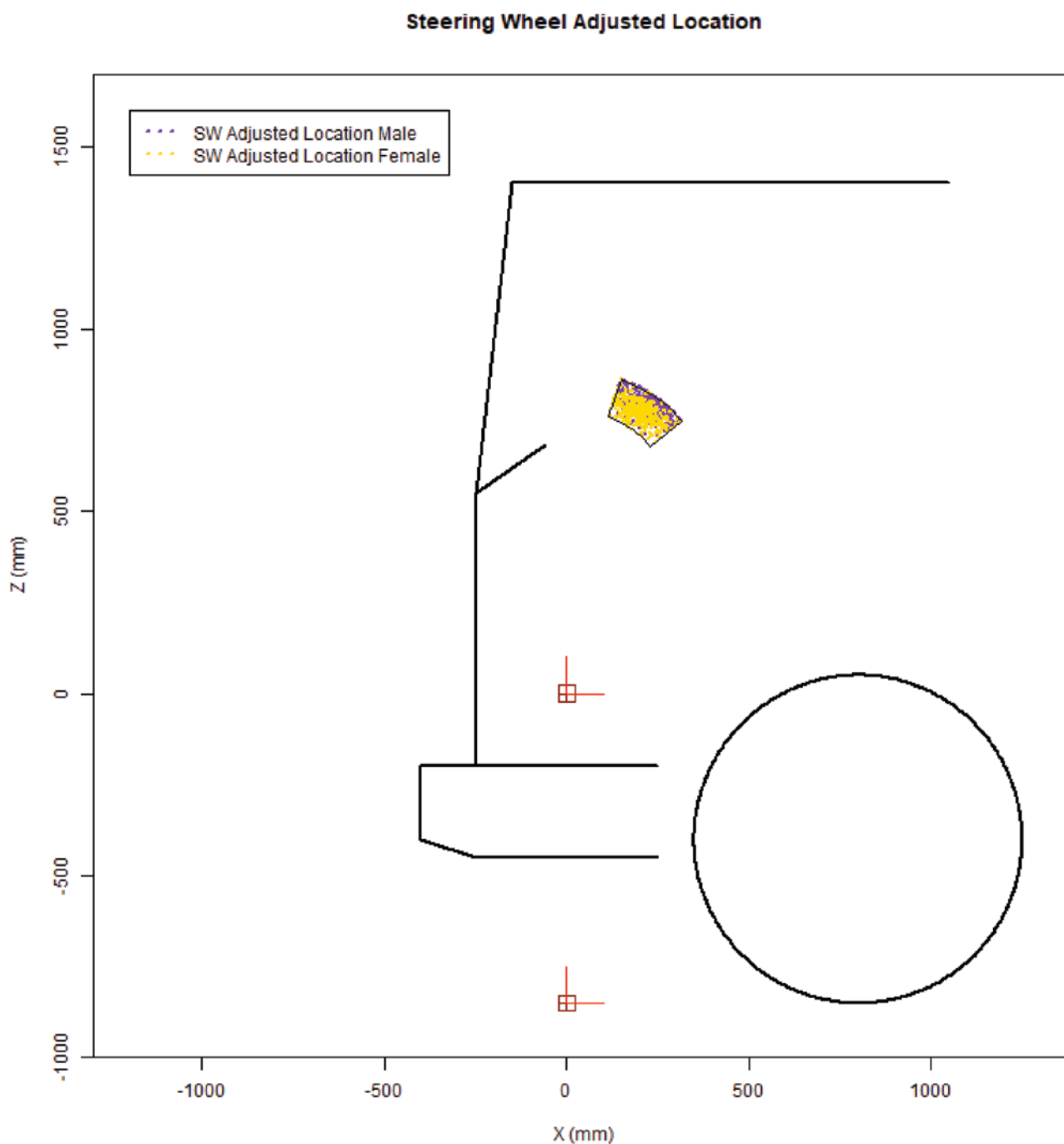


Figure 5.3. The adapted preferred steering wheel locations—those outside the adjustability envelope have been moved to the nearest location inside it.

5.2 H-Point

Once the steering wheel locations are predicted and adjusted, the cascade model can proceed to seat position. Again, 1,000 preferred seat locations were generated. Due to the variation in average size across gender, the preferred seat locations of male drivers are expected to be farther away from the AHP, and this expectation is supported by data. On average, they move the seat 54 mm more in the X direction and 15 mm more in the Z direction than female drivers (Figure 5.4).

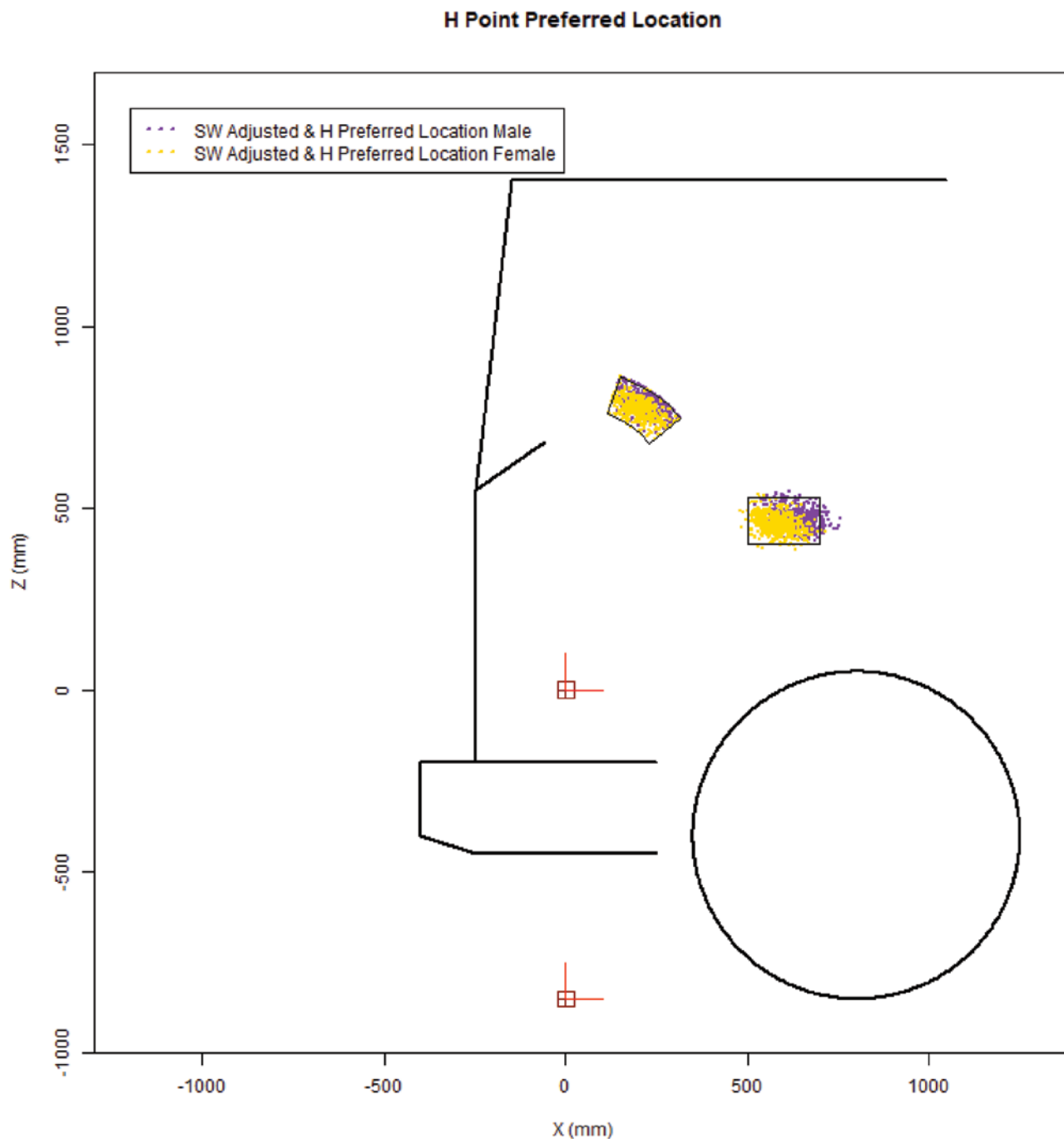


Figure 5.4. The preferred seat (*H*-point) locations for the virtual driving population.

In this work, a limited adjustment range of the seat, 500 mm to 700 mm in the X direction and 400 mm to 530 mm in the Z direction, is used to demonstrate disaccommodation. This adjustment envelope leads to a 90.6% accommodation rate for men and a 96.6% for women, with a combined rate of 93.6%. Among all the disaccommodated drivers, 47 are men and 17 are women. Disaccommodated drivers are shown in red (Figure 5.5).

Similar to disaccommodated steering wheel locations, disaccommodated seat locations are moved to the nearest point on the envelope, and the drivers are expected to adjust their posture

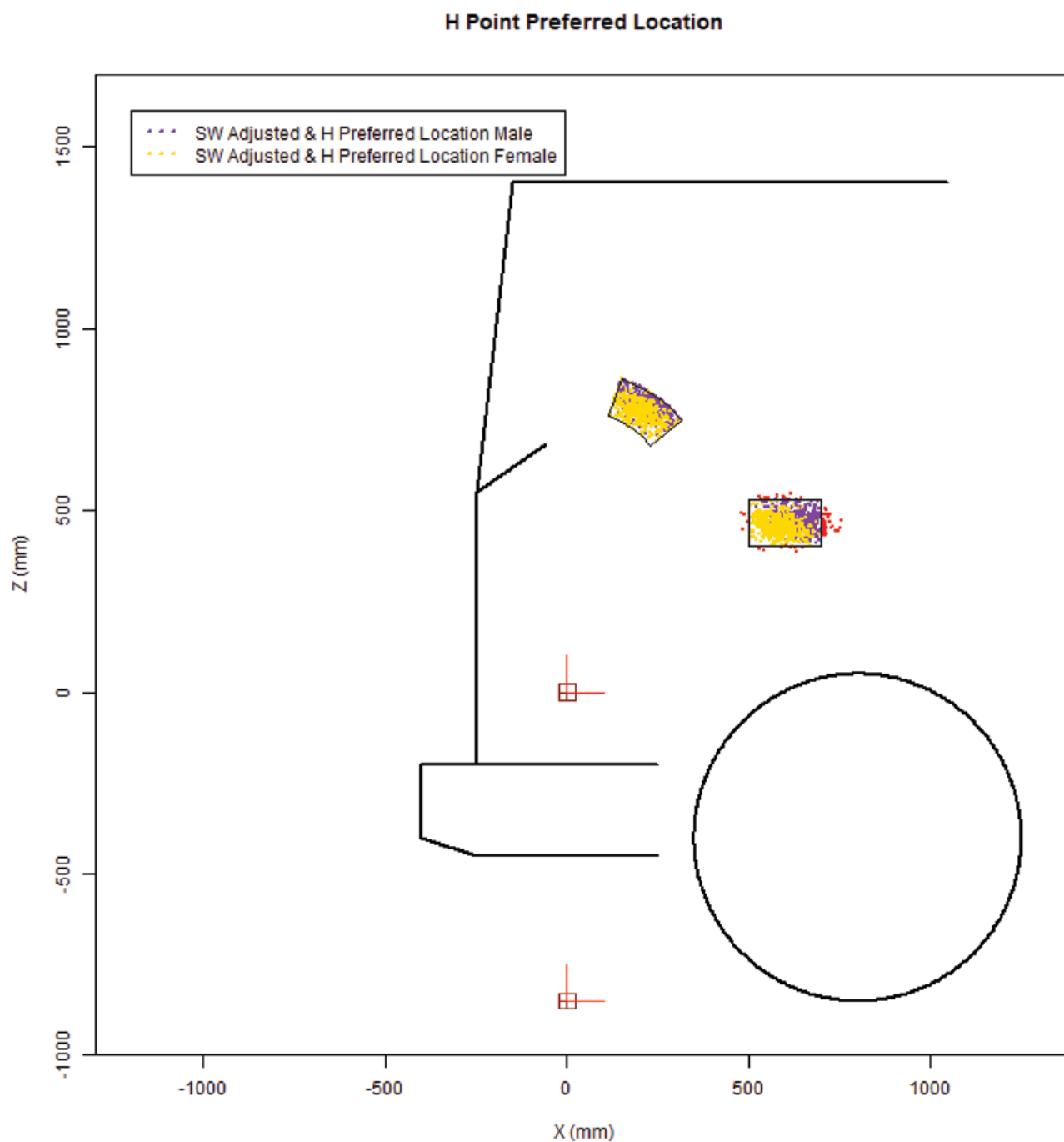


Figure 5.5. The preferred seat (H-point) locations that are not accommodated (i.e., they are outside the adjustability range).

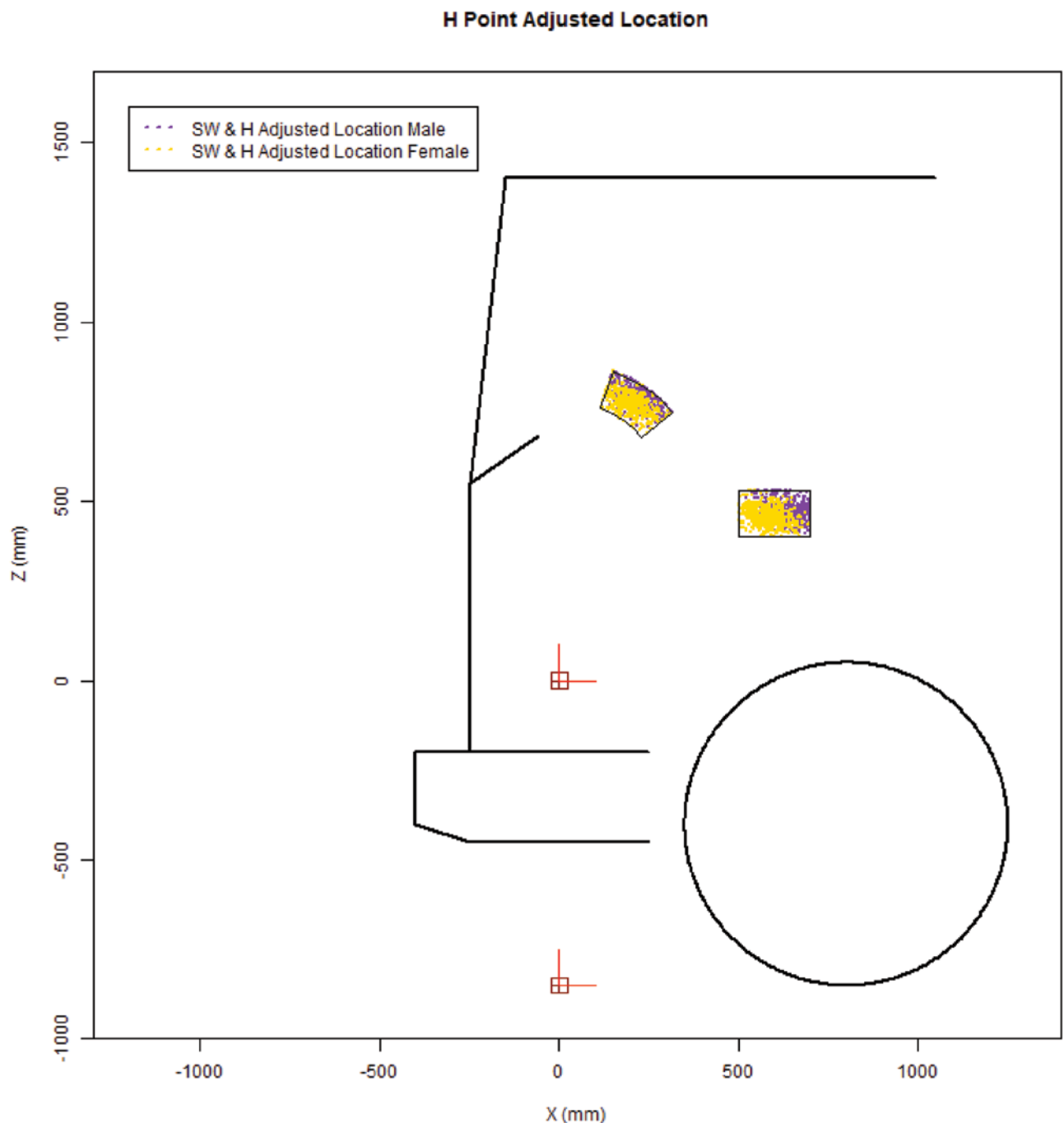


Figure 5.6. *The seat locations of disaccommodated drivers have been relocated to the nearest point inside the adjustability envelope.*

to adapt to this change. Although such adjustment is not ideal, it happens frequently. In some cases these changes are subtle and not noticed; in others they can lead to injury or reduced performance. The effect of driver self-adjustment is shown in Figure 5.6.

5.3 Eye Point

After having both steering wheel locations and seat locations successfully predicted, eye locations can be found using steering wheel and seat locations as inputs. For both men and women, the clusters of points are elliptical. Similar to seat position, the eye locations of men are farther

away from the AHP than the eye locations of women by an average of 49 mm and 66 mm in the X and Z directions, respectively (Figure 5.7).

As mentioned in Chapter 4, a main safety requirement is that drivers must be able to see 14° above the horizontal plane, and the UDLO is usually the limiting factor. Due to the large size of most buses, the UDLO is usually very high, and the upward vision requirement is rarely a concern. In this work, the UDLO is positioned significantly lower compared to other transit buses in order to demonstrate disaccommodation on this measure. For this specific bus layout, 95.4% of the male drivers and 100% of female drivers, 97.7% combined, meet the upward vision requirement. Disaccommodated drivers are shown in red in Figure 5.8.

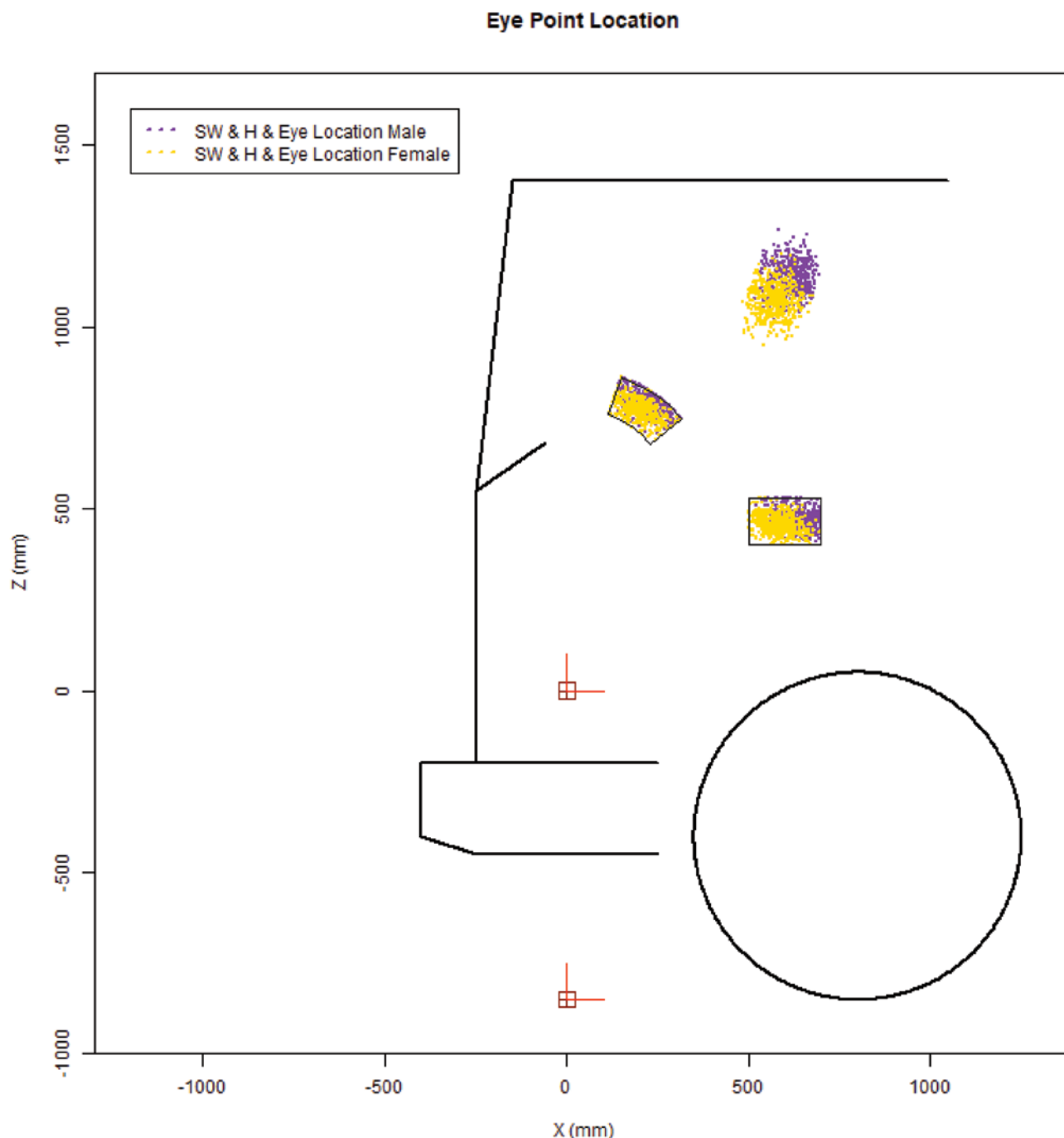


Figure 5.7. The resulting eye locations for the virtual driver population.

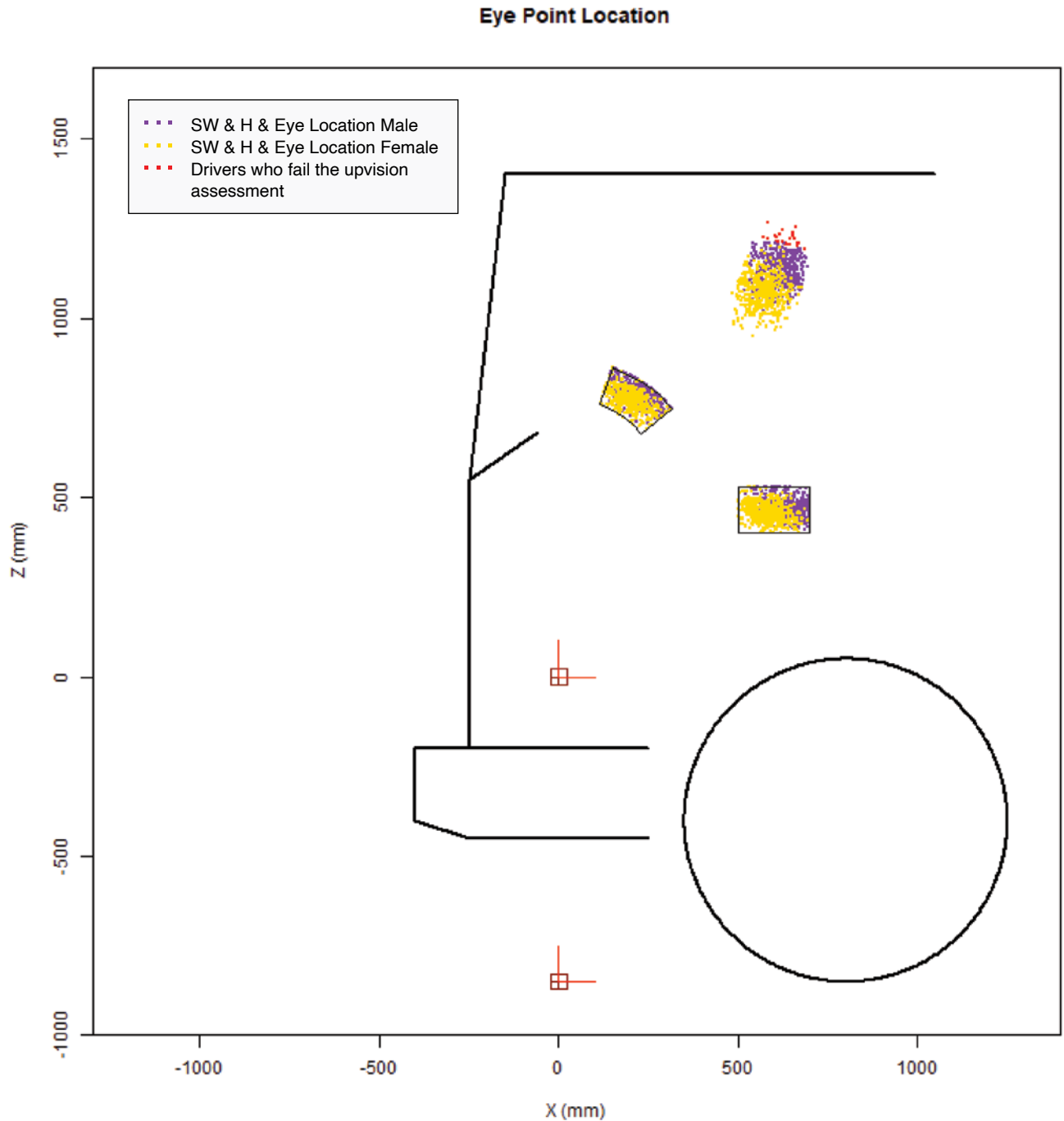


Figure 5.8. UDLO upvision disaccommodation.

In addition to a 14° upvision angle, the APTA requires all bus drivers to be able to see a 42"-tall object 24" in front of the bus. In Figure 5.9 the vertical line represents the object. When a driver looks downward, two components could block their vision: the cowl point and the tip of the dashboard. Depending on driver eye location, either one could be the limiting factor. Only when neither of them blocks driver vision is the requirement met. Given the locations of these components (Figure 5.9), 100% of the male drivers and 96.4% of the female drivers are accommodated on this requirement, which makes a 98.2% combined accommodation.

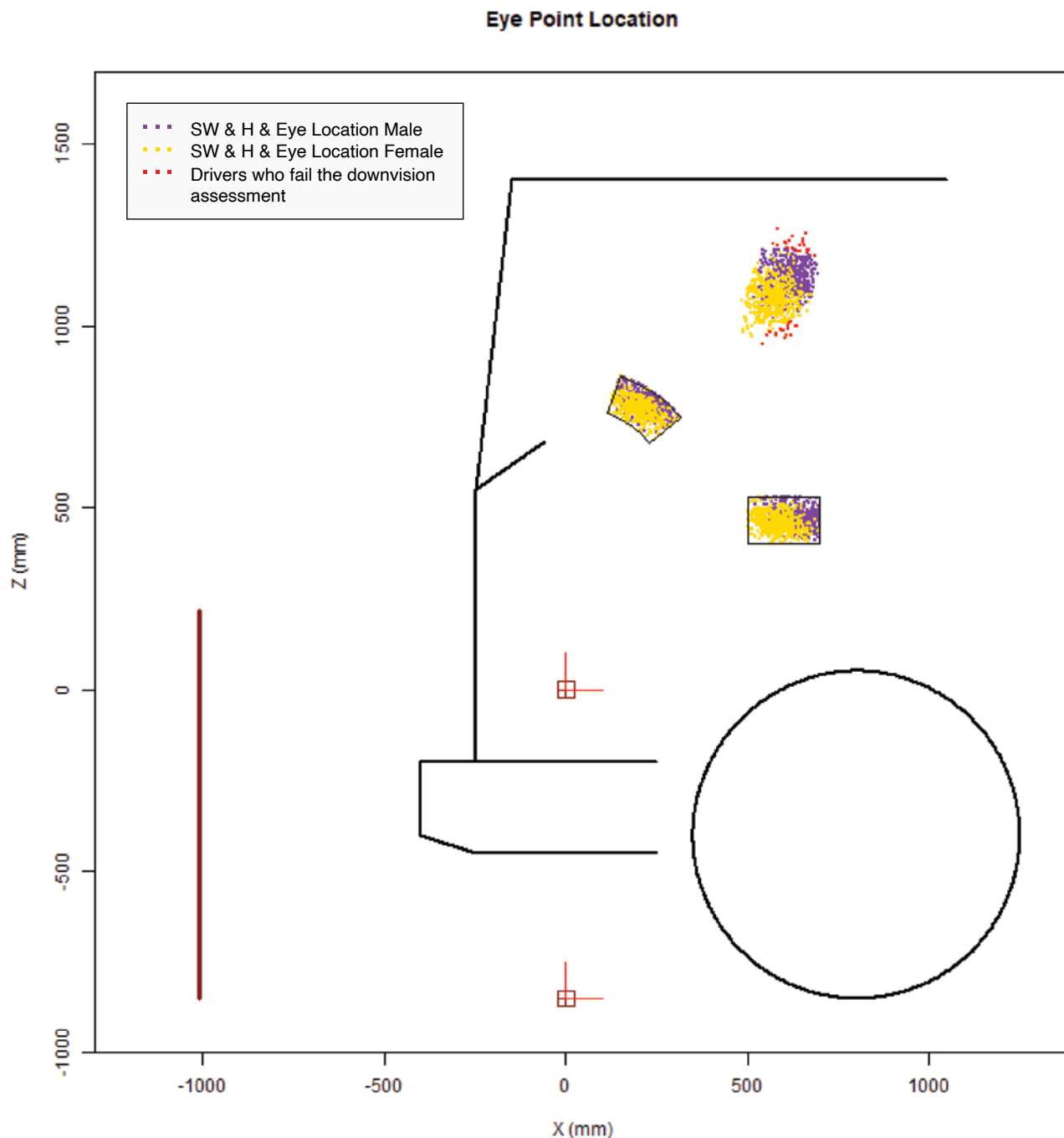


Figure 5.9. *Downvision disaccommodation.*

5.4 Overall Accommodation

Steering wheel location, seat location, and eye location are the three primary considerations in vehicle packaging, and these locations are used to assess all four requirements regarding spatial fit and vision safety (steering wheel, seat, upvision, and downvision). Through previous efforts, the accommodation rate of each requirement can be calculated, but it is of interest to study the overall accommodation. As discussed in Chapter 4, this work applies indicator functions to each virtual driver to gain a thorough understanding of what

Table 5.1. The univariate and multivariate accommodation rates of 1,000 virtual bus drivers.

Gender	Steering Wheel	Seat (H-point)	Upvision	Downvision	Overall
Men	89.6%	90.6%	95.4%	100.0%	80.6%
Women	90.4%	96.6%	100.0%	96.4%	97.0%
Combined	90.0%	93.6%	97.7%	98.2%	83.8%

limitations they are encountering; from there, the overall accommodation rate can be calculated for the 1,000 drivers (Table 5.1).

As shown in Table 5.1, the difference between men and women is noticeable. In general, male drivers tend to sit farther back and higher up with respect to the AHP. This observation is expected because of the variation in body size across genders. In this work, a small bus with limited adjustment ranges was used to effectively illustrate disaccommodation. With this specific layout, a combined population of 83.8% is accommodated; however, the accommodation rate can be improved dramatically by (1) raising the UDLO, (2) lowering the cowl point (where the lower edge of the window meets the vehicle; see Figure 2.3) and the dashboard, and (3) increasing the adjustment ranges of the steering wheel and the seat.

5.5 Other Body Landmarks

The results produced from the cascade model demonstrate its usefulness in packaging a bus as the model delivers instantaneous and quantitative feedback for a design. This work aims to establish a bridge between bus layout and accommodation so designers can effectively make proper changes to their current bus designs, which will ultimately improve drivers' overall well-being.

Besides an accurate and reliable model to predict drivers' interaction with the vehicle, another goal of this work is to provide visualization to industry users to make vehicle packaging a more intuitive process. Specifically, a full body kinematics diagram that represents a human figure would be beneficial. To do this, more body landmarks need to be predicted to indicate the locations of body joints. The first step is to locate shoulder joints using linear regressions so the driver's torso can be oriented (Figure 5.10).

A normal driving posture is when a driver is operating a vehicle without taking additional actions, such as spinning the steering wheel or braking. While drivers are maintaining a normal driving posture, their hands are expected to be placed on the lower quarter of the steering wheel. With hand location, shoulder location, and body dimensions being known, drivers' upper limbs can be configured using inverse kinematics. Similarly, a driver's foot tends to gently tap on the accelerator pedal while driving, so their ankle joint is relatively static to the AHP. With information on their leg lengths, drivers' lower limbs can also be configured (Figure 5.11).

5.6 "Average" Driver

Chapter 2 discussed the percentile model and demonstrated that the percentile approach is incapable of consistently producing accurate posture prediction. One of the arguments is that an n th-percentile person does not exist due to human variability. In spite of that weakness, the model can be used as a visualization tool to show driving postures because an n th-percentile person can certainly exist in a virtual world. In Figure 5.12, the green lines represent an "average" man with average body dimensions throughout, and the orange lines represent an "average" woman.

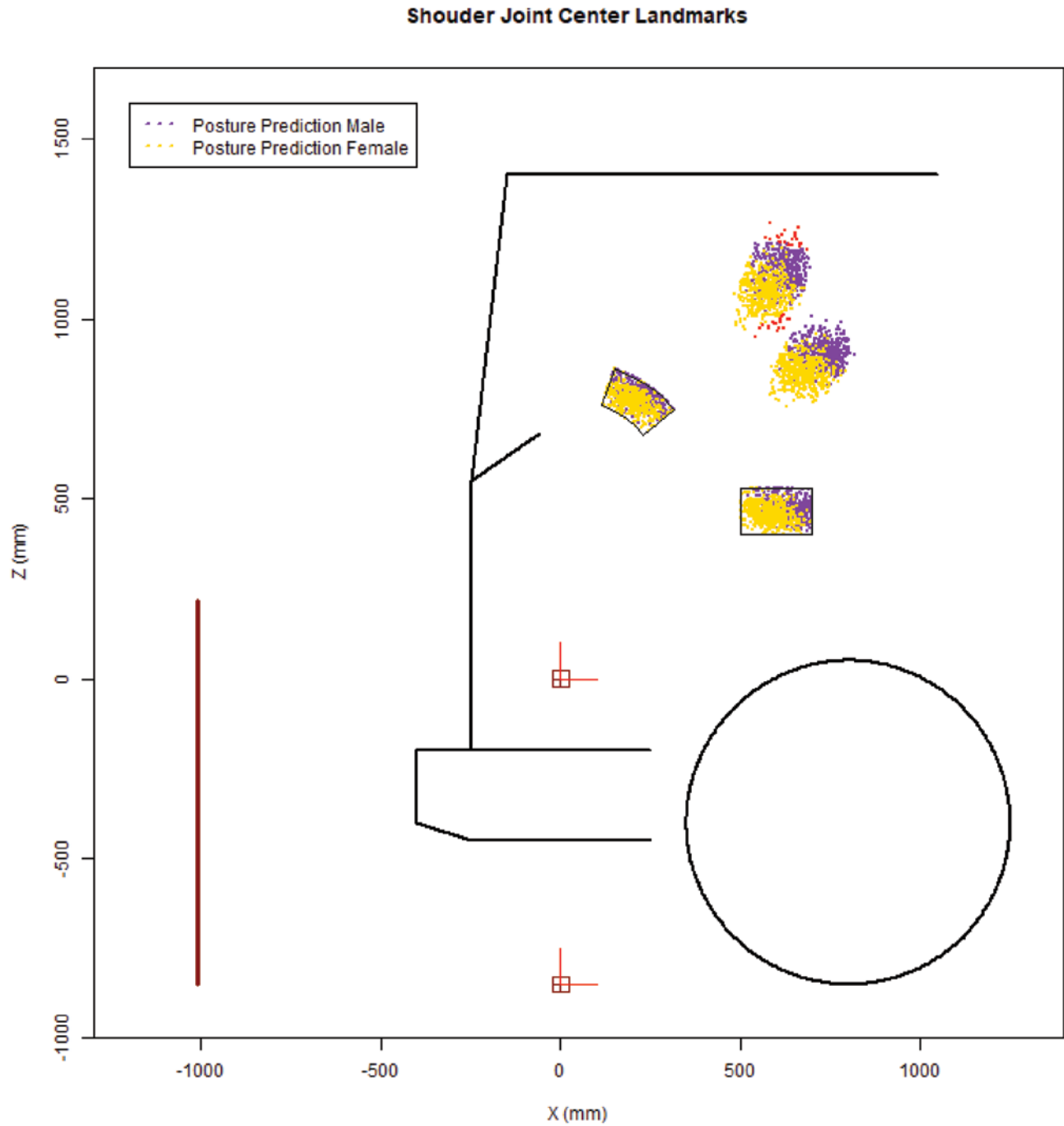


Figure 5.10. *The predicted shoulder locations for the virtual population of drivers.*

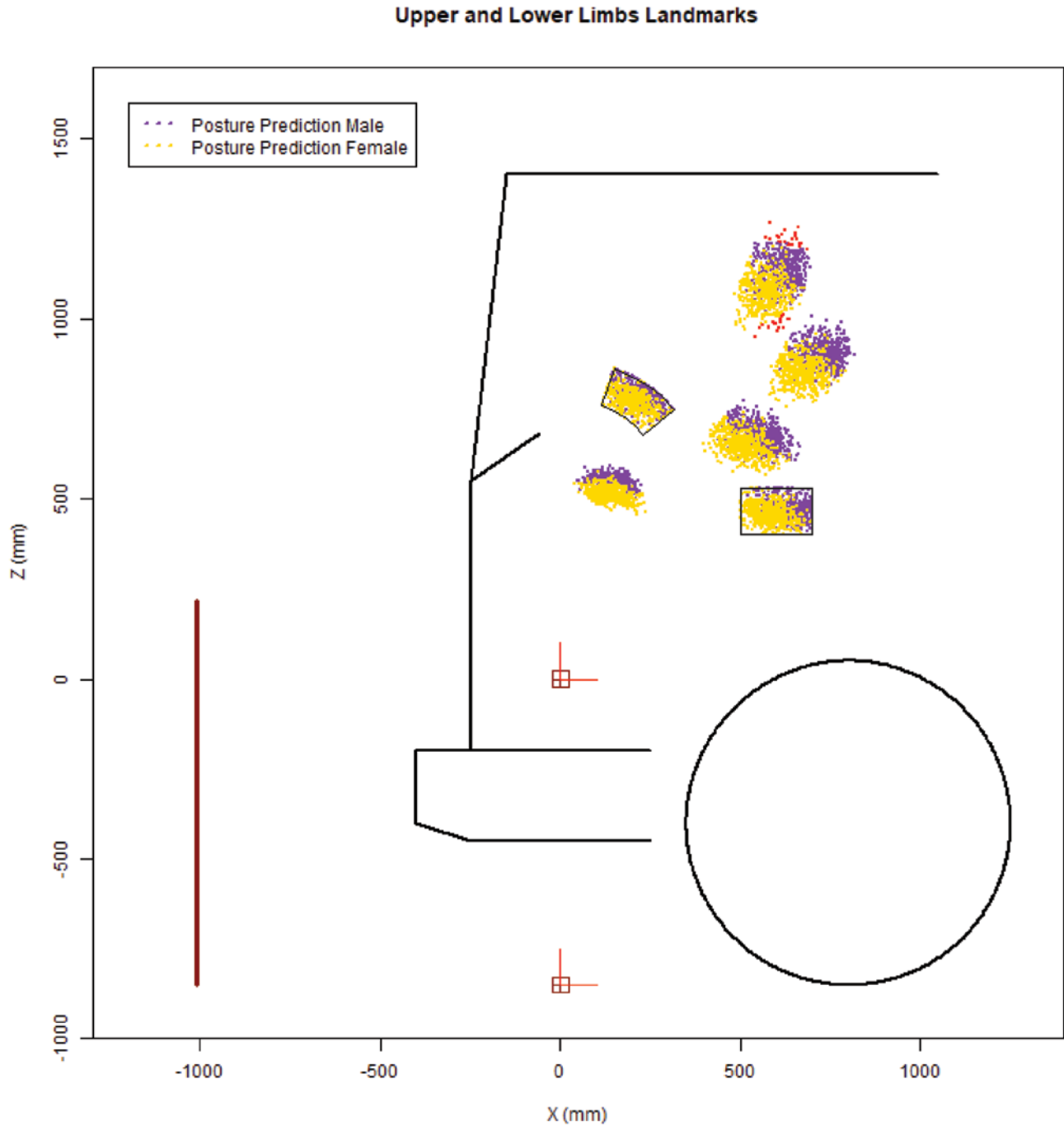


Figure 5.11. Predicted elbow and knee locations have been added to the plot.

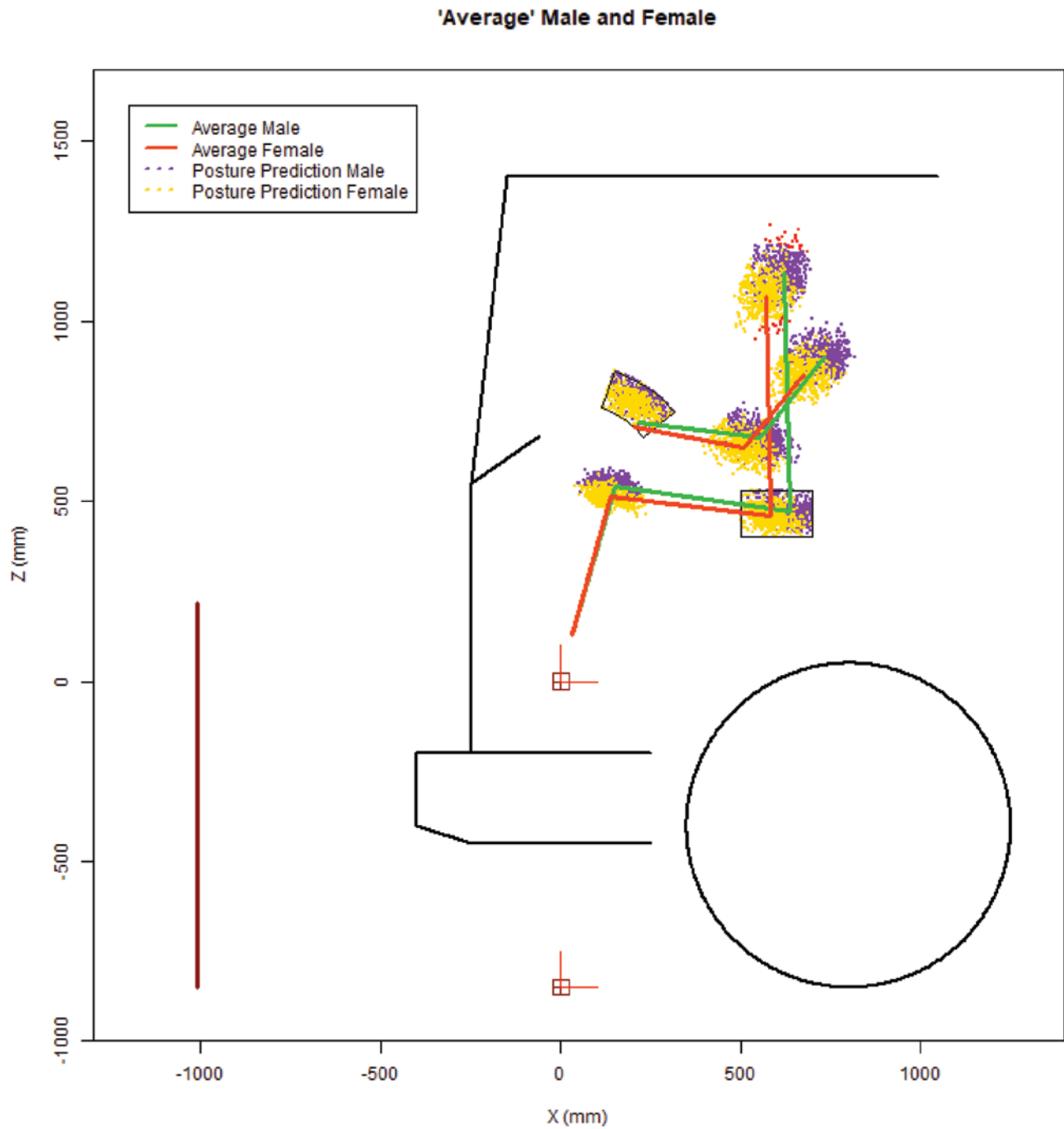


Figure 5.12. Stick figures representing the “average” man and woman superimposed on the distribution of locations across the population.

Figure 5.13 shows how the average locations for an entire population can vary from the preferred location for a single “average” driver. The plot shows the average joint center and component locations for 500 virtual men that have been postured using the model. Plotted against this is the representation of a man who is 50th-percentile by stature. The two drivers have significantly different postures, and it would be inaccurate to assume a driver with 50th-percentile stature would be 50th-percentile on other body dimensions. This limitation was identified more than 60 years ago (46).

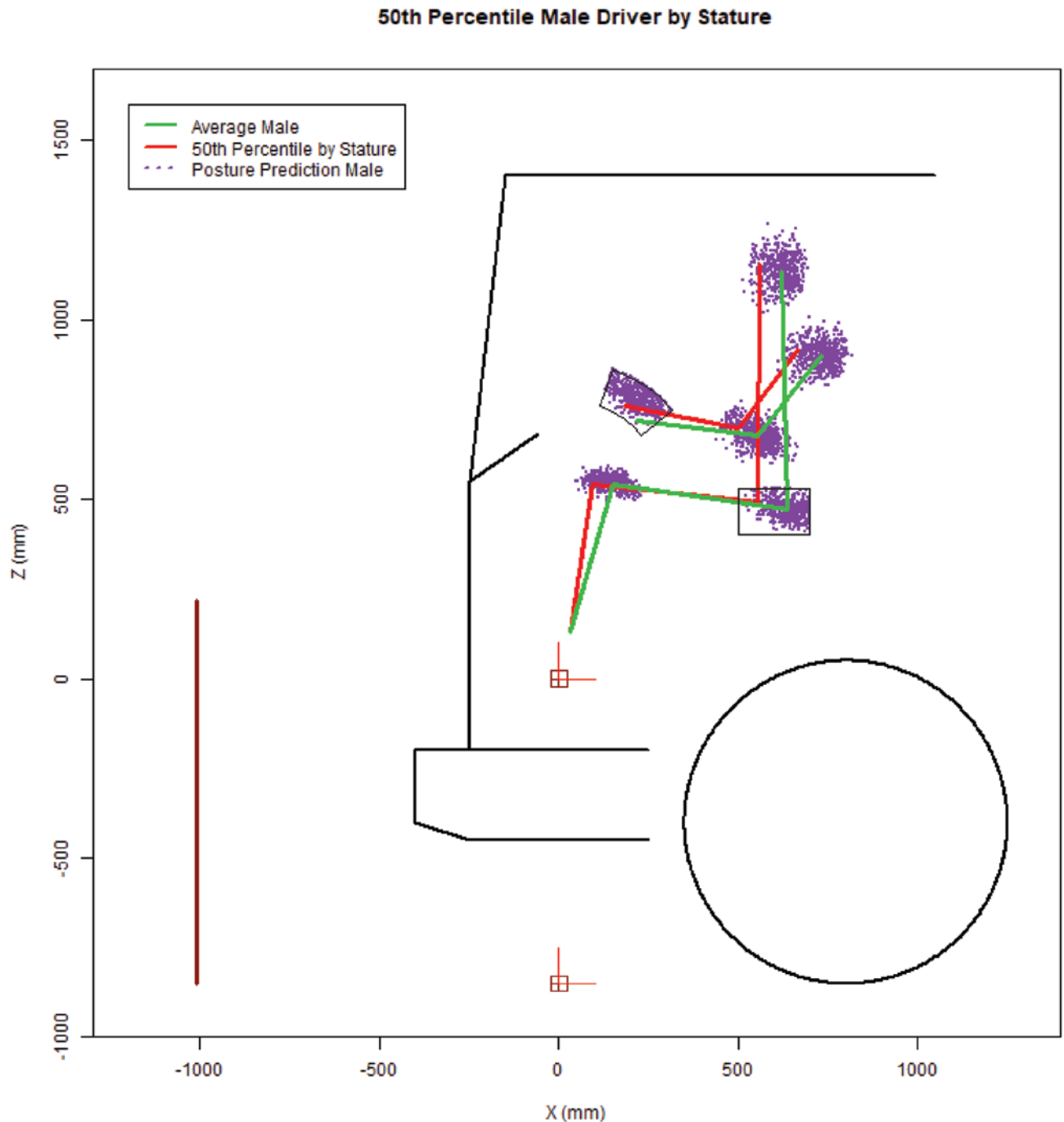


Figure 5.13. The locations of 500 drivers and their average plotted with a single “average” male driver.

5.7 RULA

This work dedicates a large amount of effort to driver posture prediction and configuration of each driver's posture as joints and links. It is of interest to use this information to investigate musculoskeletal health, because bus drivers are known for their critical work environment. As discussed in Chapter 3, they operate the vehicle in a spatially limited workstation and are expected to maintain the same posture for hours. Under such circumstances, they are likely to develop fatigue and musculoskeletal symptoms, which not only deteriorate health but also increase the likelihood of an accident. In fact, this is one of the reasons bus drivers leave the bus transportation industry (111).

Aiming to quantitatively study drivers' posture-related fatigue, a rapid upper limb assessment (RULA) is used. RULA is a method of estimating the risks of upper limb fatigue and disorders through work-related postures. It receives inputs such as body angles and force requirements to predict individual workers' ergonomic risk factor (5). In recent years, RULA has been widely used for assembly workers who repetitively perform certain tasks and has proved a valuable tool to evaluate workers' risk factors (112). Although RULA puts a great emphasis on the upper limbs, factors such as leg support and torso angle are also considered, which makes it a suitable method to assess bus drivers' work conditions. The RULA worksheet is shown in Figure 5.14.

After carefully estimating the force loads in the upper and lower body while driving with a normal posture, a RULA is carried out for each driver. The final RULA score, indicating the ergonomic risk factor, is the outcome of the assessment. On a scale of 1 to 7, the associated actions to be taken are:

- 1–2: acceptable posture
- 3–4: further investigation, change may be needed
- 5–6: further investigation, change soon
- 7: investigate and implement change

The results show that all 1,000 virtual drivers scored 3, which indicates their driving postures put them at low ergonomic risk, and the need for a posture change is minimal. Although drivers may experience discomfort at times, especially when driving for too long, ergonomic risk is not likely to become a major concern. In addition, drivers' postures vary, but the variation is not large enough to dramatically impact ergonomic risk factors. Therefore, it is unnecessary to repetitively conduct RULAs for each virtual driver after conducting it once.

RULA Employee Assessment Worksheet

Task Name: _____

Date: _____

A. Arm and Wrist Analysis

Step 1: Locate Upper Arm Position:



Step 1a: Adjust...
 If shoulder is raised: +1
 If upper arm is abducted: +1
 If arm is supported or person is leaning: -1

Upper Arm Score

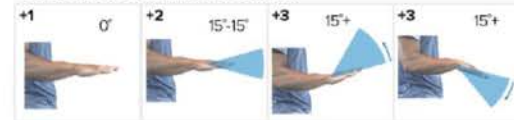
Step 2: Locate Lower Arm Position:



Lower Arm Score

Step 2a: Adjust...
 If either arm is working across midline or out to side of body: Add +1

Step 3: Locate Wrist Position:



Step 3a: Adjust...
 If wrist is bent from midline: Add +1

Step 4: Wrist Twist:

If wrist is twisted in mid-range: +1
 If wrist is at or near end of range: +2

Wrist Twist Score

Wrist Score

Step 5: Look-up Posture Score in Table A:

Using values from steps 1-4 above, locate score in Table A

Posture Score A

Step 6: Add Muscle Use Score

If posture mainly static (i.e. held >1 minute),
 Or if action repeated occurs 4X per minute: +1

Muscle Use Score

Step 7: Add Force/Load Score

If load < 4.4 lbs. (intermittent): +0
 If load 4.4 to 22 lbs. (intermittent): +1
 If load 4.4 to 22 lbs. (static or repeated): +2
 If more than 22 lbs. or repeated or shocks: +3

Force / Load Score

Step 8: Find Row in Table C

Add values from steps 5-7 to obtain Wrist and Arm Score. Find row in Table C.

Wrist & Arm Score

Scores

Table A		Wrist Score						
		1	2	3	4			
Upper Arm	Lower Arm	Wrist Twist	Wrist Twist	Wrist Twist	Wrist Twist			
		1 2	1 2	1 2	1 2			
1	1	1	2	2	2	3	3	3
	2	2	2	2	2	3	3	3
	3	2	3	3	3	3	4	4
2	1	2	3	3	3	3	4	4
	2	2	3	3	3	3	4	4
	3	3	3	4	4	4	4	5
3	1	3	3	4	4	4	4	5
	2	3	4	4	4	4	4	5
	3	4	4	4	4	4	5	5
4	1	4	4	4	4	4	5	5
	2	4	4	4	4	4	5	5
	3	4	4	4	5	5	5	6
5	1	5	5	5	5	5	6	6
	2	5	6	6	6	6	7	7
	3	6	6	6	7	7	7	8
6	1	7	7	7	7	7	8	8
	2	8	8	8	8	8	9	9
	3	9	9	9	9	9	9	9

Table C		Neck, Trunk, Leg Score						
		1	2	3	4	5	6	7+
Wrist / Arm Score	1	1	2	3	3	4	5	5
	2	2	2	3	4	4	5	5
	3	3	3	3	4	4	5	6
	4	4	3	3	3	4	5	6
	5	4	4	4	5	6	7	7
	6	4	4	5	6	6	7	7
	7	5	5	6	6	7	7	7
	8+	5	5	6	7	7	7	7

Scoring (final score from Table C)
 1-2 = acceptable posture
 3-4 = further investigation, change may be needed
 5-6 = further investigation, change soon
 7 = investigate and implement change

RULA Score

B. Neck, Trunk and Leg Analysis

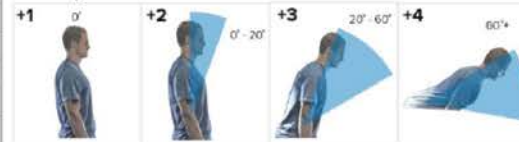
Step 9: Locate Neck Position:



Neck Score

Step 9a: Adjust...
 If neck is twisted: +1
 If neck is side bending: +1

Step 10: Locate Trunk Position:



Trunk Score

Step 10a: Adjust...
 If trunk is twisted: +1
 If trunk is side bending: +1

Step 11: Legs:
 If legs and feet are supported: +1
 If not: +2

Leg Score

Neck Posture Score	Table B: Trunk Posture Score											
	1	2	3	4	5	6						
1	1	3	2	3	3	4	5	5	6	6	7	7
2	2	3	2	3	4	5	5	5	6	7	7	7
3	3	3	3	3	4	4	5	5	6	6	7	7
4	4	5	5	5	6	6	7	7	7	7	8	8
5	7	7	7	7	7	8	8	8	8	8	8	8
6	8	8	8	8	8	8	8	9	9	9	9	9

Step 12: Look-up Posture Score in Table B:

Using values from steps 9-11 above, locate score in Table B

Posture B Score

Step 13: Add Muscle Use Score

If posture mainly static (i.e. held >1 minute),
 Or if action repeated occurs 4X per minute: +1

Muscle Use Score

Step 14: Add Force/Load Score

If load < 4.4 lbs. (intermittent): +0
 If load 4.4 to 22 lbs. (intermittent): +1
 If load 4.4 to 22 lbs. (static or repeated): +2
 If more than 22 lbs. or repeated or shocks: +3

Force / Load Score

Step 15: Find Column in Table C

Add values from steps 12-14 to obtain Neck, Trunk and Leg Score. Find Column in Table C.

Neck, Trunk, Leg Score

Figure 5.14. An example RULA worksheet (10).

Discussion and Bus Packaging Software Tools

This work aimed to provide increased understanding of anthropometric variability of U.S. bus drivers and their postural preferences while driving. To achieve this, a cascade posture prediction approach was used with linear regression models verified for posture prediction. Using this method, a total of 1,000 virtual drivers were successfully postured in a given bus cab. Based on the accommodation conditions shown in the model, proper design recommendations can be made. This chapter discusses the recommendations and presents an overview of the cascade model and its software applications.

6.1 Observation and Reflection

As discussed, a driver's body landmarks and the vehicle interior components, such as the steering wheel and seat, are all measured from the AHP. Intuitively, smaller drivers tend to posture themselves closer to the AHP for comfort and task-oriented considerations. However, this observation is not always true due to human variability and preference unrelated to anthropometry. As research has shown, an n th-percentile person, who has all n th-percentile body dimensions, does not exist. In fact, people vary tremendously from each other, and anthropometric variability and preference are expected to contribute enormously to the final driving posture of a driver. Even among people with similar body dimensions, a large degree of variation still exists, as shown in the "average" male and 50th-percentile-stature male comparison in Chapter 5. This observation indicates that human variability in preference plays a critical role in how drivers posture themselves in a bus.

Although there has been a lot of literature on the distribution of locations of the H-point and the driver eye point, research on steering wheel location is limited. In some vehicles, steering wheels have only one mode of adjustment (tilting), and drivers are expected to achieve a comfortable driving posture by moving the seat. In the case of buses and most other large vehicles, the steering wheels are designed to move on two axes with rotating and telescoping mechanisms. In the cascade model developed for buses and trucks, steering wheel location prediction is the first step and serves as an input for seat location prediction and eye location prediction. Therefore, it is critical to select a proper pivot location and provide an adequate adjustment range for the steering wheel. These factors not only improve drivers' hand grip comfort, but also make it easier to accommodate the preferred seat and eye locations.

In this work, a spatially limited bus cab was chosen to demonstrate disaccommodated conditions. The cab layout accommodates the majority of the preferred body configurations, which are the centers of the clusters of points shown in Chapter 5. In other words, for each body landmark (indicated as a cluster of points) the highest frequency of occurrence is at the center. Extending outward, the frequency of occurrence decreases. The farther the distance, the larger the decrease. Researchers have found that body dimensions can be approximated as Gaussian

distributions. Since drivers' posture is predicted using linear regression models with variance, it is implied that drivers' posture is also normally distributed in the dimensional space of each predicted measure.

6.2 Cascade Model Overview

This work uses estimated anthropometry of U.S. bus drivers. This data passes through a sequence of posture prediction models and becomes an invaluable part of representing preferred driving posture. Two critical design concerns, spatial fitting and driving safety, are analyzed for accommodation during each step of the prediction process. Spatial fitting is usually limited by the adjustment envelope, and drivers can sometimes compromise on a less desirable posture and achieve comfort by adjusting the rest of their bodies to adapt. Driving safety is assessed by driver's ability to maintain adequate vision during driving. The outcomes of the analysis indicate the overall quality of a bus package and indicate directions to improve the design.

The posture prediction models are carried out in a cascading manner such that the output of the previous step becomes the input of the next step. Starting with steering wheel location prediction, the cascading process then directs its focus to seat location and eye location, which are the critical reference points in vehicle packaging. Following that, other body landmarks can be configured, such as shoulder joint, elbow joint, knee joint, and ankle joint. A schematic diagram of the cascading approach is shown in Figure 4.2.

6.3 Applications

The objective of this work was to investigate the effect of human variability in vehicle packaging and deliver tools to assist in the design of workstations for U.S. bus drivers. The goals were met by applying the fundamental principles of the cascading posture prediction model throughout this research in the use of linear models that incorporate residual variance to predict landmark locations for each virtual driver and reverse kinematics to configure body posture. The outcomes of this research are delivered in an Excel spreadsheet.

The spreadsheet tool is primarily for industry users who are packaging buses and assessing candidate designs. Due to the complexity of the subject and the learning curve of using a new tool, an intuitive software tool with visuals is highly desirable. In the tool, users can change the bus geometry, adjustment range of the components, and driver demographics. The tool automatically performs posture prediction for each virtual driver and assesses the design. Results are presented in two forms: (1) a table that summarizes the accommodation rates of each of the four design objectives (steering wheel location, seat location, upvision, and downvision) and the overall accommodation rate, and (2) a pictorial representation of the bus layout and the body landmarks. It allows users to see how the drivers are accommodated so they can make proper adjustments to the design.

In the Excel spreadsheet the inputs are used to construct a frontal layout of a bus, a seat track adjustment envelope, and a steering wheel adjustment envelope (Figure 6.1). An example of the table outputs that display univariate and multivariate accommodation rates is shown in Figure 6.2, and an example of the pictorial outputs is shown in Figure 6.3.

6.4 Limitations and Future Work

This work primarily studies bus drivers' posture and uses it to assess bus packages in the X-Z plane because most of the packaging components are designed to be adjustable only in this plane. For example, the steering wheel and the seat are two of the most important design considerations when packaging a bus. They are fixed in the Y direction but are adjustable in the

Bus Geometry (mm)	
ST_X1	475
ST_X2	700
ST_Z1	400
ST_Z2	550
SW_Pivot_X	20
SW_Pivot_Z	500
SW_Diameter	450
SW_Telescop_min	275
SW_Telescop_max	400
SW_Angle_min	20
SW_Angle_max	50
AHP_X	0
AHP_Z	850
Cowl_X	-250
Cowl_Z	1400
Db_X	-60
Db_Z	1550
Bumper_X	-450
Bumper_Z	650
UDLO_X	-150
UDLO_Z	2400

ST	Seat Track
SW	Steering Wheel
Rf	Roof
Db	Dashboard

Figure 6.1. The Excel inputs to the bus packaging tool.

	Up Vision	Down Vision	H point	SW	Total	RULA
Male	100.0%	99.8%	91.8%	94.4%	87.6%	3.0
Female	100.0%	90.2%	98.0%	90.6%	83.0%	3.0
Total	100.0%	97.9%	93.0%	93.6%	86.7%	3.0

Figure 6.2. The Excel outputs from the bus packaging tool.

X-Z plane. By default they are expected to reside in the center plane on the driver's side so the distance from the driver's left hand to the components is the same as from their right hand. In addition to spatial fitting, a driver's central vision is also mainly determined in the X-Z plane due to the windshield setup. By analyzing the two-dimensional accommodation, the majority of design questions can be answered. The software presented can consistently provide predictable results. However, with additional time and resources, a three-dimensional analysis can be performed by augmenting the spatial fitting assessment and the vision safety assessment in the Y direction. For instance, opaque areas of bus structure create blind spots that cannot be effectively monitored by the driver. By knowing a driver's eye point in three dimensions, designers can identify the effective range of the driver's peripheral vision and make appropriate design modifications. With a three-dimensional analysis, parameters such as seat width can also be assessed.

An Excel spreadsheet was developed to help industry users package the driver workstation of a bus. The output summary table quantitatively estimates the percentage of people to be accommodated, and the graphic indicates how to modify the bus layout to improve the accommodation rate. This tool is expected to facilitate the iterative design process and help engineers as they explore vehicle packaging options and the consequences of different decisions. For instance, if a user wants to improve the accommodation rate of upward vision, they can raise the ceiling or lower the seat adjustment envelope. It will be the user's decision to do one or both. To minimize this ambiguity, future research can investigate the cost factors of the components to be packaged so design decisions can be logically made. Once cost factors are quantitatively studied, an overall cost calculation method can be developed and used as an objective function in an optimization study. By setting a target overall accommodation rate and an objective of minimizing cost, the "best" vehicle layout can be found.

62 Assessing Lifecycle and Human Costs of Bus Operator Workstation Design and Components

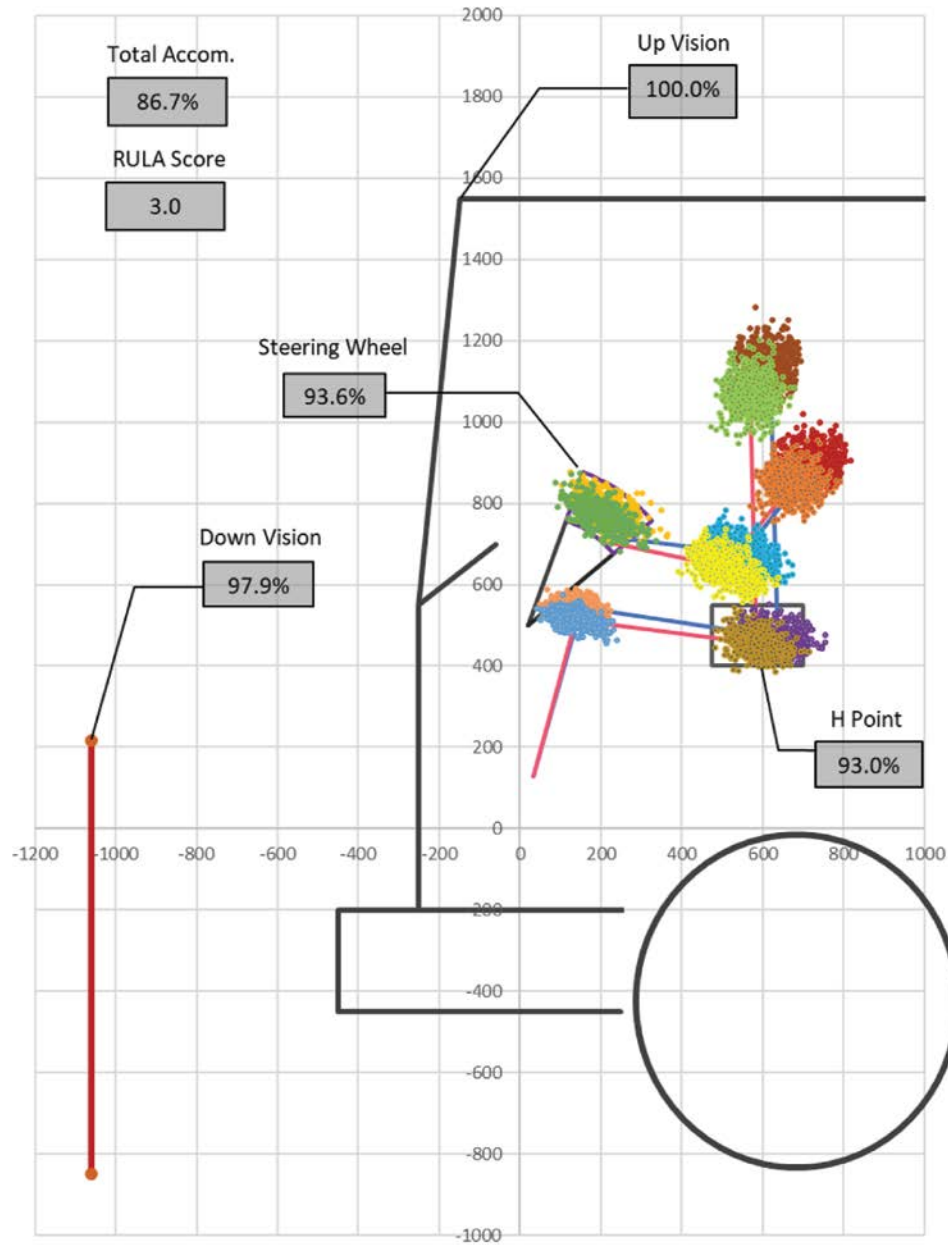


Figure 6.3. The graphical output of the Excel bus packaging tool.



References

1. SAE International. 2009. J1100_200911: Motor Vehicle Dimensions. https://www.sae.org/standards/content/j1100_200911/.
2. Poirson, E., and Delangle, M. 2013. Comparative Analysis of Human Modeling Tools. International Digital Human Modeling Symposium, June 2013, Ann Arbor, MI. <https://core.ac.uk/download/pdf/52994139.pdf>.
3. Parkinson, M. B., and Reed, M. P. 2006. Optimizing Vehicle Occupant Packaging. *SAE Transactions* Vol. 115, Section 6: Journal of Passenger Car: Mechanical Systems Journal, pp. 890–901. <https://www.jstor.org/stable/44667791>.
4. Seth, V., Weston, R. L., and Freivalds, A. 1999. Development of a Cumulative Trauma Disorder Risk Assessment Model for the Upper Extremities. *International Journal of Industrial Ergonomics* 23(4):281–291. [https://doi.org/10.1016/S0169-8141\(98\)00045-6](https://doi.org/10.1016/S0169-8141(98)00045-6).
5. McAtamney, L., and Corlett, E. N. 1993. RULA: A Survey Method for the Investigation of Work-Related Upper Limb Disorders. *Applied Ergonomics* 24(2):91–99. [https://doi.org/10.1016/0003-6870\(93\)90080-S](https://doi.org/10.1016/0003-6870(93)90080-S).
6. Moore, J. S., and Garg, A. 1995. The Strain Index: A Proposed Method to Analyze Jobs for Risk of Distal Upper Extremity Disorders. *American Industrial Hygiene Association Journal* 56(5):443–458. <https://doi.org/10.1080/15428119591016863>.
7. ISO. 2010. Method for Establishment of Eyellipses for Driver's Eye Location. ISO Standard 4513:2022(en)—Road Vehicles—Visibility. <https://www.iso.org/standard/72001.html#:~:text=This%20document%20establishes%20the%20location,percentiles%20of%20driver's%20eye%20locations>.
8. APTA. 2010. *Standard Bus Procurement Guidelines RFP*. <https://www.apta.com/research-technical-resources/standards/procurement/apta-bts-bpg-gl-001-13/>.
9. Gordon, C. C., Blackwell, C. L., Bradtmiller, B., Parham, J. L., Barrientos, P., Paquette, S. P., Corner, B. D., Carson, J. M., Venezia, J. C., Rockwell, B. M., Mucher, M., and Kristensen, S. 2015. *2012 Anthropometric Survey of U.S. Army Personnel: Methods and Summary Statistics*. United States Army Natick Soldier Research, Development and Engineering Center, Natick, MA. <https://dacowits.defense.gov/LinkClick.aspx?fileticket=EbsKcm6A10U%3D&portalid=48>.
10. Middlesworth, M. 2012. A Step-by-Step Guide to the RULA Assessment Tool. <https://ergo-plus.com/rula-assessment-tool-guide/>.
11. Lee, M. W., Yun, M. H., and Lee, J. S. 1996. High Touch: Human Factors in New Product Design. In *Proceedings of the Human Factors and Ergonomics Society 40th Annual Meeting*, pp. 401–405. <https://journals.sagepub.com/doi/pdf/10.1177/154193129604000706>.
12. Slovak, A. J. M. 1996. Review of *Human Variability and Plasticity*, ed. C. G. N. Mascie-Taylor and B. Bogin. *Journal of Epidemiology and Community Health* 50(2):230. <https://www.ncbi.nlm.nih.gov/pmc/articles/PMC1060270/>.
13. Fisher, R. A. 2016. The Causes of Human Variability. *International Journal of Epidemiology* 48(1):7–10. <https://doi.org/10.1093/ije/dyw315>.
14. White, R. M. 1976. Anthropometry as a Variable in Human Factors Engineering. In *Proceedings of the Human Factors Society Annual Meeting* 20(5):131–135. <https://doi.org/10.1177/154193127602000507>.
15. Cho, J., Freivalds, A., and Rovniak, L. S. 2017. Utilizing Anthropometric Data to Improve the Usability of Desk Bikes, and Influence of Desk Bikes on Reading and Typing Performance. *Applied Ergonomics* 60: 128–135. <https://doi.org/10.1016/j.apergo.2016.11.003>.
16. Dianat, I., Molenbroek, J., and Castellucci, H. I. 2018. A Review of the Methodology and Applications of Anthropometry in Ergonomics and Product Design. *Ergonomics* 61(12):1696–1720. <https://www.tandfonline.com/doi/full/10.1080/00140139.2018.1502817>.
17. Shan, G. B. 2008. Sport Equipment Evaluation and Optimization: A Review of the Relationship Between Sport Science Research and Engineering. *The Open Sports Sciences Journal* 1:5–11. <https://opensportssciencesjournal.com/contents/volumes/V1/TOSSJ-1-5/TOSSJ-1-5.pdf>.

18. Oh, S.-Y., Suh, D.-A., and Kim, H.-G. 2016. Last Design for Men's Shoes Using 3D Foot Scanner and 3D Printer. *The Journal of the Korea Contents Association* 16(2):186–199. https://www.researchgate.net/publication/299480842_Last_Design_for_Men's_Shoes_using_3D_Foot_Scanner_and_3D_Printer.
19. Telfer, S., and Woodburn, J. 2010. The Use of 3D Surface Scanning for the Measurement and Assessment of the Human Foot. *Journal of Foot and Ankle Research* 3(19). <https://jfootankleres.biomedcentral.com/articles/10.1186/1757-1146-3-19>.
20. Lee, Y.-C., Lin, G., and Wang, M.-J. J. 2014. Comparing 3D Foot Scanning with Conventional Measurement Methods. *Journal of Foot and Ankle Research* 7(44). <https://jfootankleres.biomedcentral.com/articles/10.1186/s13047-014-0044-7>.
21. Boorla, S. M., Eifler, T., Howard, T. J., and McMahon, C. A. 2017. Mass Production Tools and Process Readiness for Uniform Parts: Injection Molding Application. *Journal of Polymer and Composites* 5(3): 30–40. <https://engineeringjournals.stmjournals.in/index.php/JoPC/article/view/58>.
22. Ituarte, I. F., Coatanea, E., Salmi, M., Tuomi, J., and Partanen, J. 2015. Additive Manufacturing in Production: A Study Case Applying Technical Requirements. *Physics Procedia* 78:357–366. <https://doi.org/10.1016/j.phpro.2015.11.050>.
23. Luximon, Y., and Luximon, A. 2013. Sizing and Grading of Shoe Lasts. In *Handbook of Footwear Design and Manufacture* (A. Luximon, ed.), Woodhead Publishing Limited, pp. 197–215.
24. Buldt, A. K., and Menz, H. B. 2018. Incorrectly Fitted Footwear, Foot Pain and Foot Disorders: A Systematic Search and Narrative Review of the Literature. *Journal of Foot and Ankle Research* 11(43). <https://jfootankleres.biomedcentral.com/articles/10.1186/s13047-018-0284-z#citeas>.
25. Lee, M., S. J. 2019. Change in Waist Circumference with Continuous Use of a Smart Belt: An Observational Study. *JMIR mHealth and uHealth* 7(5). <https://mhealth.jmir.org/2019/5/e10737/>.
26. Yutko, J. M., Jerath, K., and Brennan, S. N. 2010. A Failure Rate Analysis of Complex Vehicles. *International Journal of Heavy Vehicle Systems* 17(1). <https://www.inderscience.com/offers.php?id=29624>.
27. Roe, R. W. 1993. Occupant Packaging. In *Automotive Ergonomics* (B. Peacock and W. Karwowski, eds.), Taylor & Francis, London, Washington, DC, pp. 11–42.
28. Zheng, L., Zhao, N., Chen, D., Hu, M., Fu, X., Stallones, L., Xiang, H., and Wang, Z. 2014. Nonfatal Work-Related Injuries Among Agricultural Machinery Operators in Northern China: A Cross-Sectional Study. *Injury* 45(3):599–604. <https://doi.org/10.1016/j.injury.2013.07.004>.
29. SAE International. 2009. J1050_200902: Describing and Measuring the Driver's Field of View. https://www.sae.org/standards/content/j1050_200902/.
30. Schmidt, S., Amereller, M., Franz, M., Kaiser, R., and Schwirtz, A. 2014. A Literature Review on Optimum and Preferred Joint Angles in Automotive Sitting Posture. *Applied Ergonomics* 45(2)Part B:247–260. <https://doi.org/10.1016/j.apergo.2013.04.009>.
31. Al-Hinai, N., Al Kindi, M., and Shamsuzzoha, A. 2018. An Ergonomic Student Chair Design and Engineering for Classroom Environment. *International Journal of Mechanical Engineering and Robotics Research* 7(5): 534–543. https://www.researchgate.net/publication/327682845_An_Ergonomic_Student_Chair_Design_and_Engineering_for_Classroom_Environment.
32. Lin, L. 2018. Bias Caused by Sampling Error in Meta-Analysis with Small Sample Sizes. *PLoS One* 13(9). <https://journals.plos.org/plosone/article?id=10.1371/journal.pone.0204056>.
33. Abras, C., Maloney-Krichmar, D., and Preece, J. 2004. User-Centered Design. In *Encyclopedia of Human Computer Interaction* (W. Bainbridge, ed.), Sage Publications, Thousand Oaks, CA, pp. 445–456.
34. Norman, D. A. 2005. Human-Centered Design Considered Harmful. *Interactions* 12(4):14–19. <https://doi.org/10.1145/1070960.1070976>.
35. Burchett, H. E. D., Mayhew, S. H., Lavis, J. N., and Dobrow, M. J. 2012. When Can Research from One Setting Be Useful in Another? Understanding Perceptions of the Applicability and Transferability of Research. *Health Promotion International* 28(3):418–430. <https://doi.org/10.1093/heapro/das026>.
36. Mathiassen, S. E., Wells, R. P., Winkel, J., Forsman, M., and Medbo, L. 2002. Tools for Integrating Engineering and Ergonomics Assessment of Time Aspects in Industrial Production. In *Human in a Complex Environment: Proceedings of the 34th Annual Congress of the Nordic Ergonomics Society* (D. Caldenfors, J. Eklund, and L. Kiviloog, eds.), Oct. 1–3, 2002, Kolmården, Sweden, pp. 579–584. https://www.researchgate.net/publication/295513830_Tools_for_integrated_engineering_and_ergonomic_assessment_of_time_aspects_in_industrial_production.
37. Reed, M. P. 2005. *Development of a New Eyellipse and Seating Accommodation Model for Trucks and Buses*. UMTRI-2005-30. University of Michigan Transportation Research Institute, Ann Arbor, MI. <https://rosap.nhtl.bts.gov/view/dot/20426>.
38. Fubini, E., Micheletti Cremasco, M., and Occeili, C. 2012. Human Variability and Ergonomic Design. *Journal of Biological Research* 85(1). <https://doi.org/10.4081/jbr.2012.4134>.
39. Yousaf, K., Iftikhar, A., and Javed, A. 2012. Comparative Analysis of Automatic Vehicle Classification Techniques: A Survey. *International Journal of Image, Graphics and Signal Processing* 4(9). <https://doi.org/10.5815/ijigsp.2012.09.08>.

40. Classes of Comparable Automobiles, 40 CFR § 600.315-08 (2013).
41. SAE International. 2010. J941_201003. Motor Vehicle Drivers' Eye Locations. https://www.sae.org/standards/content/j941_201003/.
42. SAE International. 2008. J826_202106: Devices for Use in Defining and Measuring Vehicle Seating Accommodation. https://www.sae.org/standards/content/j826_202106/.
43. Parkinson, M. B., Reed, M. P., Kokkolaras, M., and Papalambros, P. 2007. Optimizing Truck Cab Layout for Driver Accommodation. *Journal of Mechanical Design* 129(11):1110–1117. <https://doi.org/10.1115/1.2771181>.
44. Damon, A., and McFarland, R. A. 1955. The Physique of Bus and Truck Drivers: With a Review of Occupational Anthropology. *American Journal of Physical Anthropology* 13(4):711–742. <https://doi.org/10.1002/ajpa.1330130412>.
45. Mehta, C. R., Gite, L. P., Pharade, S. C., Majumder, J., and Pandey, M. M. 2008. Review of Anthropometric Considerations for Tractor Seat Design. *International Journal of Industrial Ergonomics* 38(5–6):546–554. <https://doi.org/10.1016/j.ergon.2007.08.019>.
46. McFarland, R. A., Damon, A., and Stoudt, H. W., Jr. 1958. Anthropometry in the Design of the Driver's Work-space. *American Journal of Physical Anthropology* 16(1):1–23. <https://doi.org/10.1002/ajpa.1330160102>.
47. Haslegrave, C. M. 1986. Characterizing the Anthropometric Extremes of the Population. *Ergonomics* (2): 281–301. <https://doi.org/10.1080/00140138608968265>.
48. Huynh, N., Uddin, M., and Minh, C. C. 2017. "Data Analytics for Intermodal Freight Transportation Applications." In *Data Analytics for Intelligent Transportation Applications*, ed. M. Chowdhury, A. Apon, and K. Dey, pp. 241–262. Elsevier Inc.
49. Fromuth, R. C., and Parkinson, M. 2009. Predicting 5th and 95th Percentile Anthropometric Segment Lengths from Population Stature. In *ASME 2008 Conference Proceedings: International Design Engineering Technical Conference & Computers and Information in Engineering*, pp. 581–588. <https://doi.org/10.1115/DETC2008-50091>.
50. Khademi, A. 2016. Applied Univariate, Bivariate, and Multivariate Statistics. *Journal of Statistical Software* 72(2):1–4. <https://doi.org/10.18637/jss.v072.b02>.
51. Hertzberg, H. T. E. 1955. Some Contributions of Applied Physical Anthropology to Human Engineering. *Annals of the New York Academy of Sciences* 63(4):616–629. <https://nyaspubs.onlinelibrary.wiley.com/doi/abs/10.1111/j.1749-6632.1955.tb32114.x>.
52. Das, S., and Sengupta, A. K. 1996. Industrial Workstation Design: A Systematic Ergonomics Approach. *Applied Ergonomics* 27(3):157–163. [https://doi.org/10.1016/0003-6870\(96\)00008-7](https://doi.org/10.1016/0003-6870(96)00008-7).
53. Schultz, K. L., Batten, D. M., and Sluchak, T. J. 1998. Optimal Viewing Angle for Touch-Screen Displays: Is There Such a Thing? *International Journal of Industrial Ergonomics* 22(4–5):343–350. [https://doi.org/10.1016/S0169-8141\(97\)00087-5](https://doi.org/10.1016/S0169-8141(97)00087-5).
54. Schneider, L. W., Reed, M. P., Roe, R. W., Manary, M. A., Flannagan, C. A. C., Hubbard, R. P., and Rupp, G. L. 1999. ASPECT: The Next-Generation H-Point Machine and Related Vehicle and Seat Design and Measurement Tools. SAE Technical Paper 1999-01-0962. <https://doi.org/10.4271/1999-01-0962>.
55. Colombo, G., and Cugini, U. 2005. Virtual Humans and Prototypes to Evaluate Ergonomics and Safety. *Journal of Engineering Design* 16(2):195–203. <https://doi.org/10.1080/09544820500031542>.
56. Robinette, K. M., and McConville, J. T. 1981. An Alternative to Percentile Models. *SAE Transactions* Vol. 90, Section 1: 810010–810234, pp. 938–946. <https://www.jstor.org/stable/44631724>.
57. Garneau, C. J., and Parkinson, M. B. 2011. A Comparison of Methodologies for Designing for Human Variability. *Journal of Engineering Design* 22(7):505–521. <https://doi.org/10.1080/09544820903535404>.
58. Meunier, P., Tack, D., Ricci, A., Bossi, L., and Angel, H. 2000. Helmet Accommodation Analysis Using 3D Laser Scanning. *Applied Ergonomics* 31(4):361–369. [https://doi.org/10.1016/S0003-6870\(00\)00006-5](https://doi.org/10.1016/S0003-6870(00)00006-5).
59. Ekşioğlu, M. 2004. Relative Optimum Grip Span as a Function of Hand Anthropometry. *International Journal of Industrial Ergonomics* 34(1):1–12. <https://doi.org/10.1016/j.ergon.2004.01.007>.
60. Park, B. K. D., and Reed, M. P. 2017. Characterizing Vehicle Occupant Body Dimensions and Postures Using a Statistical Body Shape Model. SAE Technical Paper 2017-01-0497. <https://doi.org/10.4271/2017-01-0497>.
61. Braess, H. H., and Seiffert, U. W., eds. 2009. *Handbook of Automotive Engineering*. SAE International.
62. Christiaans, H. H. C. M., and Bremner, A. 1998. Comfort on Bicycles and the Validity of a Commercial Bicycle Fitting System. *Applied Ergonomics* 29(3):201–211. [https://doi.org/10.1016/S0003-6870\(97\)00052-5](https://doi.org/10.1016/S0003-6870(97)00052-5).
63. Yakou, T., Yamamoto, K., Koyama, M., and Hyodo, K. 1997. Sensory Evaluation of Grip Using Cylindrical Objects. *JSME International Journal Series C Mechanical Systems, Machine Elements and Manufacturing* 40(4):730–735. <https://doi.org/10.1299/jsmec.40.730>.
64. Seidl, A. 1997. RAMSIS—A New CAD Tool for Ergonomic Analysis of Vehicles Developed for the German Automotive Industry. SAE Technical Paper 970088. <https://doi.org/10.4271/970088>.
65. Mahdjoub, M., Monticolo, D., Gomes, S., and Sagot, J.-C. 2009. A Collaborative Design for Usability Approach Supported by Virtual Reality and a Multi-Agent System Embedded in a PLM Environment. *Computer-Aided Design* 42(5):402–413. <https://doi.org/10.1016/j.cad.2009.02.009>.

66. Garneau, C., and Parkinson, M. 2008. "Validating Models of Censored Driver Behavior in Trucks and Buses." Technical report, *International Truck and Engine*.
67. Reed, M., and Flannagan, C. 2000. Anthropometric and Postural Variability: Limitations of the Boundary Manikin Approach. SAE Technical Paper 2000-01-2172. <https://doi.org/10.4271/2000-01-2172>.
68. Reed, M. P., Manary, M., Flannagan, C. A. C., and Schneider, L. W. 2002. A Statistical Method for Predicting Automobile Driving Posture. *Human Factors* 44(4):557–568. <https://doi.org/10.1518/0018720024496917>.
69. Reed, M. P., Manary, M. A., Flannagan, C. A. C., and Schneider, L. W. 2000. Effects of Vehicle Interior Geometry and Anthropometric Variables on Automobile Driving Posture. *Human Factors* 42(4):541–552. <https://doi.org/10.1518/001872000779698006>.
70. Freivalds, A. 2011. *Biomechanics of the Upper Limbs: Mechanics, Modeling and Musculoskeletal Injuries*, 2nd ed. CRC Press, Taylor and Francis, Boca Raton, London, New York.
71. Magnusson, M. L., Pope, M. H., Wilder, D. G., and Areskou, B. 1996. Are Occupational Drivers at an Increased Risk for Developing Musculoskeletal Disorders? *Spine* 21(6):710–717. <https://doi.org/10.1097/00007632-199603150-00010>.
72. Van Der Beek, A., and Frings-Dresen, M. H. W. 1995. Physical Workload of Lorry Drivers: A Comparison of Four Methods of Transport. *Ergonomics* 38(7):1508–1520. <https://doi.org/10.1080/00140139508925205>.
73. Gruber, G. 1976. *Relationships Between Wholebody Vibration and Morbidity Patterns Among Interstate Truck Drivers*. DHEW-PUB-NIOSH77-167. National Institute for Occupational Safety and Health, Division of Biomedical and Behavioral Science, Cincinnati, OH.
74. Tse, J. L. M., Flin, R., and Mearns, K. 2006. Bus Driver Well-Being Review: 50 Years of Research. *Transportation Research Part F: Traffic Psychology and Behaviour* 9(2):89–114. <https://doi.org/10.1016/j.trf.2005.10.002>.
75. Gobel, M., Springer, J., and Scherff, J. 1998. Stress and Strain of Short Haul Bus Drivers: Psychophysiology as a Design Oriented Method for Analysis. *Ergonomics* 41(5):563–580. <https://doi.org/10.1080/001401398186757>.
76. Pope, M. H., Goh, K. L., and Magnusson, M. L. 2002. Spine Ergonomics. *Annual Review of Biomedical Engineering* 4(1):49–68. <https://doi.org/10.1146/annurev.bioeng.4.092101.122107>.
77. Silverstein, B., Welp, E., Nelson, N., and Kalat, J. 1998. Claims Incidence of Work-Related Disorders of the Upper Extremities: Washington State, 1987 through 1995. *American Journal of Public Health* 88(12):1827–1833. <https://doi.org/10.2105/AJPH.88.12.1827>.
78. Szeto, G. P. Y., and Lam, P. 2007. Work-Related Musculoskeletal Disorders in Urban Bus Drivers of Hong Kong. *Journal of Occupational Rehabilitation* 17(2):181–198. <https://doi.org/10.1007/s10926-007-9070-7>.
79. Alperovitch-Najenson, D., Katz-Leurer, M., Santo, Y., Golman, D., and Kalichman, L. 2010. Upper Body Quadrant Pain in Bus Drivers. *Archives of Environmental & Occupational Health* 65(4):218–223. <https://doi.org/10.1080/19338244.2010.486422>.
80. Massaccesi, M., Pagnotta, A., Soccetti, A., Masali, M., Masiero, C., and Greco, F. 2003. Investigation of Work-Related Disorders in Truck Drivers Using RULA Method. *Applied Ergonomics* 34(4):303–307. [https://doi.org/10.1016/S0003-6870\(03\)00052-8](https://doi.org/10.1016/S0003-6870(03)00052-8).
81. Singh, Y. K. 2005. *Instructional Technology in Education*. APH Publishing Corporation, New Delhi.
82. Cuban, L. 2001. *Oversold and Underused: Computers in the Classroom*. Harvard University Press, Cambridge, MA.
83. Smith, G. 2018. Step Away from Stepwise. *Journal of Big Data* 5(32). <https://doi.org/10.1186/s40537-018-0143-6>.
84. Owsley, C., and McGwin, G. J. 2010. Vision and Driving. *Vision Research* 50(23):2348–2361. <https://doi.org/10.1016/j.visres.2010.05.021>.
85. Plantard, P., Muller, A., Pontonnier, C., Dumont, G., Shum, H. P. H., and Multon, F. 2017. Inverse Dynamics Based on Occlusion-Resistant Kinect Data: Is It Usable for Ergonomics? *International Journal of Industrial Ergonomics* 61:71–80. <https://doi.org/10.1016/j.ergon.2017.05.010>.
86. Borbély, B. J., and Szolgay, P. 2017. Real-Time Inverse Kinematics for the Upper Limb: A Model-Based Algorithm Using Segment Orientations. *BioMedical Engineering OnLine* 16(21). <https://doi.org/10.1186/s12938-016-0291-x>.
87. Pizzolato, C., Reggiani, M., Modenese, L., and Lloyd, D. G. 2017. Real-Time Inverse Kinematics and Inverse Dynamics for Lower Limb Applications Using OpenSim. *Computer Methods in Biomechanics and Biomedical Engineering* 20(4):436–445. <https://doi.org/10.1080/10255842.2016.1240789>.
88. de Leva, P. 1996. Adjustments to Zatsiorsky-Seluyanov's Segment Inertia Parameters. *Journal of Biomechanics* 29(9):1223–1230. [https://doi.org/10.1016/0021-9290\(95\)00178-6](https://doi.org/10.1016/0021-9290(95)00178-6).
89. Reed, M. P. 2012. *UMTRI Truck Driver Posture Prediction*. University of Michigan Transportation Research Institute.
90. Dove, L. A. 1986. *Teachers and Teacher Education in Developing Countries*. Croom Helm, London, Dover, NH.
91. Roebuck, J. A., Jr. 1995. *Anthropometric Methods: Designing to Fit the Human Body*. Human Factors and Ergonomics Society, Santa Monica, CA.

92. Robinette, K. M. 1998. Multivariate Methods in Engineering Anthropometry. In *Proceedings of the Human Factors and Ergonomics Society 42nd Annual Meeting*, pp. 719–721. <https://journals.sagepub.com/doi/pdf/10.1177/154193129804201012>.
93. Albin, T. J., and Molenbroek, J. 2016. Stepwise Estimation of Accommodation in Multivariate Anthropometric Models Using Percentiles and an Average Correlation Value. *Theoretical Issues In Ergonomics Science* 18(1):79–94. <https://doi.org/10.1080/1463922X.2016.1149254>.
94. Gordon, C. C., Churchill, T., Clauser, C. E., Bradtmiller, B., McConville, J. T., Tebbetts, I., and Walker, R. A. 1989. *1988 Anthropometric Survey of U.S. Army Personnel: Methods and Summary Statistics*. United States Army Natick Research, Development and Engineering Center, Natick, MA. https://mreed.umtri.umich.edu/mreed/downloads/anthro/ansur/Gordon_1989.pdf.
95. Waller, P., and Green, P. 1997. Human Factors in Transportation. In *Handbook of Human Factors and Ergonomics*, 2nd ed. (G. Salvendy, ed.), Wiley, Hoboken, NJ.
96. Ogden, C. L., Fryar, C. D., Carroll, M. D., and Flegal, K. M. 2004. *Mean Body Weight, Height, and Body Mass Index: United States 1960–2002*. Advance Data from Vital and Health Statistics, No. 347. U.S. Department of Health and Human Services, Centers for Disease Control and Prevention, National Center for Health Statistics, Hyattsville, MD.
97. Fryar, C. D., Gu, Q., Ogden, C. L., and Flegal, K. M. 2016. *Anthropometric Reference Data for Children and Adults: United States, 2011–2014*. Vital and Health Statistics, Ser. 3, No. 39. U.S. Department of Health and Human Services, Centers for Disease Control and Prevention, National Center for Health Statistics, Hyattsville, MD.
98. Schneider, L. W., Robbins, D. H., Pflueg, M. A., and Snyder, R. G. 1983. *Development of Anthropometrically Based Design Specifications for an Advanced Adult Anthropomorphic Dummy Family, Volume 1*. Final report. University of Michigan Transportation Research Institute, Ann Arbor, MI.
99. Robbins, D. H. 1983. *Anthropometric Specifications for Mid-Sized Male Dummy, Volume 2*. University of Michigan Transportation Research Institute, Ann Arbor, MI.
100. Robbins, D. H. 1983. *Anthropometric Specifications for Small Female and Large Male Dummies, Volume 3*. University of Michigan Transportation Research Institute, Ann Arbor, MI.
101. Reddie, M., and Parkinson, M. B. 2022. A Comparison of Approaches to Reweighting Anthropometric Data. *Ergonomics* 65(10):1397–1409. <https://doi.org/10.1080/00140139.2022.2039409>.
102. Nadadur, G., and Parkinson, M. B. 2014. A Z-Score-Based Method to Synthesize Anthropometric Datasets for Global User Populations. In *ASME 2013 Conference Proceedings: International Design Engineering Technical Conference & Computers and Information in Engineering*. <https://doi.org/10.1115/DETC2013-12845>.
103. Parkinson, M. B., and Reed, M. P. 2010. Creating Virtual User Populations by Analysis of Anthropometric Data. *International Journal of Industrial Ergonomics* 40(1):106–111. <https://doi.org/10.1016/j.ergon.2009.07.003>.
104. Bureau of Labor Statistics. n.d. Bus Drivers. In *Occupational Outlook Handbook*, U.S. Department of Labor, Washington, DC. <https://www.bls.gov/ooh/transportation-and-material-moving/bus-drivers.htm>.
105. Courtney, A. J., and Evans, W. A. 1987. A Preliminary Investigation of Bus Cab Design for Cantonese Drivers. *Journal of Human Ergology* 16(2):163–171. <https://doi.org/10.11183/jhe1972.16.163>.
106. Schweitzer, M. M. 1980. World War II and Female Labor Force Participation Rates. *The Journal of Economic History* 40(1):89–95. <https://www.jstor.org/stable/2120427>.
107. Bureau of Labor Statistics. 2010. Women in the Labor Force: A Databook. U.S. Department of Labor, Washington, DC. <https://www.bls.gov/cps/wlf-intro-2010.htm>.
108. Census Bureau. n.d. National Population by Characteristics: 2010–2019. Annual Estimates of the Resident Population by Sex, Race, and Hispanic Origin for the United States: April 1, 2010 to July 1, 2019. <https://www.census.gov/data/tables/time-series/demo/popest/2010s-national-detail.html>.
109. NHTSA. n.d. National Automotive Sampling System: Crashworthiness Data System. U.S. Department of Transportation, Washington, DC. <https://www.nhtsa.gov/national-automotive-sampling-system/crashworthiness-data-system>.
110. Courtney, A. J., and Wong, M. H. 1985. Anthropometry of the Hong Kong Male and the Design of Bus Driver Cabs. *Applied Ergonomics* 16(4):259–266. [https://doi.org/10.1016/0003-6870\(85\)90089-4](https://doi.org/10.1016/0003-6870(85)90089-4).
111. May, J. F., and Baldwin, C. L. 2009. Driver Fatigue: The Importance of Identifying Causal Factors of Fatigue When Considering Detection and Countermeasure Technologies. *Transportation Research Part F: Traffic Psychology and Behaviour* 12(3):218–224.
112. Kim, J. Y., Choi, J. W., and Kim, H. J. 1999. The Relation Between Work-Related Musculoskeletal Symptoms and Rapid Upper Limb Assessment (RULA) Among Vehicle Assembly Workers. *Korean Journal of Preventive Medicine* 32(1):48–59.



APPENDIX A

Data Processing in Excel

Stature	ESH	BMI	UpperLeg	LowerLeg	UpperArm	LowerArm	ESH/Stature	Stature-ESH
1740.0	931.1	23.18	447.2	429.8	281.9	335.8	0.535	809.0
1675.3	863.4	22.85	430.5	413.8	271.4	323.3	0.515	811.9
1665.6	902.1	29.96	428.1	411.4	269.8	321.5	0.542	763.5
1683.0	860.7	23.35	432.5	415.7	272.6	324.8	0.511	822.4
1833.0	936.8	24.51	471.1	452.8	297.0	353.8	0.511	896.3
1804.5	908.0	25.84	463.7	445.7	292.3	348.3	0.503	896.5
1719.1	894.4	23.34	441.8	424.6	278.5	331.8	0.520	824.7
1834.6	939.0	25.93	471.5	453.1	297.2	354.1	0.512	895.6
1653.2	856.9	26.30	424.9	408.4	267.8	319.1	0.518	796.4
1782.4	921.2	23.11	458.1	440.3	288.8	344.0	0.517	861.3
1842.9	946.4	26.53	473.6	455.2	298.6	355.7	0.514	896.5
1762.9	919.9	25.60	453.1	435.4	285.6	340.2	0.522	843.0
1643.9	845.6	24.81	422.5	406.0	266.3	317.3	0.514	798.4
1711.8	881.7	18.61	439.9	422.8	277.3	330.4	0.515	830.1
1839.1	957.0	21.60	472.7	454.3	297.9	355.0	0.520	882.1
1817.6	955.5	29.10	467.1	449.0	294.5	350.8	0.526	862.1
1869.5	994.6	26.53	480.5	461.8	302.9	360.8	0.532	874.9
1899.8	961.2	21.37	488.2	469.2	307.8	366.7	0.506	938.6
1739.1	912.7	31.28	447.0	429.6	281.7	335.7	0.525	826.4
1765.4	879.9	20.34	453.7	436.0	286.0	340.7	0.498	885.5
1747.2	897.9	27.87	449.0	431.6	283.1	337.2	0.514	849.3

Figure A.1. Virtual U.S. bus driver body dimensions.

SW_pref_X	SW_pref_Z	SW_X	SW_Z	H_pref_X	H_pref_Z	H_X	H_Z	Eye_X	Eye_Z
276.5	749.8	276.5	749.8	656.9	441.6	656.9	441.6	655.1	1117.8
182.7	814.0	182.7	814.0	579.0	496.7	579.0	496.7	561.1	1118.4
164.1	803.9	164.1	803.9	563.4	479.1	563.4	479.1	552.9	1140.4
194.0	774.7	194.0	774.7	605.6	463.8	605.6	463.8	583.7	1084.0
187.2	845.6	187.2	845.6	631.2	529.6	631.2	529.6	608.0	1213.0
186.2	820.5	186.2	820.5	642.2	507.4	642.2	507.4	609.9	1169.6
187.6	779.9	187.6	779.9	601.4	468.5	601.4	468.5	586.8	1115.8
104.8	846.0	141.8	834.8	609.3	519.4	609.3	519.4	584.2	1206.6
180.6	738.9	180.6	738.9	600.7	429.2	600.7	429.2	577.8	1050.4
238.3	756.8	238.3	756.8	662.7	452.0	662.7	452.0	646.3	1120.7
167.8	830.4	167.8	830.4	629.9	515.4	629.9	515.4	605.4	1209.3
273.0	782.4	273.0	782.4	674.8	470.6	674.8	470.6	657.8	1141.6
187.4	770.0	187.4	770.0	592.6	456.8	592.6	456.8	569.5	1066.9
198.8	798.4	198.8	798.4	591.0	487.8	591.0	487.8	581.4	1118.0
221.7	747.1	221.7	747.1	662.8	446.6	662.8	446.6	652.4	1142.0
210.6	791.0	210.6	791.0	655.7	477.1	655.7	477.1	637.0	1181.3
185.6	786.0	185.6	786.0	640.4	475.8	640.4	475.8	632.9	1207.8
237.5	817.6	237.5	817.6	687.5	511.5	687.5	511.5	665.7	1210.0
240.9	805.1	240.9	805.1	656.2	484.6	656.2	484.6	630.9	1157.1
147.6	827.8	147.6	827.8	590.0	516.4	590.0	516.4	564.5	1147.6
215.4	809.0	215.4	809.0	641.6	492.3	641.6	492.3	613.5	1148.9

Figure A.2. Virtual U.S. bus driver primary reference points.

Grip X	Grip Z	Hip X	Hip Z	Shoulder X	Shoulder Z	Elbow X	Elbow Z	Elbow Angle	Knee X	Knee Z	Knee Angle
276.5	669.2	625.0	442.4	765.5	876.4	611.1	640.6	118.4	186.3	529.2	99.9
182.7	762.3	548.8	491.5	669.1	897.1	497.2	687.1	115.9	120.1	532.3	96.9
164.1	755.7	495.7	487.8	649.8	902.1	479.4	692.9	118.0	70.5	537.6	88.7
194.0	714.5	572.7	459.1	691.8	863.7	513.7	657.2	120.7	145.7	527.9	96.8
187.2	796.6	592.3	532.9	724.3	972.5	536.8	742.2	120.4	122.8	571.6	96.9
186.2	768.7	596.3	510.3	723.2	936.8	530.6	716.9	122.7	135.3	561.6	97.1
187.6	722.2	568.6	466.5	696.7	885.6	515.8	673.9	122.2	133.0	540.4	94.2
141.8	808.0	562.8	525.0	698.8	964.5	491.4	751.7	125.2	94.2	576.9	91.6
180.6	676.2	552.3	428.6	680.2	828.5	496.8	633.4	125.6	137.9	522.4	92.3
238.3	683.9	631.1	451.9	760.8	884.3	581.3	658.1	124.2	182.0	541.9	98.6
167.8	784.5	580.3	522.5	719.6	964.8	521.0	741.9	124.9	109.7	576.5	93.3
273.0	707.3	630.1	474.1	767.6	903.4	610.6	664.8	116.2	181.4	537.0	102.1
187.4	710.8	552.0	453.1	673.3	849.3	498.5	648.4	119.8	134.9	520.8	95.5
198.8	740.6	583.1	477.7	696.7	894.5	523.3	678.2	117.9	146.9	534.9	98.4
221.7	675.9	639.1	447.1	772.2	896.8	576.7	672.0	130.4	179.6	557.6	95.5
210.6	729.3	592.5	488.8	745.5	931.3	560.3	702.4	124.6	131.8	565.7	93.4
185.6	729.7	590.8	486.8	747.3	948.3	546.3	721.8	130.4	119.7	581.3	89.6
237.5	754.0	665.1	512.1	790.5	966.0	602.8	722.1	122.7	180.7	573.1	101.3
240.9	739.1	581.6	496.2	732.0	917.3	572.2	685.3	115.4	137.2	544.5	98.0
147.6	787.0	573.0	508.7	681.9	925.9	481.9	721.4	123.3	121.6	554.7	96.1
215.4	748.9	584.9	497.4	720.2	916.1	547.7	691.7	117.8	138.5	546.2	98.1

Figure A.3. Virtual U.S. bus driver secondary body landmarks.

70 Assessing Lifecycle and Human Costs of Bus Operator Workstation Design and Components

Up_Vision	Down_Vision	H_point	SW	Total	RULA
1	1	1	1	1	3
1	1	1	1	1	3
1	1	1	1	1	3
1	1	1	1	1	3
1	1	1	1	1	3
1	1	1	1	1	3
1	1	1	1	1	3
1	1	1	0	0	3
1	1	1	1	1	3
1	1	1	1	1	3
1	1	1	1	1	3
1	1	1	1	1	3
1	1	1	1	1	3
1	1	1	1	1	3
1	1	1	1	1	3
1	1	1	1	1	3
1	1	1	1	1	3
1	1	1	1	1	3
1	1	1	1	1	3
1	1	1	1	1	3
1	1	1	1	1	3
1	1	1	1	1	3
1	1	1	1	1	3

Figure A.4. *U.S. bus driver accommodation virtual assessment.*



APPENDIX B

U.S. Bus Driver Demographics

B.1 Bus Driver Demographics: Gender

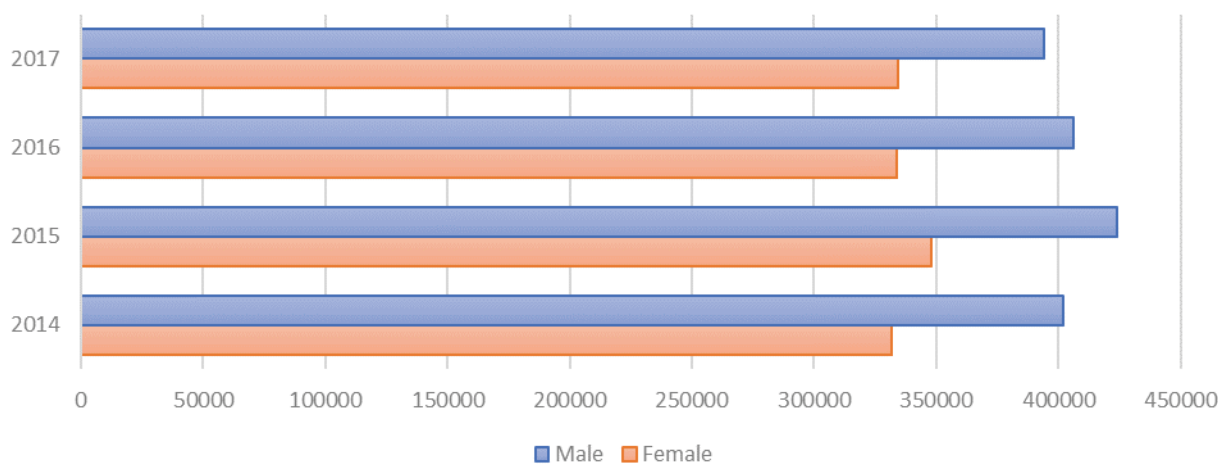


Figure B.1. U.S. bus driver male-to-female ratio, 2014–2017.

B.2 Bus Driver Demographics: Ethnicity

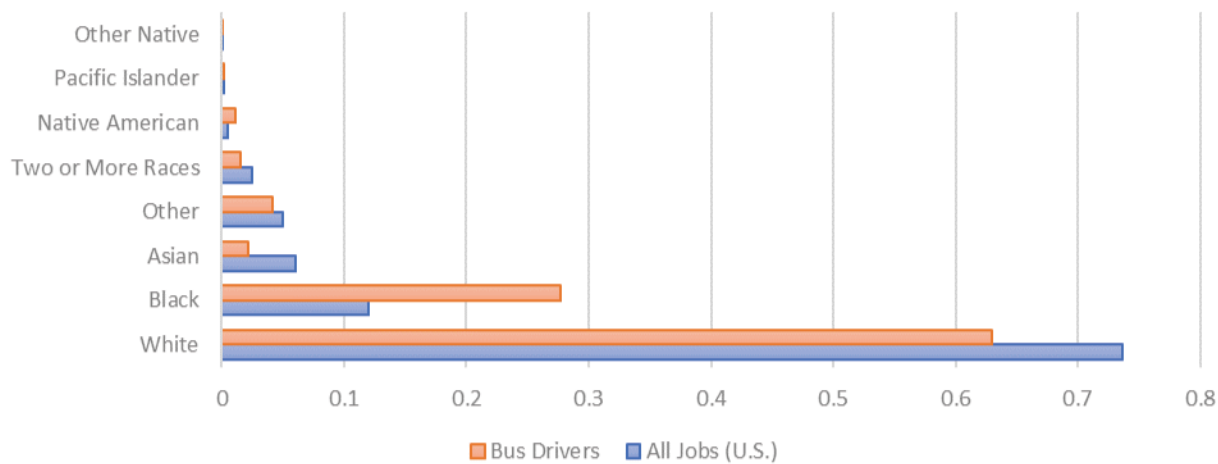


Figure B.2. U.S. bus driver racial diversity, 2017.

72 Assessing Lifecycle and Human Costs of Bus Operator Workstation Design and Components

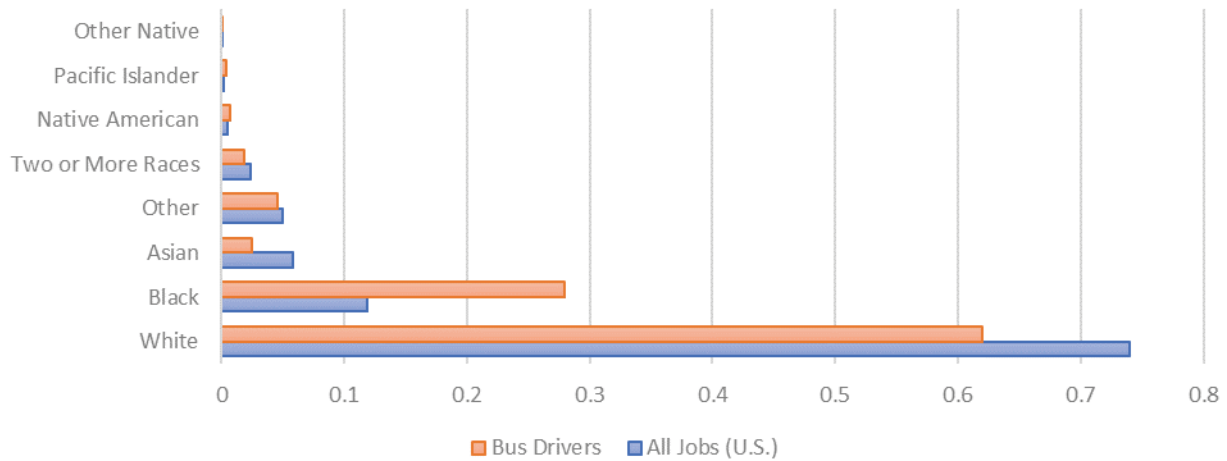


Figure B.3. U.S. bus driver racial diversity, 2016.

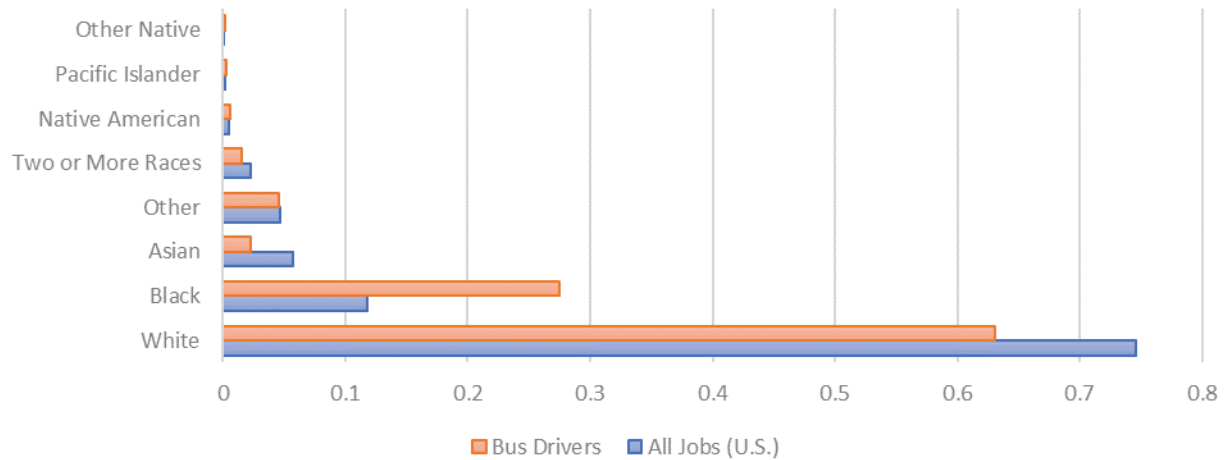


Figure B.4. U.S. bus driver: racial diversity, 2015.

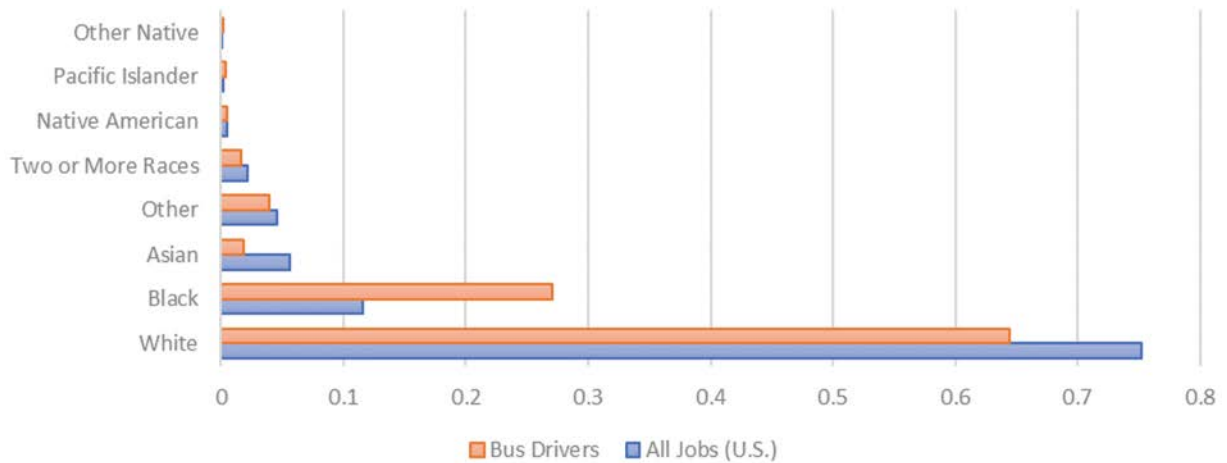


Figure B.5. U.S. bus driver racial diversity, 2014.

B.3 Bus Driver Demographics: Age

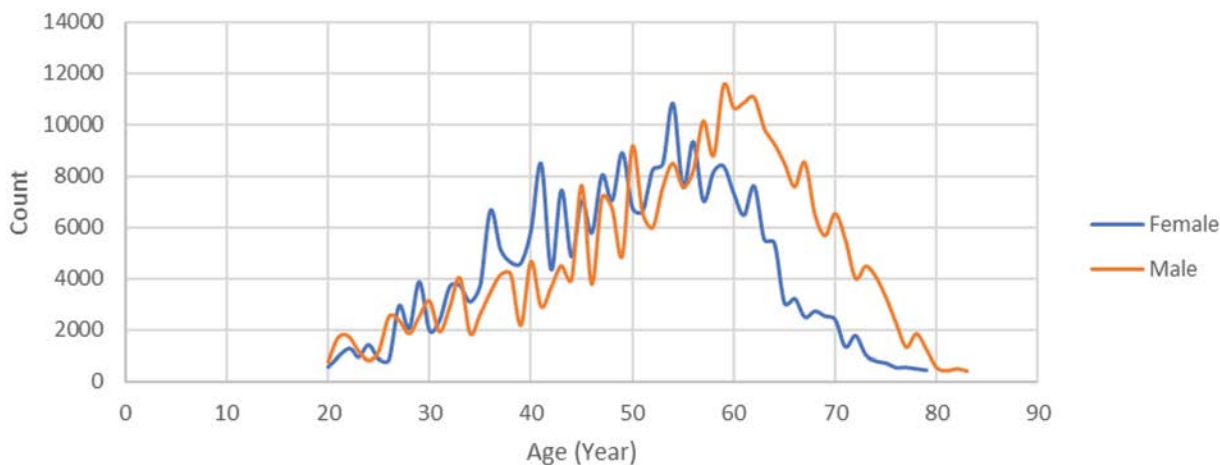


Figure B.6. U.S. bus driver male and female age distribution, 2017.

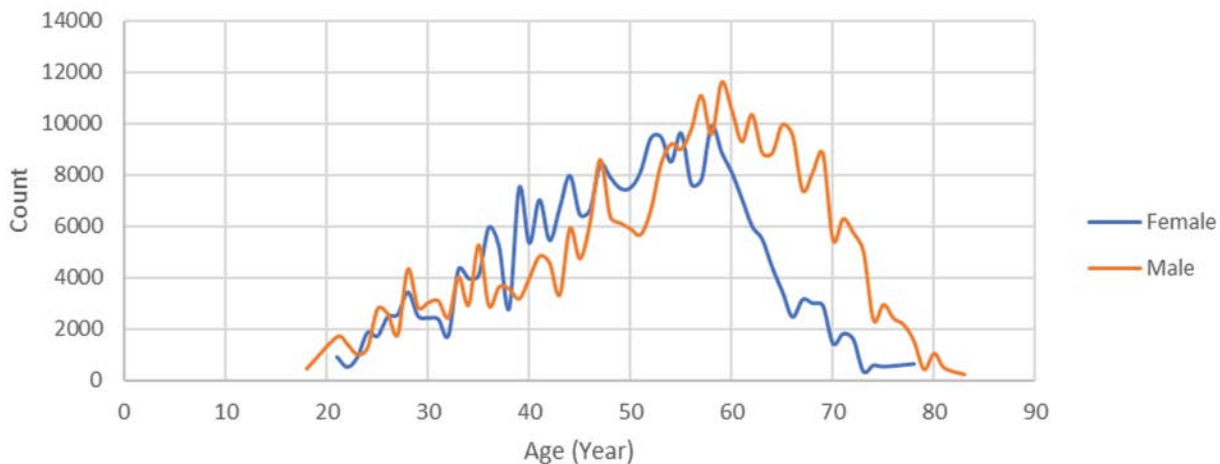


Figure B.7. U.S. bus driver male and female age distribution, 2016.

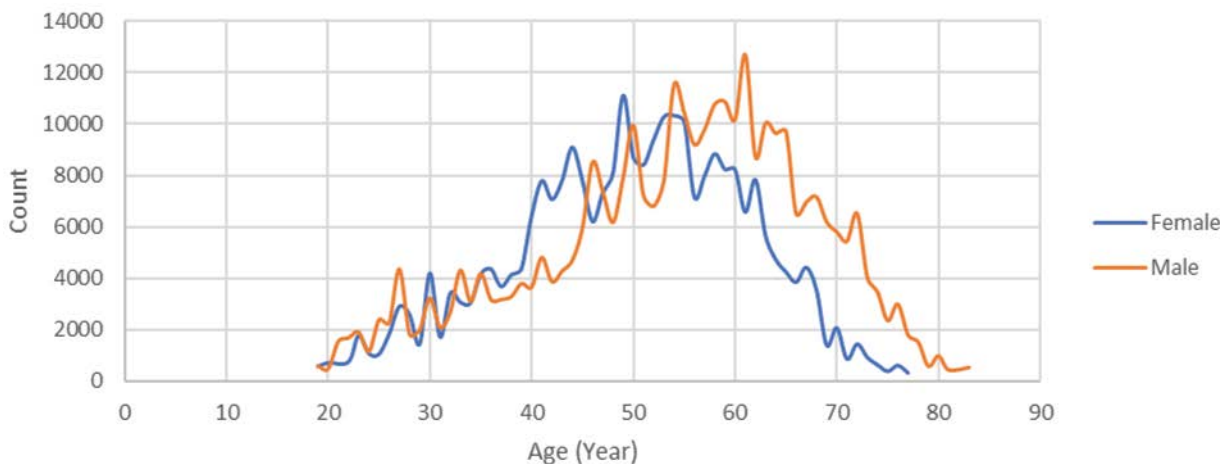


Figure B.8. U.S. bus driver male and female age distribution, 2015.

74 Assessing Lifecycle and Human Costs of Bus Operator Workstation Design and Components

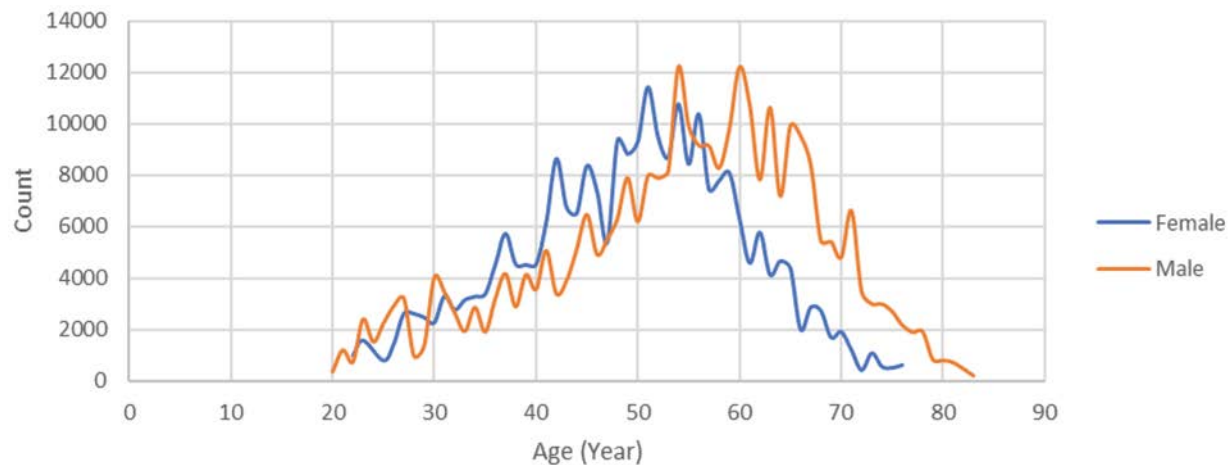


Figure B.9. U.S. bus driver male and female age distribution, 2014.

Abbreviations and acronyms used without definitions in TRB publications:

A4A	Airlines for America
AAAAE	American Association of Airport Executives
AASHO	American Association of State Highway Officials
AASHTO	American Association of State Highway and Transportation Officials
ACI-NA	Airports Council International-North America
ACRP	Airport Cooperative Research Program
ADA	Americans with Disabilities Act
APTA	American Public Transportation Association
ASCE	American Society of Civil Engineers
ASME	American Society of Mechanical Engineers
ASTM	American Society for Testing and Materials
ATA	American Trucking Associations
CTAA	Community Transportation Association of America
CTBSSP	Commercial Truck and Bus Safety Synthesis Program
DHS	Department of Homeland Security
DOE	Department of Energy
EPA	Environmental Protection Agency
FAA	Federal Aviation Administration
FAST	Fixing America's Surface Transportation Act (2015)
FHWA	Federal Highway Administration
FMCSA	Federal Motor Carrier Safety Administration
FRA	Federal Railroad Administration
FTA	Federal Transit Administration
GHSA	Governors Highway Safety Association
HMCRP	Hazardous Materials Cooperative Research Program
IEEE	Institute of Electrical and Electronics Engineers
ISTEA	Intermodal Surface Transportation Efficiency Act of 1991
ITE	Institute of Transportation Engineers
MAP-21	Moving Ahead for Progress in the 21st Century Act (2012)
NASA	National Aeronautics and Space Administration
NASAO	National Association of State Aviation Officials
NCFRP	National Cooperative Freight Research Program
NCHRP	National Cooperative Highway Research Program
NHTSA	National Highway Traffic Safety Administration
NTSB	National Transportation Safety Board
PHMSA	Pipeline and Hazardous Materials Safety Administration
RITA	Research and Innovative Technology Administration
SAE	Society of Automotive Engineers
SAFETEA-LU	Safe, Accountable, Flexible, Efficient Transportation Equity Act: A Legacy for Users (2005)
TCRP	Transit Cooperative Research Program
TEA-21	Transportation Equity Act for the 21st Century (1998)
TRB	Transportation Research Board
TSA	Transportation Security Administration
U.S. DOT	United States Department of Transportation

Transportation Research Board
500 Fifth Street, NW
Washington, DC 20001

ADDRESS SERVICE REQUESTED

**NATIONAL
ACADEMIES** *Sciences
Engineering
Medicine*

The National Academies provide independent, trustworthy advice that advances solutions to society's most complex challenges.

www.nationalacademies.org

ISBN 978-0-309-70985-9

